VDA Verband der Automobilindustrie

FAT Forschungsvereinigung Automobiltechnik

# FAT-Schriftenreihe 318

## Air Quality Modelling on the Contribution of Brake Wear Emissions to Particulate Matter Concentrations Using a High-Resolution Brake Use Inventory

# Air Quality Modelling on the Contribution of Brake Wear Emissions to Particulate Matter Concentrations Using a High-Resolution Brake Use Inventory

**Ricardo Energy & Environment**

Dan Wakeling
Dr. Tim Murrells
Dr. David Carslaw
Dr. John Norris
Dr. Jess Virdo

Das Forschungsprojekt wurde mit Mitteln der Forschungsvereinigung Automobiltechnik e.V. (FAT) gefördert.

# Executive summary

This is the final report for the FAT project 1.40 "Air Quality Modelling on the Contribution of Brake Wear Emissions to Particulate Matter Concentrations Using a High-Resolution Brake Use Inventory". In this project, a highly spatially resolved brake wear emissions inventory has been developed using real vehicle measurements data, covering over 150,000 km driven, together with emission factors from contemporary literature emission rates. This spatially resolved brake wear emissions inventory has been modelled using Ricardo's RapidAir air quality model to investigate how this affects ambient particulate matter concentrations at a high spatial resolution. Furthermore, the model is used to compare current approaches for estimating brake wear emissions where emissions are assumed to be constant along each road link and with a more refined approach that accounts for the spatial variability of emissions.

In the first part of the project, an innovative approach was developed to estimate brake use on a highly resolved spatial and temporal basis. Real vehicle measurements data has been analysed, and estimates made of the energy dissipated to brakes each second. These estimates have been validated against measured records of brake use within these datasets, where possible. The approach developed for estimating the energy dissipation to the brakes can be extended and applied to datasets without a record of brake use (e.g. PEMS data).

In the second part of the project, contemporary estimates of brake wear emission rates were distributed according to the spatial and temporal energy dissipation inventory. A literature review was undertaken to consider the most appropriate brake wear emission rates to use. The brake wear emissions inventory was analysed to investigate the relationship between brake wear emissions and variables including the speed limit of the road, the road type classification, the time of day, and gradient of the road, with important relationships observed in many cases. Road gradient for example was found to be a particularly significant influencing factor. This information could be used by air quality practitioners if they have information available on these variables.

In the final part of the project, the spatially resolved brake wear emissions inventory has been used as an input to the RapidAir model to investigate impacts on ambient particulate matter ($PM_{10}$) concentrations at a high spatial resolution. In general, it was found that the contribution of brake wear to ambient urban $PM_{10}$ was below 1 µg $m^{-3}$, but the contribution can be as high as 5.7 µg $m^{-3}$ at busy junctions. Comparisons with current modelling assumptions (i.e. constant emission rates along each road link) were made to understand the effect of using the new approach. This modelling showed that the contribution of brake wear to $PM_{10}$ concentrations was more spatially variable using the new approach, with larger contributions more focussed around busy road junctions.

Additional model runs were made to determine the sensitivity of the results to the brake wear emission factor and fleet composition used, and to investigate the effect of regenerative braking on the contribution of brake wear emissions to $PM_{10}$ concentrations. An interesting aspect of the regenerative brake scenario is that it has the effect of largely removing brake wear emissions from areas that could be considered urban i.e. where personal exposure is of importance, while leaving only a few small areas of emissions where the hardest braking conditions occur. This is because most urban locations are not associated with the highest braking energies. This behaviour of the regenerative braking scenario could therefore be of importance for exposure to particulate matter in urban populations.

The main focus of the work was to reapportion brake wear emissions according to data on the location and intensity of vehicle braking. In most locations the brake wear contribution is lower in the spatially resolved model, however there are few locations of high intensity braking where the brake wear contribution is predicted to be significantly higher. Eleven receptor sites were chosen for the air quality modelling and the contribution of brake wear to ambient $PM_{10}$ concentrations at one site was over 3 times higher (3.9 µg $m^{-3}$ difference) using the more refined spatially resolved emissions inputs. In the regenerative braking scenario, the brake wear contribution to $PM_{10}$ was reduced significantly (from 5.7 µg $m^{-3}$ to 1.6 µg $m^{-3}$) at the receptor location with the highest contribution of brake wear to ambient $PM_{10}$ concentrations.

The results of the air quality modelling could be used to inform the siting of measurement stations to help understand and verify the contribution of brake wear to ambient $PM_{10}$ concentrations, which itself is highly uncertain. Currently, air quality monitoring sites are not specifically located in regions where brake wear emissions could be high. The approach adopted in this work could be used to help design ambient measurement site choice to maximise the contribution made from brake wear emissions. Locations at busy road junctions were found to often be associated with the highest brake wear emissions.

The approach used (analysing the high frequency energy changes from vehicle measurements data) lends itself to a more sophisticated approach to understanding the contribution of brake wear to ambient $PM_{10}$ concentrations in future. The energy-based approach is well-suited for considering a range of scenarios, for example the effect of regenerative braking, as has been covered within this project.

# Table of contents

# 1 Introduction

Fine particulate matter (PM) is present in the ambient air as a complex mixture of solid and liquid particles of organic and inorganic substances. The most health relevant particulates are those with a diameter of 10 microns or less, (≤ $PM_{10}$), which can penetrate and lodge deep inside the lungs. A growing body of research has pointed towards the smaller particles, in particular PM less than 2.5 µm in diameter ($PM_{2.5}$), as a metric even more closely associated with adverse health effects. There is a close, quantitative relationship between exposure to high concentrations of small particulates ($PM_{10}$ and $PM_{2.5}$) and increased mortality or morbidity, both daily and over time.

The EU Ambient Air Quality Directive sets a limit on ambient concentrations of $PM_{10}$ of 50 µg $m^{-3}$ not to be exceeded more than 35 times a year and an annual mean limit of 40 µg $m^{-3}$. The limit on annual mean concentrations of $PM_{2.5}$ concentrations is 25 µg $m^{-3}$ [(1)]. Under certain meteorological conditions, these limits can be exceeded in European cities.

A major source of PM in urban areas has been emissions from road traffic, particularly near roadsides. Exhaust emissions of PM from road vehicles have been declining in recent years. This decrease has been the result of the successful introduction of various abatement technologies driven by ever tighter vehicle emission regulations. As the importance of exhaust emissions has declined, the emissions of PM from non-exhaust sources have become relatively more prominent. These non-exhaust emissions include $PM_{10}$ and $PM_{2.5}$ arising from the mechanical wear of brake, tyre and road surface material and traffic-induced resuspension of road dust. Emissions from these non-exhaust sources are not currently controlled.

In FAT (2017), a review and summary of the current evidence base for the contribution of brake wear to Particulate Matter (PM) air quality in Europe was carried out, alongside a scoping study on how uncertainties in brake wear emission estimates can be reduced. Key results included:

(1) That there are few articles in the literature that explicitly provided an estimate of contribution of the brake wear to concentrations of PM in the air, and that there are considerable uncertainties in such estimates;
(2) An analysis of national emissions inventory data that shows that the contribution of non-exhaust emissions, relative to exhaust emissions of PM, is expected to increase considerably up to 2030;
(3) That future and emerging vehicle technologies, such as regenerative braking, will affect brake wear emission rates, which is not accounted for in national emissions inventories.

FAT (2017) also developed a potential innovative approach for demonstrating the typical pattern and likely magnitude of brake use expected in real journeys, to better spatially apportion braking intensity. This approach showed how spatially variable braking is, which is not reflected well in emissions inventories, and not well-researched to date.

[1] The EU Ambient Air Quality Directive also sets a National exposure reduction targets for $PM_{2.5}$ to be achieved by 2020. See Air Quality Expert Group (2012).

This project has developed an air quality modelling approach, further developing and applying the higher resolution understanding of brake use from FAT (2017), to better inform emissions from brake wear and how this affects ambient PM concentrations at a high spatial and temporal resolution.

In order to achieve the project aims, the project has been split into three work packages:

- In **Work Package 1**, an innovative approach has been developed to estimate brake use on a highly resolved spatial and temporal basis. Real vehicle measurements data, covering over 150,000 km driven has been analysed, and estimates made of the energy dissipated to brakes each second. These estimates have been validated against measured records of brake use within these datasets, where possible. The approach developed for estimating the energy dissipation to the brakes can be extended and applied to datasets without a record of brake use e.g. Portable Emissions Measurement Systems (PEMS) data.

- In **Work Package 2**, contemporary estimates of brake wear emission rates were distributed according to the spatial and temporal energy dissipation inventory. A literature review was undertaken to consider the most appropriate brake wear emission rates to use. The brake wear emissions inventory was analysed to investigate the relationship between brake wear emissions and variables including the speed limit of the road, the road type classification, the time of day, and gradient of the road. This information could be used by air quality practitioners if they have information available on these variables.

- In **Work Package 3**, the spatially resolved brake wear emissions inventory has been used as an input to the RapidAir model to investigate impacts on ambient particulate matter ($PM_{10}$) concentrations at a high spatial resolution. Comparisons with current modelling assumptions (i.e. constant emission rates along each road link) were made to understand the effect of using the new approach. Additional model runs were made to determine the sensitivity of the results to the brake wear emission factor and fleet composition used, and to investigate the effect of regenerative braking on the contribution of brake wear emissions to particulate matter concentrations.

Consideration has also been given for how the results of this work could be applied to other European locations – including Germany. This is covered in section 5 of the report.

# 2 Work Package 1 - Spatial-temporal brake use inventory

In Work Package 1, a brake use inventory has been developed that captures both the duration and magnitude of braking necessary for mapping brake use at a high spatial and temporal resolution. Using estimates of the energy dissipated through braking, an inventory has been constructed on example routes that provides a directly relevant proxy for brake wear based on the energy lost by vehicles during braking. Estimates of the average energy dissipation for different road types, vehicle types, and traffic situations have also been developed, so that estimates of energy dissipation can be applied more widely, where dynamic vehicle measurements data is not available. This forms the basis of the generalised brake wear emission factors in Work Package 2.

An example brake use inventory was developed in FAT (2017), based on high frequency dynamic vehicle measurements data from 19 passenger cars tested as part of UK Department for Transport research in 2016. This data was analysed to produce a proxy for brake intensity; Vehicle Specific Power. The data did not include a measure of whether the brake pedal was used, or the strength of brake use however, and so an assumption was made as to at which level of negative Vehicle Specific Power brakes were applied at. The brake use inventory developed in Work Package 1 has been refined and improved relative to the approach used in FAT (2017) by:

- Analysing more dynamic vehicle measurements data (over 100 times more kilometres driven), allowing more robust conclusions to be made;
- Replacing the proxy for brake use (Vehicle Specific Power) by the more appropriate proxy of modelled energy dissipated to the brakes;
- Verifying and calibrating the modelled brake use and intensity, based on the estimated energy dissipated to the brakes, using a measure of brake use;
- Analysing patterns in brake use and intensity by the speed limit of the road, and the road type, to draw more general conclusions.

### 2.1.1 Activity datasets

Three vehicle activity datasets have been analysed within this project:

- **euroFOT**: activity dataset of one vehicle, largely around western Germany.
- **DfT**: UK Department for Transport (DfT) dataset that was used in FAT project 1.39, with data from 38 vehicles measured in central England; (The UK Department for Transport, 2016).
- **Leeds**: University of Leeds dataset on the activity of 20 vehicles and 79 vehicles, across most areas of England, and some of Wales, although concentrated around the cities of Leeds and Leicester.

Table 1 summarises key details on these three activity datasets considered, and further detail on the activity datasets is also provided in the text below this. A small amount of data was available from other vehicle measurement campaigns; however, this was disregarded for analysis due to insufficient high quality and high frequency data within these datasets. None of the data given below was collected specifically for this project.

**Table 1 Summary of key details on the three activity datasets considered.**

| Dataset | Area covered | Kilometres driven (km) | Vehicle(s) used | Measure of brake use | Description |
|---|---|---|---|---|---|
| euroFOT | Largely western Germany, with some data in southern Germany, southern Netherlands, and eastern Belgium | 23,750 | Ford Mondeo Station Wagon | Yes | Activity of one driver. |
| Leeds | Largely Leeds and Leicester, though many roads covered across England and north Wales. | 129,000 | Skoda Fabia Elegance 1.4 litre estate | Yes | Activity of 79 drivers collected. Included in the dataset was a measure of the speed limit of the road, age group and gender group of the driver, and other measures. |
| DfT | Central England. 38 vehicles repeated a given route incorporating a mix of urban, rural, and motorway roads | 2,600 | 19 Euro 5 and 19 Euro 6 light-duty diesel vehicles | No | Further details of the measurement programme are given in The UK Department for Transport (2016) |

Further details on the vehicle measurements datasets used are given in Appendix A.1.

### 2.1.2 Comparison to the Worldwide Harmonised Light Vehicle Test Procedure driving cycle

The Worldwide Harmonised Light Vehicle Test Procedure (WLTP) driving cycle is used as a global test cycle across different world regions, so that pollutant and $CO_2$ emissions as well as fuel consumption values would be comparable worldwide. Grigoratos, Giorgio and Heinz (2016) undertook analyses of the WLTP typical driving conditions to narrow down the range of driving conditions to be taken into consideration as far as non-exhaust particle emissions are concerned and will improve the comparability of future studies.

The analyses done by Grigoratos, Giorgio and Heinz (2016) have been replicated using the vehicle measurements datasets used in this project. This has been done to determine the similarity in driving and braking behaviour between the WLTP drive cycle and the vehicle measurements datasets used in this project. Overall, there was very good agreement between the driving and braking behaviour between the WLTP drive cycle and the vehicle measurements datasets used in this project.

An analysis showing the effect of driver behaviour is presented within this section of the report. Some further results on the analyses to replicate the analyses done by Grigoratos, Giorgio and Heinz (2016) using the data from this project are presented in Appendix A.2 and the full analysis can be found here (**to create web link**).

#### 2.1.2.1 Effect of Driver Behaviour

The effect of driver behaviour was considered by looking at patterns in the data split by the 79 drivers in the Leeds data and the single driver from the euroFOT data. Figure 1 shows the importance of driver behaviour on the brake phase duration distributions by “v_max” group (facets running from left to right). As considered in Grigoratos, Giorgio and Heinz (2016), “v_max” is the maximum speed in a “short trip”, where a short trip is consecutive data with v_max > 1 km/h.

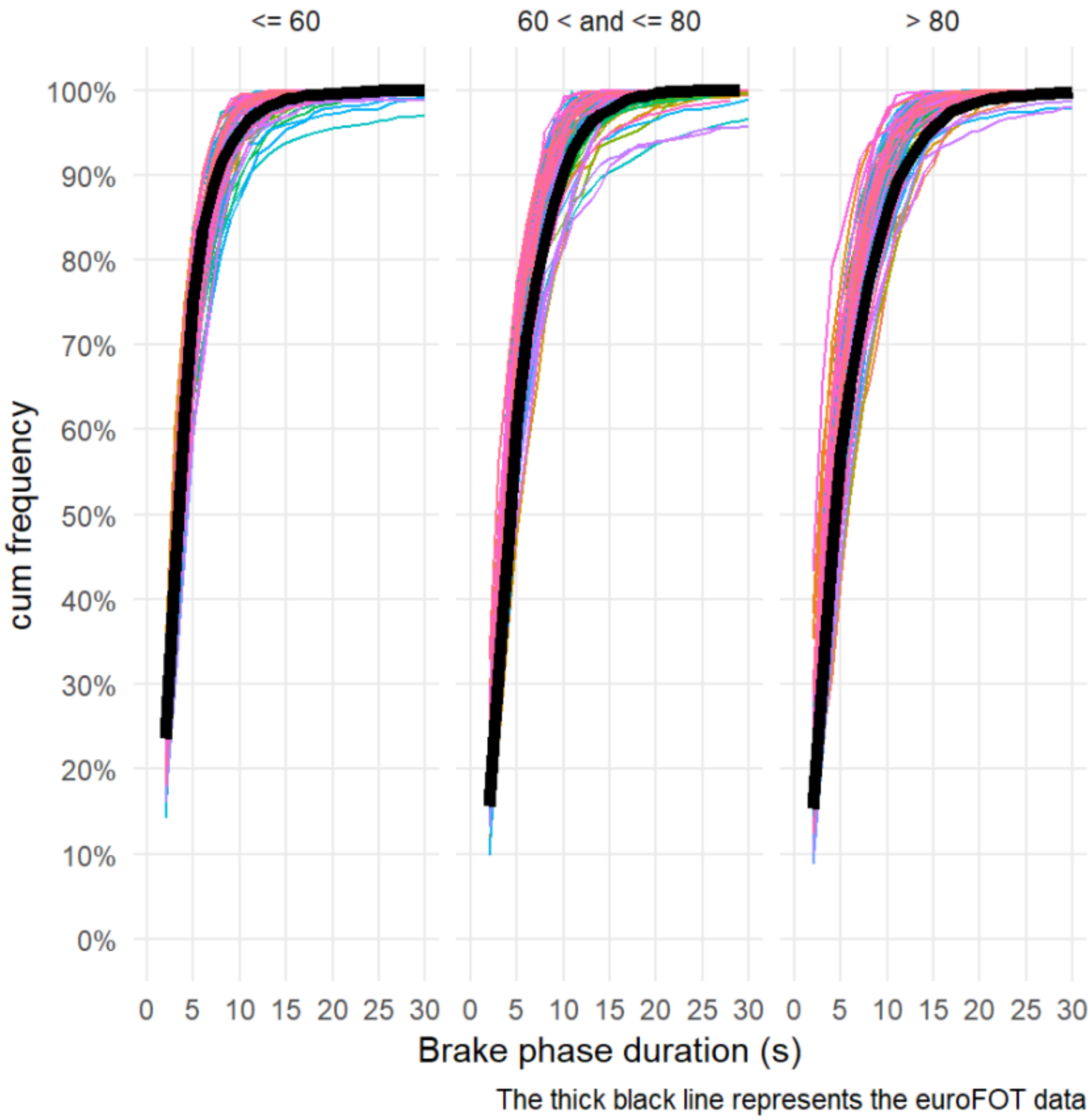


**Figure 1 Comparison of the euroFOT and Leeds brake phase duration distributions, split by the driver. The different coloured lines represent different drivers within the Leeds data, and the thick black line represents the driver from the euroFOT data.**

## 2.2 Calculations of energy going to the brakes

The principal approach used in this study is to apportion brake wear emission rates according to the energy dissipated to the brakes. This section describes how estimates of the energy going to the brakes were made. The estimates of energy to the brakes is used to apportion brake wear emission rates for the activity datasets analysed, such that the brake use and brake wear emission rate is linearly dependent on the estimated energy going to the brakes. Figure 2 summarises how estimates of energy going to the brakes were made for the vehicle measurement datasets.

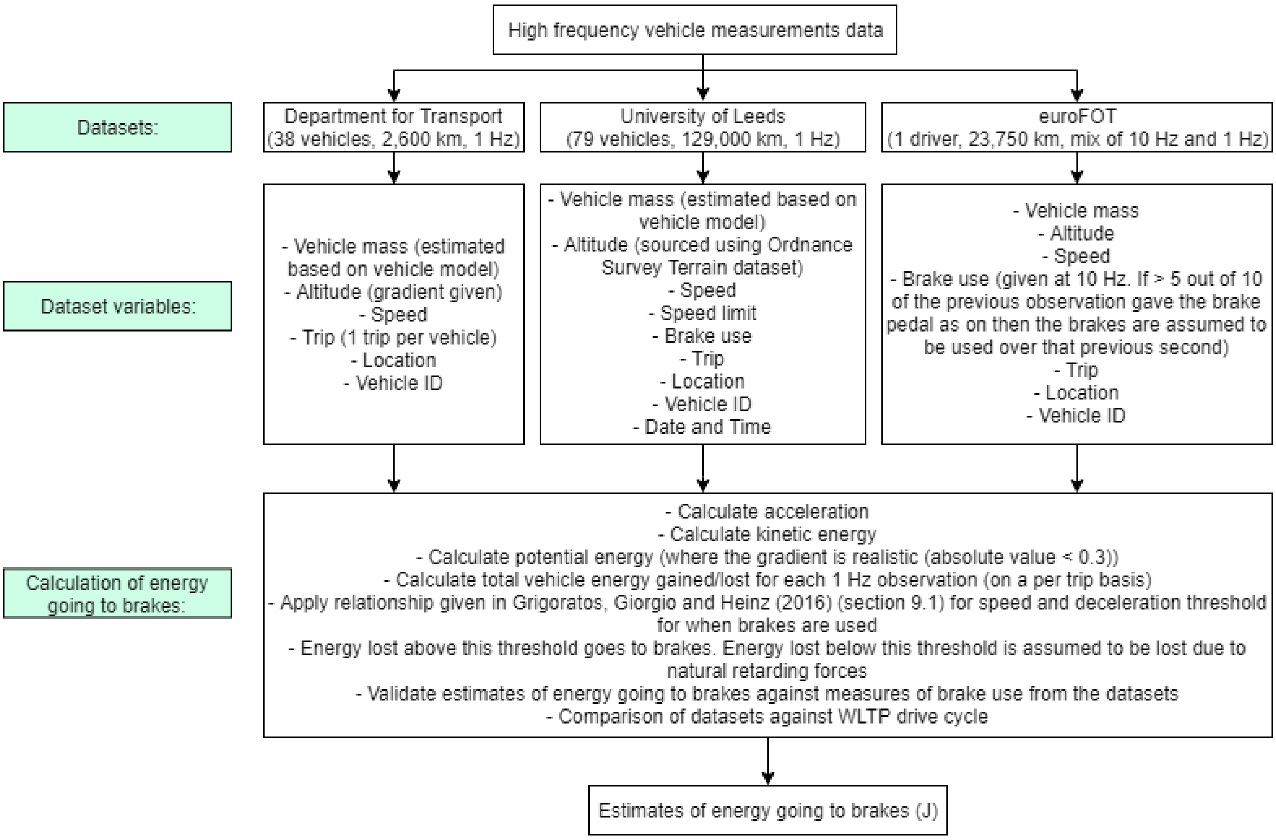


**Figure 2 Flow chart summarising how estimates of energy going to the brakes were made for the vehicle measurements datasets.**

The text immediately below outlines the approach used to generate estimates of the energy going to the brakes from the vehicle measurements datasets. Further details on the methodology used are given in Appendix A.2.

Data was available or collected on the vehicle mass, speed, and altitude. Using this data, the acceleration, kinetic energy and potential energy of the vehicles was calculated at a 1 Hz resolution. From this the energy gained or lost was calculated at a 1 Hz resolution, and on a per trip basis.

A vehicle can lose speed and energy through natural retarding forces, so consideration was needed to determine at what energy threshold the brakes were applied at. The approach used was to apply the deceleration threshold defined as "a_threshold" on page 25 of Grigoratos, Giorgio and Heinz (2016). This threshold also factors in the vehicle speed.

Vehicle energy losses below this threshold were assumed to occur due to natural retarding forces, including drag, rolling resistance, and engine braking. Vehicle energy losses above this threshold were assumed to go the brakes. As a result, calculations of the energy going to the brakes were made at a 1 Hz resolution.

The calculation of energy going to the brakes can be summarised in the below equation.

$$\mathrm{E}_{\mathrm{to\_brakes}} = \mathrm{E}_{\mathrm{loss}} - \mathrm{E}_{\mathrm{loss\_thresh}}$$

where $\mathrm{E}_{\mathrm{to\_brakes}}$ is the energy calculated to go to the brakes, $\mathrm{E}_{\mathrm{loss}}$ is the energy loss calculated for the vehicle given the change in kinetic and potential energy, and $\mathrm{E}_{\mathrm{loss\_thresh}}$ is the energy loss at the threshold point from the “a_threshold” on page 25 of Grigoratos, Giorgio and Heinz (2016), for the vehicle’s speed and deceleration at that time.

Energy is calculated to go the brakes where $\mathrm{E}_{\mathrm{loss}} - \mathrm{E}_{\mathrm{loss\_thresh}} > 0$.

The euroFOT and Leeds datasets included a measure of whether the brakes were used or not. The calculations of braking energy were validated against the recorded measure of brake use available from the euroFOT and Leeds datasets. The results showed a good predicted accuracy (94-96%).

# 3 Work Package 2 - Brake wear emission factor estimates

In Work Package 1, a highly spatially resolved brake use inventory has been developed that estimates the location and intensity of brake use from real vehicle measurements data, according to the calculated energy dissipated to the brakes. In Work Package 2, contemporary brake wear emission rates are reviewed, applied, and related to the brake use inventory from Work Package 1, to produce highly spatially and temporally resolved emissions rates for brake wear. Furthermore, brake wear emissions are analysed according to variables such as the speed limit of the road and the road type classification to generate emission rate relationships that can be used for air quality modelling where highly resolved vehicle measurements data is not available.

## 3.1 Development of highly resolved brake wear emission rates

### 3.1.1 Review and application of contemporary brake wear emission rates

To identify the most applicable emission rates to use, sources such as the EMEP 2016 Guidebook (EMEP (2016)), the USEPA's MOVES model for estimating traffic emissions (United States Environmental Protection Agency (2014)), and the latest scientific literature have been reviewed. The USEPA's MOVES model uses emission rates in (g/hr) as a function of deceleration ($m/s^2$), whereas the (EMEP (2016) Guidebook uses average speed-related g/km emission factors. Consideration is given as to which approach is most appropriate for a modern European context, and the brake use inventory developed in Work Package 1.

Literature articles have been reviewed to find appropriate brake wear $PM_{10}$ emission factors for cars and other light duty vehicles (LDVs). Table 2 shows the emission factors found, the type of study, and the literature source. Brake wear emission factors show a wide range of values, indicating that there are large uncertainties. An appropriate average from reviewing Table 2 is **6 mg/km**.

**Table 2 Brake wear $PM_{10}$ emission factors for cars and LDVs obtained from literature articles.**

| Reference | Type of study | Emission factor (mg/km) |
|---|---|---|
| Garg *et al.* (2000) via Grigoratos and Martini (2015) | Brake dynamometer study | 2.9-7.5 |
| Hagino et al. (2015) | Brake dynamometer study | 0.24-0.64 |
| Hagino et al. (2016) | Brake dynamometer study | 0.04-1.4 |
| Rauterberg-Wulff (1999) via Grigoratos and Martini (2015) | Receptor modelling (highway tunnel) | 1 |
| Abu-Allaban *et al.* (2003) via Grigoratos and Martini (2015) | Receptor modelling | 0-80 |
| Luhana et al. (2004) via Grigoratos and Martini (2015) | Receptor modelling | 8.8 |
| Bukowiecki et al. (2009a) via Grigoratos and Martini (2015) | Receptor modelling (urban street canyon) | 8 |
| Bukowiecki et al. (2009a) via Grigoratos and Martini (2015) | Receptor modelling (highway) | 1.6 |
| Westerlund and Johansson (2002) | Emissions modelling | 17 |
| Lawrence, Sokhi and Ravindra (2016) | Source apportionment modelling | 3.8-4.4 |
| USEPA (1995) via Grigoratos and Martini (2015) | Emission inventory | 7.9 |
| Lükewille et al. (2001) via Grigoratos and Martini (2015) | Emission inventory | 1.8-4.9 |
| Boulter et al. (2006) via Grigoratos and Martini (2015) | Emission inventory (RAINS model) | 3.8 |
| Boulter et al. (2006) via Grigoratos and Martini (2015) | Emission inventory (MOBILE 6.2 model) | 7.8 |
| Barlow et al. (2007) via Grigoratos and Martini (2015) | Emission inventory | 4.0-8.0 |
| NAEI (2012) via Grigoratos and Martini (2015) | Emission inventory | 7 |
| TNO CEPMEIP Database (2007)[2] | Emission inventory | 6.0-7.5 |
| NERI (2004)[3] | Emission inventory | 7.5-13.4 |
| EEA (2003) via Lawrence, Sokhi and Ravindra (2016) | Emission inventory | 7.3 |

[2] http://www.air.sk/tno/cepmeip/em_factors.php

[3] http://www.dmu.dk/Pub/AR236.pdf

### 3.1.2 Method for apportioning emissions according to the highly resolved brake use inventory

As mentioned previously, the brake wear emissions are apportioned in the vehicle measurements datasets according to the calculations of energy going to the brakes. Figure 3 outlines the approach used to do this.

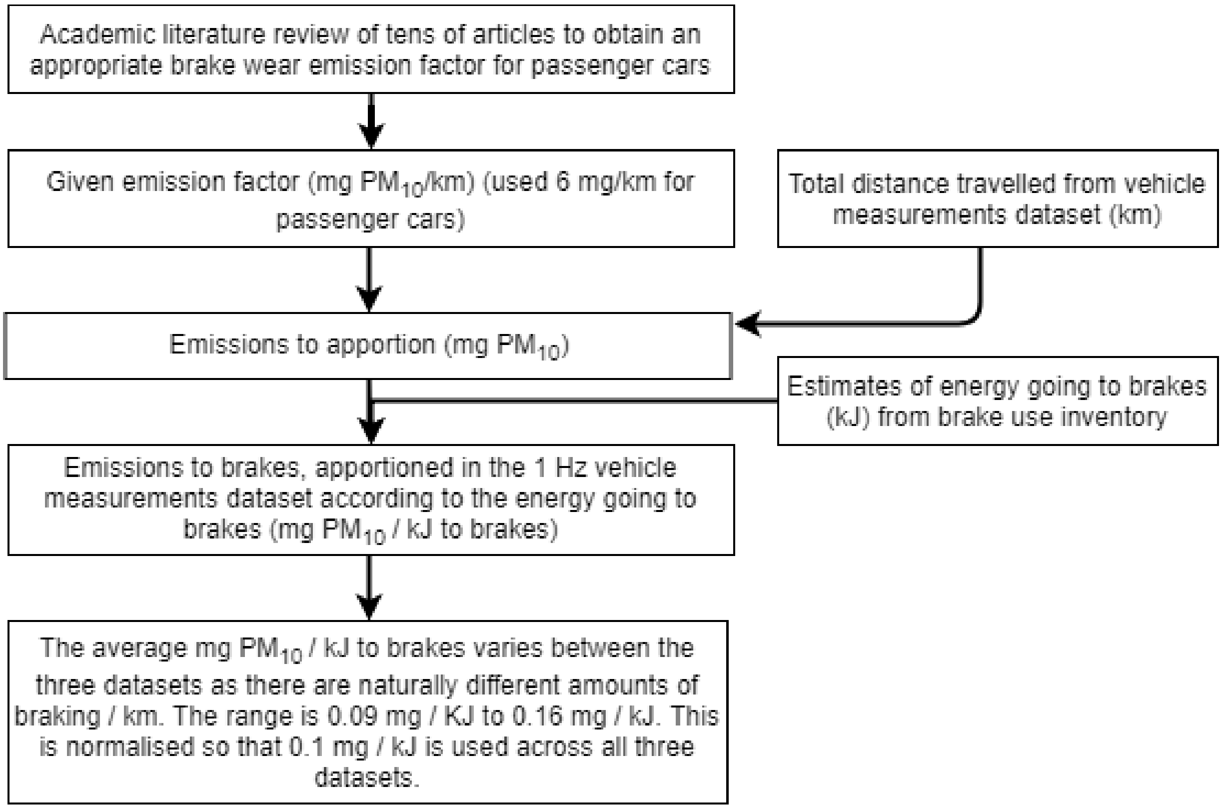


**Figure 3 Flow chart summarising how estimates of emissions from the brakes were made based on the energy going to the brakes from the highly resolved brake use inventory.**

Given that there were large amounts of vehicle measurements data analysed (over 150,000 vehicle kilometres driven), it is considered that applying the average from the literature review is appropriate. If less data were used, it may not be appropriate to apply this factor because the data may not be robust and large enough. It is also considered that the emission factor of 6 mg/km considers a wide range of brake pad types that may be in the fleet.

The final energy-based brake wear emission rate applied was **0.1 mg/kJ** to the brakes, as shown in the final box of Figure 3.

### 3.1.3 Comparisons/validation against other literature sources

Comparisons have been made to the brake wear emission rates developed in this study against other literature sources. The United States Environmental Protection Agency (US EPA) have developed the MOtor Vehicle Emission Simulator (MOVES), which is a is a state-of-the-science emission modelling system. Brake wear emission rates are based on $PM_{2.5}$ emission rates vs a deceleration curve/function.

Some literature articles have experimentally researched the mass of particles released over set drive cycles, or from initial speeds and fixed deceleration rates. Therefore, emission rates can be expressed as mg/stop (i.e. braking event), rather than mg/km. Factors in mg/stop have also be generated from the model developed in this project for comparison. These comparisons are given in Appendix A.4.

### 3.1.4 Scaling for other vehicle types

The work described above has been to develop highly spatially resolved emission rates using high resolution vehicle measurements data for passenger cars. Of all the vehicle types on the road in the UK and Germany, passenger cars are estimated to contribute the most to emissions from vehicle brake wear. In both Germany and the UK in 2016, 65% of vehicle brake wear emissions were estimated to come from passenger cars (Hausmann *et al.* (2018); Wakeling *et al.* (2018)). Whilst passenger cars have lower brake wear emission rates per kilometre than heavier vehicles (e.g. heavy-duty vehicles), they dominate the kilometres driven for both countries, and hence contribute the most to emissions from vehicle brake wear. In 2016, passenger cars were estimated to contribute 84% of the total distance driven by vehicle type in Germany (Hausmann *et al.* (2018)), and 78% of the total distance driven by vehicle type in the UK (Wakeling *et al.* (2018)). These figures are also larger in urban areas, as passenger cars have a larger proportion of their activity in urban areas relative to Heavy Duty Vehicles (HDVs).

When modelling the impact of road vehicles on air quality however, it is important to consider appropriate emission rates, to account for significant differences in emission rates between vehicle types. Vehicle brake wear emission rates can vary by orders of magnitude between vehicle types, largely due to differences in vehicle weights. A short review has been undertaken to identify appropriate scaling factors to apply for different vehicle type groups.

The USEPA MOVES model considers brake wear emissions for LDVs and a further seven vehicle categories, including HDVs (US EPA, 2011). They acknowledge that there are several reasons (e.g. use of drums, engine downshifting, exhaust braking, “jake” braking, larger discs/drums (lower temperatures) etc.) which would reduce the relative rate of brake emissions for the kinetic energy lost. In developing the MOVES methodology, the authors reviewed the existing literature for an applicable heavy duty to light duty ratio. and opted for a simple ratio of 7.5. To factor in different weights in different vehicle classes, they opted for an assumption that the emission rate is linearly proportional to the vehicle weight.

The UK and German national emissions inventories provide brake wear emission factors for different vehicle types (Hausmann *et al.* (2018); Wakeling *et al.* (2018)). The UK emissions inventory also provides brake wear emission factors disaggregated by road type (Urban, Rural, and Motorway). The UK emissions inventory brake wear emission factors were developed based on the Tier 2 method in the EMEP/EEA Emissions Inventory Guidebook (EMEP (2016)) derived from a review of measurements by the UNECE Task Force on Emissions Inventories[4]. Emission factors are provided in g/km for different vehicle types with speed correction factors, which imply higher emission factors at lower speeds. The German emissions inventory brake wear emission factors are derived from a literature study from 2006.

[4] http://vergina.eng.auth.gr/mech0/lat/PM10/

Table 3 shows the vehicle-type specific scaling factors applied to brake wear emission factors, relative to those used for passenger cars, for both the UK and German emissions inventory. For example, this gives motorcycle emission factors as 0.5 times the emission factor for passenger cars. These scaling factors have been calculated based on the difference between the mg/km emission rates by vehicle type used. The scaling factors for the UK and Germany given in Table 3 are similar despite them being based on different methodological approaches. For heavy-goods vehicles the factors are also significantly less than that used by US EPA (2011). **For scaling brake wear emissions by vehicle type, the scaling factors given in Table 3 from the German emissions inventory were applied**.

**Table 3 Vehicle type-specific scaling factors applied to brake wear emission factors, relative to those used for passenger cars, for both the UK and German emissions inventory.**

| Vehicle Type | UK | Germany |
|---|---|---|
| Light-goods vehicles | 1.6 | 1.6 |
| Heavy-goods vehicles | 4.4 | 4.3 |
| Buses | 4.4 | 3.9 |
| Motorcycles | 0.5 | 0.5 |

### 3.1.5 Other influencing variables on brake wear emissions

The literature review undertaken as part of this Work Package also identified two other potential influencing factors on the release of brake wear emissions; brake material temperature, and a lag in the release of particles from braking. This is covered in more detail in Appendix A.5.

Although temperature may be an important influencing factor on brake wear emissions, the evidence reviewed suggests that there is no clear temperature dependency relationship for typical drive cycles on $PM_{10}$. There would also be significant uncertainties in trying to model this effect. Estimates would need to be made for the rates of cooling of the brake materials, which would vary significantly across the range of pad materials used.

There is some evidence that brake particles may be emitted some time after the braking event. It is not clear what the mechanism for this is though, nor conclusive evidence on what this lag value should be.

## 3.2 Generalised brake wear emission factors

The previous section describes the development of a highly spatially resolved brake emissions inventory by combining the highly spatially resolved brake use inventory with contemporary brake wear emission factors. This emissions inventory is used as an input for the air quality modelling described in section 4.

The highly resolved nature of the data used lends itself to a wide range of analyses by dataset variables such as speed limit of the road and road type. The results of these analyses may be useful to air quality practitioners who have information on such variables, but not high frequency vehicle measurements data to develop a highly spatially resolved brake wear emissions inventory. This sub section of the report presents the results of these analyses. An analysis on the effect of vehicle speed on average brake wear emission factors is also shown in Appendix A.6.

### 3.2.1 Speed limit

The Leeds dataset included a field giving the speed limit of the road the vehicle was on. The relationship between the estimated brake wear emissions and the speed limit of the road is presented below.

In Figure 4 the data is grouped by speed limit of the road (miles per hour (mph)), and the calculated average emission rate is presented for each road speed limit. The average emission rate is calculated as the sum of the emissions (mg) divided by the distance travelled (km) in the 1 Hz dataset. Data was also available for 20 mph speed limit roads, however there were too few observations to draw a robust analysis, and so this data was omitted for this speed limit relationship analysis.

In Figure 4, there is a clear relationship of higher average brake wear emission rates on lower speed limit roads. This relationship is expected as vehicles tend to brake more often per kilometre travelled on lower speed limit roads. Figure 5 shows the proportion of observations where the brakes were used (%) by speed limit of the road (mph). The determination of whether the brakes were used is based on the measured brake use from the 1 Hz vehicle measurements dataset. Around four times as many observations showed braking behaviour on 30 mph roads relative to 70 mph roads.

The black dots in Figure 4 show the brake wear emission rates from the UK's National Atmospheric Emissions Inventory (Wakeling *et al.* (2018)). The UK's National Atmospheric Emissions Inventory provides emission rates by road type (urban, rural, and motorway), and these are matched with the 30 mph, 50 mph, and 70 mph speed limit roads respectively in Figure 4. The pattern between the data analysed in this project and the UK's National Atmospheric Emissions Inventory is similar, though the speed limit to emission rate relationship is more extreme in the UK's National Atmospheric Emissions Inventory.

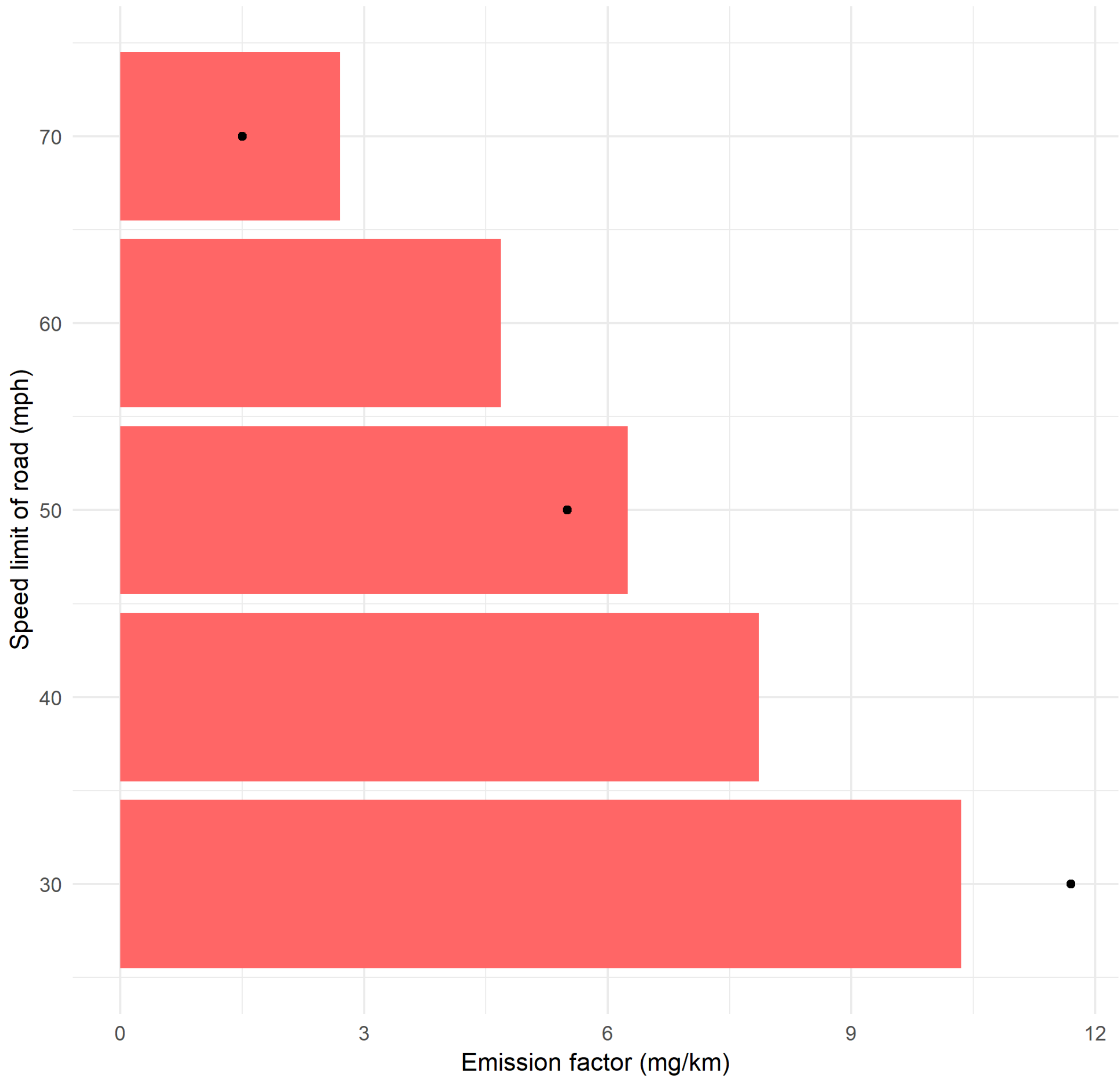


**Figure 4 Brake wear emission factor ($PM_{10}$ mg/km) by speed limit of road. The black dots in show the brake wear emission rates from the UK's National Atmospheric Emissions Inventory, matched with the 30 mph, 50 mph, and 70 mph speed limit roads respectively.**

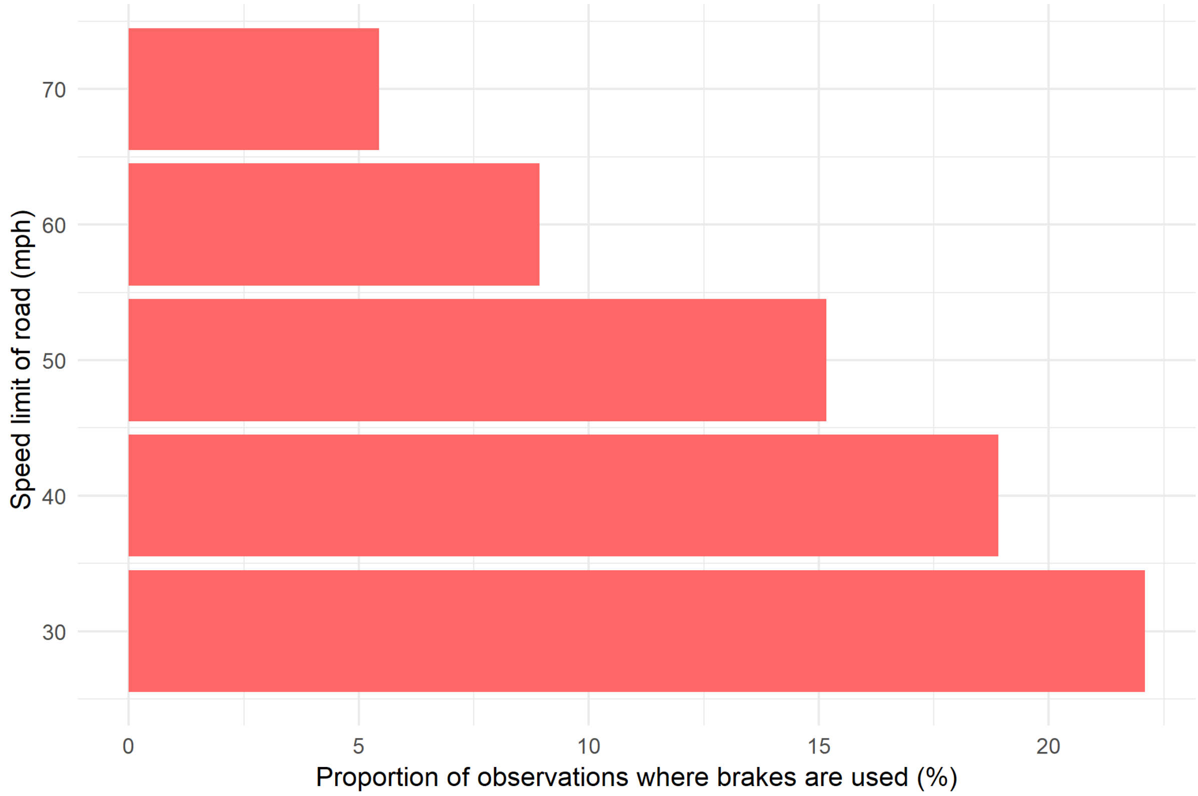


**Figure 5 Proportion of observations where the brakes are used (%) by speed limit of the road (mph).**

The Leeds dataset has been analysed further to investigate how braking behaviour varies by the speed limit of the road. The average brake wear emission factors presented in Figure 4 are useful, however the highly spatially resolved nature of the data allows more detailed analyses to be conducted. Emissions from the brakes (mg $PM_{10}$) have been estimated for each of the valid 1 Hz observations, apportioned according to the estimated energy dissipated by the brakes. Figure 6 shows the density of the estimated emissions from the brakes, by the speed limit of the road. The density represents the relative number of observations by the “Emissions from brakes” values on the x-axis. This shows that more of the braking events have very low emissions at the lower speed limit roads, and vice versa. Figure 7 displays the same data, but with the x-axis limited at the low end to 1.25 mg/s, making the pattern clearer to see. Although average emission rates are lower for high speed limit roads (Figure 4) as vehicles brake less frequently on these roads, when they do brake, the emissions are more severe. This is as vehicles typically travel at higher speeds on higher speed limit roads and therefore more energy is needed to reduce the vehicle’s speed and kinetic energy. As a result, it may be expected that emissions from brakes on higher speed limit roads may be more spatially variable, with few highly localised areas of high brake wear emissions, which could lead to high $PM_{10}$ concentrations.

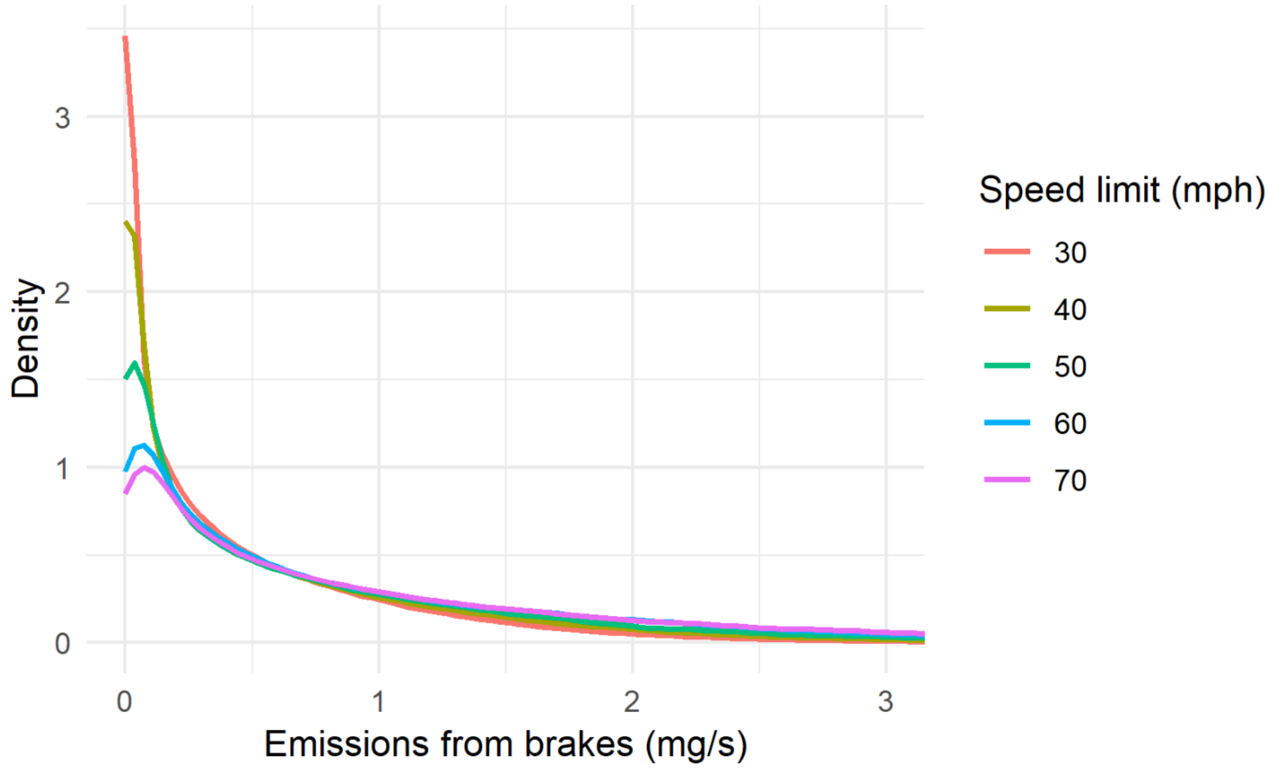


**Figure 6 Density of the estimated emissions from the brakes, by the speed limit of the road.**

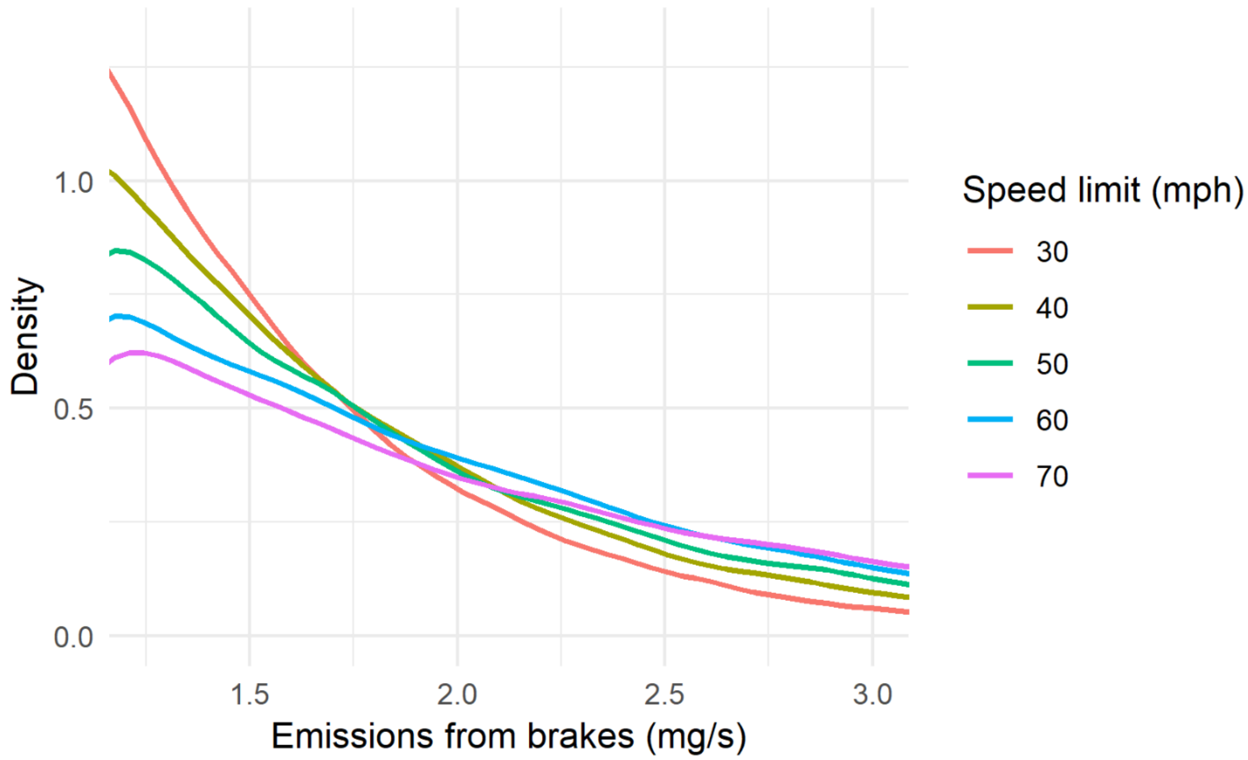


**Figure 7 Density of the estimated emissions from the brakes, by the speed limit of the road, with the x-axis limited at the low end to 1.25 mg/s.**

### 3.2.2 Road type

The type of road is another variable that has a significant effect on brake wear emissions. The varying characteristics between road types leads to different driver behaviour, and as a result, different braking behaviour and emissions.

Information on the road type classification was obtained from OpenStreetMap, which is a wiki world map built by volunteers and released with an open-content license[5]. Users add features to the map such as boundary regions, bicycle lanes, and the type of road. The type of road is classified with the key "highway". Further information about the "highway" key is available here: https://wiki.openstreetmap.org/wiki/Key:highway.

The OpenStreetMap data has been downloaded in the areas where vehicle measurements datasets are available. This includes the location of the nodes, so the data can be joined to the vehicle measurements data sets used in this project.

Note that as OpenStreetMap is user-generated by volunteers, there may be some inconsistencies between assigned classifications. For example, the classification between "primary" and "secondary" roads is quite subjective as it is based on the "importance" of the road. Also, the road classifications vary between countries, including between the UK and Germany.

Figure 8 shows the calculated average emission factor (mg/km) by the road type classification from OpenStreetMap and vehicle measurement dataset. Only road types where there were more than 2,000 observations for each road type and dataset (euroFOT and Leeds) are shown. The road types ending in "_link" are slip roads/ramps leading from that road type to a lower-class road type (e.g. "motorway_link" is a slip road coming from a motorway). Figure 8 shows that the average brake wear emission factors are up to an order of magnitude larger on "link"-equivalent roads (e.g. larger for "motorway_link" than "motorway"), although the difference is less pronounced for trunk roads in the Leeds data set. This pattern is as expected as vehicles will tend to brake much more often on link type roads. Also, the average emission factors are lower on the "motorway" and "trunk" roads which are the highest-class roads that typically have the highest speed limits. This aligns with the results found in section 3.2.1. The patterns are broadly similar between the euroFOT and Leeds datasets, however there is not always a clear agreement. As mentioned above, there are differences in the road classifications between countries, and as the two measurements datasets were collected using different instruments and on different vehicles, this adds extra reason for potential discrepancies. Also, the euroFOT data is based on measurements from one driver, whereas the Leeds dataset is collected from 79 drivers. Driver behaviour is a key influencing factor and the effect of driver behaviour is briefly covered in section 2.1.2.

[5] https://wiki.openstreetmap.org/wiki/About_OpenStreetMap

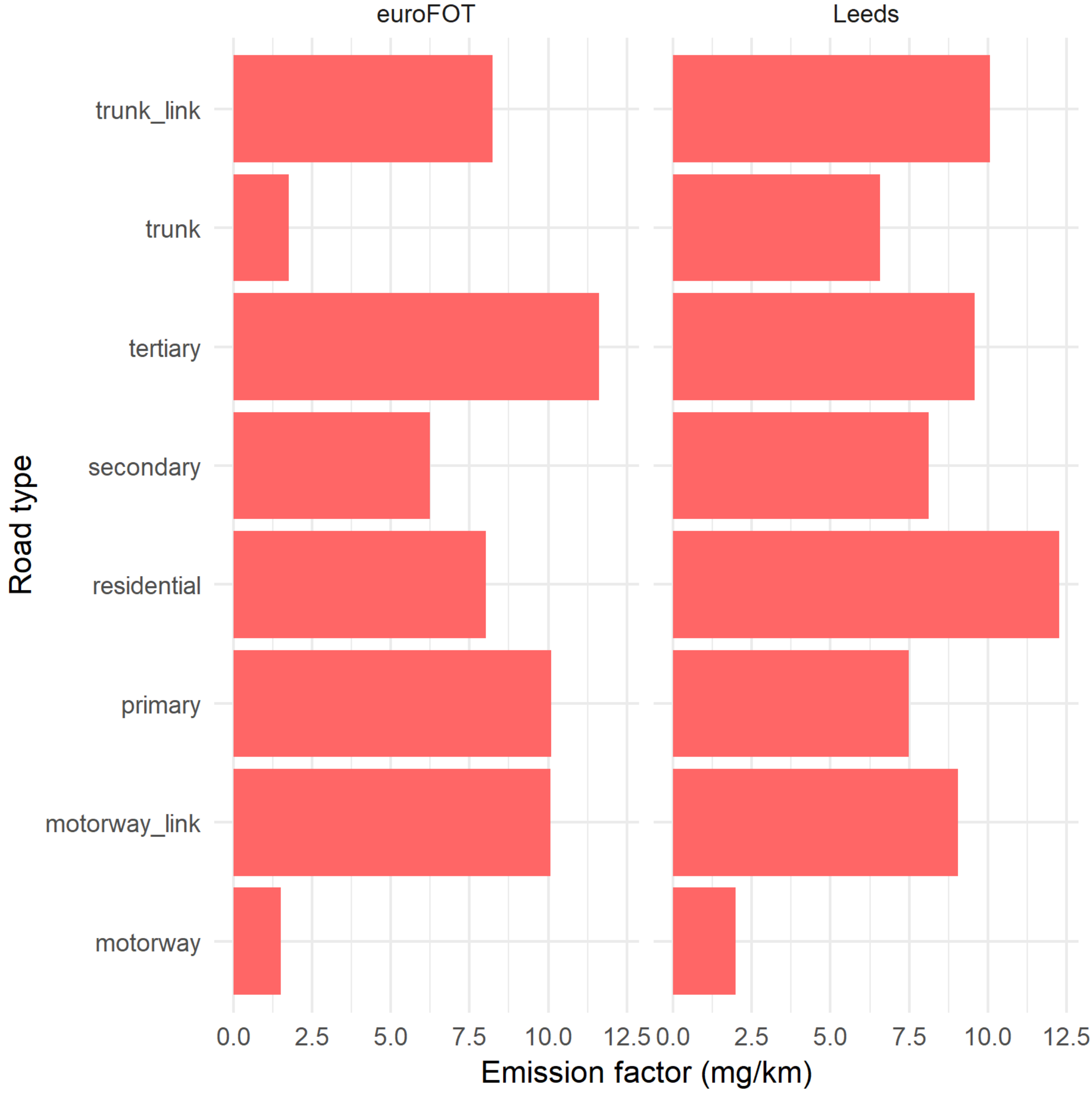


**Figure 8 Calculated average brake wear emission factor (mg/km) by road type and vehicle measurement dataset.**

### 3.2.3 Temporal changes

#### 3.2.3.1 Time of day

The Leeds dataset included a field giving the date and time of each 1 Hz observation. The relationship between the estimated brake wear emissions and the time of day from the Leeds dataset is discussed below.

Figure 9 shows the calculated average brake wear emission factor (mg/km) by hour of the day. On the x-axis, where the hour of day is given as “7” for example, that includes observations from 07:00:00 until 07:59:59. Note that the y-axis begins at 4 mg/km. Each hour of the day grouping included over 6,000 observations, and all hour of the day groupings from 07:00 until 18:00 had over 500,000 observations included.

Figure 9 shows that there is not a strong, clear relationship between hour of the day and the average brake wear emission factor. The largest emission factors are found for the typical peak hours beginning at 07:00 and ending at 19:00 and the lowest emission factors are found at times when traffic volume is typically lower (00:00 – 02:00, and 06:00). This pattern is expected as roads are typically more congested at peak hours and so vehicles brake more often.

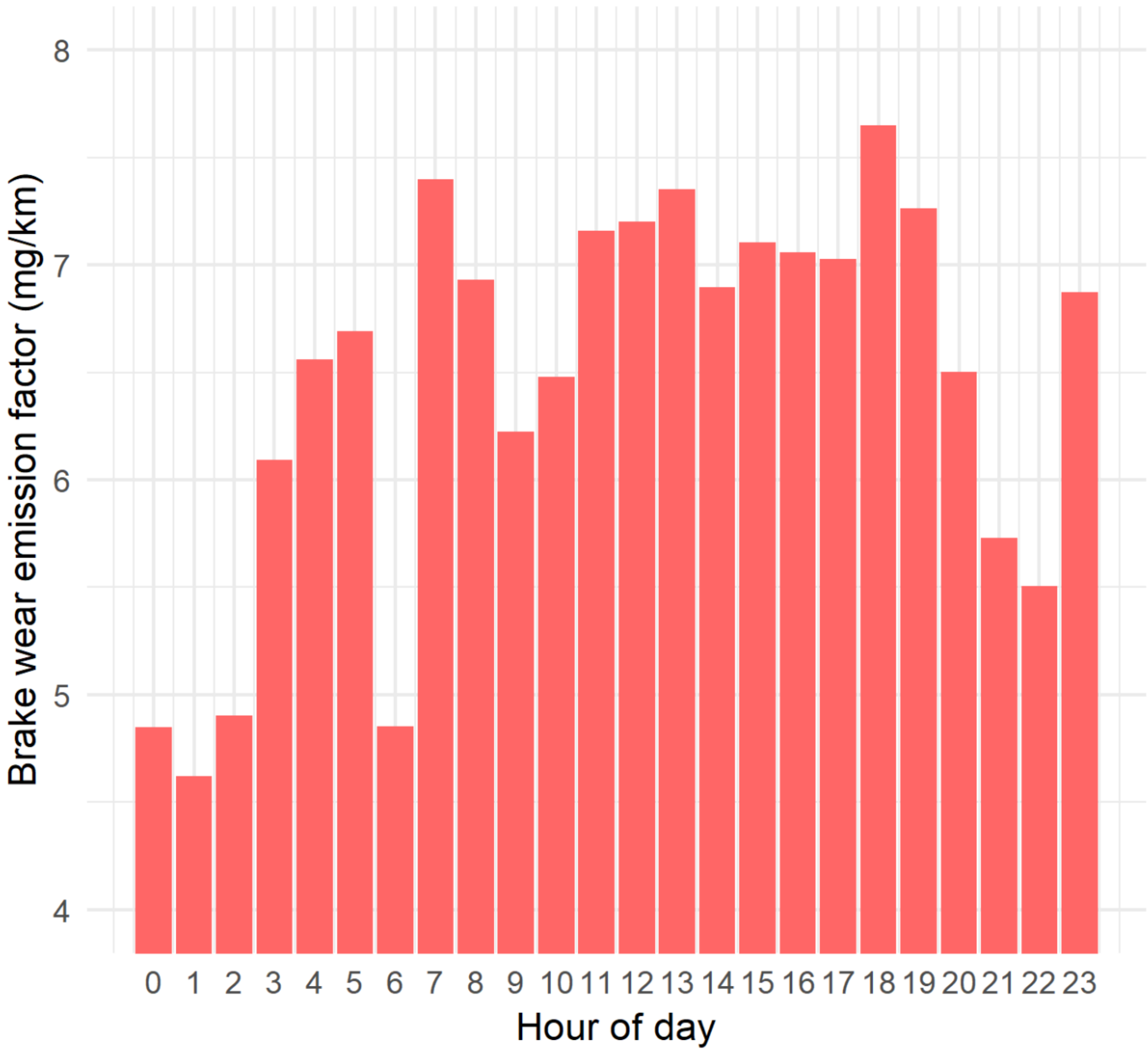


**Figure 9 Brake wear emission factor (mg/km) by hour of the day. Note, the y-axis starts at 4 mg/km.**

It may have been expected that there would be a stronger relationship between the hour of the day and the average brake wear emission factor, with emission factors significantly higher at busier times of the day when vehicles are expected to brake more. The average brake wear emission factors from 03:00 - 06:00 are similar however to the average brake wear emission factors at busier times of the day. To help explain the patterns seen, Figure 10 shows the relationships for other related variables by the hour of the day. These related variables are the average emissions from brakes in braking events (mg/s), the average vehicle speed (mph), the average speed limit (mph), and the proportion of observations where the brakes were applied.

As may be expected, the proportion of observations where the brakes were applied are largest during the typical peak hours between 07:00 – 19:00. The average brake wear emissions in braking events (mg/s) are significantly larger between 03:00 and 06:00, indicating that on average more energy is released per second when vehicles brake during these hours. Although the vehicles don’t brake as often between 03:00 and 06:00, when they do brake they release more energy and hence the average emission rates (Figure 9) are similar to those during peak hours.

Karl *et al.* (2017) give traffic counts for Innsbruck, Austria, a city they considered representative for Central Europe. These traffic counts are from July – October 2015. Figure 2 of Karl *et al.* (2017) shows the diurnal variation in traffic count data. This shows that the peak hours are from 07:00 – 19:00. The data in this project has been split into “peak” hours (07:00 – 18:59), and non-peak hours (19:00 – 06:59). The average brake wear emission rates are 7.0 mg/km and 6.2 mg/km for peak and non-peak hours respectively[6]. Although there are more braking events in peak hours (18% of observations, compared to 15% for non-peak hours), less energy is released per second when vehicles brake during peak hours. So overall, there is little difference in the average brake wear emission rates.

[6] The values of 7.0 mg/km and 6.2 mg/km are larger than the average passenger car emission factor of 6 mg/km as the Leeds data was corrected upwards slightly to use an average energy-based emission rate of 0.1 mg/kJ.

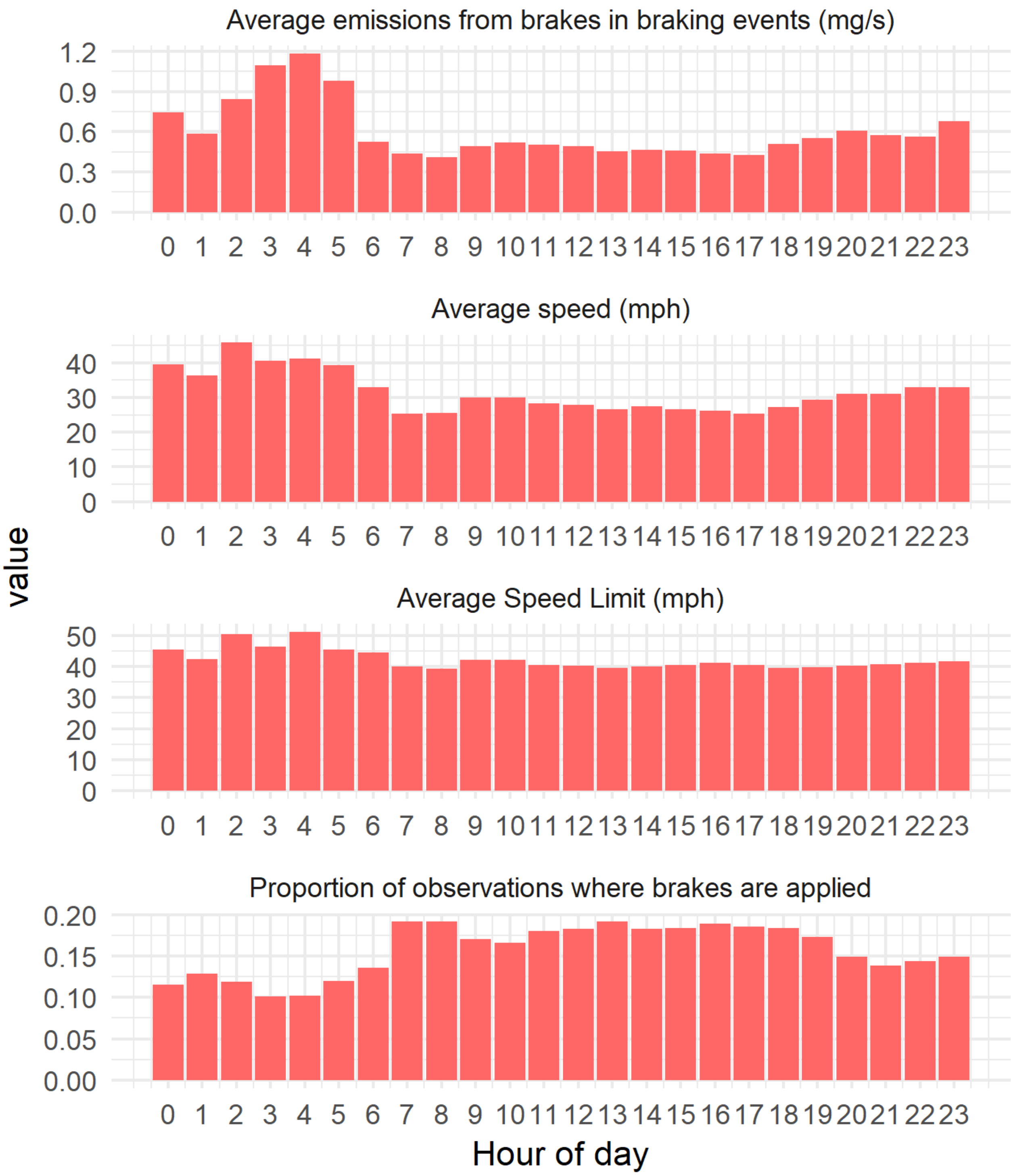


**Figure 10 Relationship for the average emissions from brakes in braking events (mg/s), the average vehicle speed (mph), the average speed limit (mph), and the proportion of observations where the brakes were applied as a function of the hour of the day.**

#### 3.2.3.2 Weekend / weekday

The Leeds dataset included a field giving the date of each observation. Therefore, the day of the week could be identified and consequently whether an observation was made on a weekday or on a weekend. The relationship between the estimated brake wear emissions and whether the observation was made on a weekday or weekend is discussed below.

The average brake wear emission factors calculated were 7.2 mg/km and 6.1 mg/km respectively for weekday and weekend. Given the extra congestion and lower average speeds on weekdays this may have been expected, although the difference may have been expected to be larger. The relationship and explanation for this is similar to that described for the difference between peak hours and non-peak hours in section 3.2.3.1. Although there are more braking events on weekdays (18% of observations, compared to 15% for weekends), less energy is released per second when vehicles brake during peak hours. So overall, there is little difference in the average brake wear emission rates.

### 3.2.4 Gradient

The gradient of the road is hypothesised to be a significant variable affecting brake wear emission rates, with emissions hypothesised to increase significantly as the road gradient becomes more negative. Road gradient has been calculated on all three vehicle measurements datasets used in this project based on altitude data available within the raw dataset or externally sourced. The relationship between the estimated brake wear emissions and the gradient of the road is discussed below.

For this analysis, the gradients were averaged over one minute of observations. For each observation, the change in altitude from the observation 30 seconds before to the observation 30 seconds after, combined with the distance travelled over that minute, was used to calculate the gradient averaged over one minute. If there were gaps in the data (i.e. there was not one minute of valid consecutive data for that observation), then that observation was excluded from the analysis. The data was averaged over one minute as there is less uncertainty when looking at the changes in altitude over longer timescales and distances (i.e. one minute instead of one second). By averaging over one minute, this helps identify longer hills and avoids the inclusion of changes in altitude in the data over one second that are large and likely unrealistic.

The calculated gradients were split into 1% groups (e.g. 0.08, 0.07, 0.06 etc.). Gradient groups with less than 1,500 observations were excluded to provide a more robust analysis, leaving gradients between -8% and +8% inclusive. The average brake wear emission factor was estimated as the sum of emissions (mg) divided by the distance travelled (km) within each gradient group.

Figure 11 shows the calculated average brake wear emission factor (mg/km) by the gradient group of the road. This shows, as hypothesised, a highly significant relationship between the road gradient and the average brake wear emission rate. At a -8% gradient the emission rate is >55 mg/km and at a +8% gradient the emission rate is <1 mg/km. Although only gradients between -8% and +8% inclusive were included, it is reasonable to extrapolate the trend found for more steep gradients not shown, although these are rare. The smoothed fit shown in Figure 11 is calculated using a loess curve fit.

The pattern in Figure 11 should be similar for vehicles of varying mass. The change in potential energy is a function of the mass as a first order variable, so as the mass changes, the change in potential energy changes linearly too. A linear relationship has also been used in the US EPA MOVES model (United States Environmental Protection Agency (2014)) for considering different HGV vehicle weight classes. The relationship may be proportionate rather than linear as this excludes other influencing factors such as the shape and aerodynamics of the vehicle, however a linear relationship is what the model outputs, and is a good approximation. Figure 12 shows the average brake wear emission factor (mg/km) by the gradient of the road (averaged over one minute of observations), also with the vehicle mass doubled in the model for comparison.

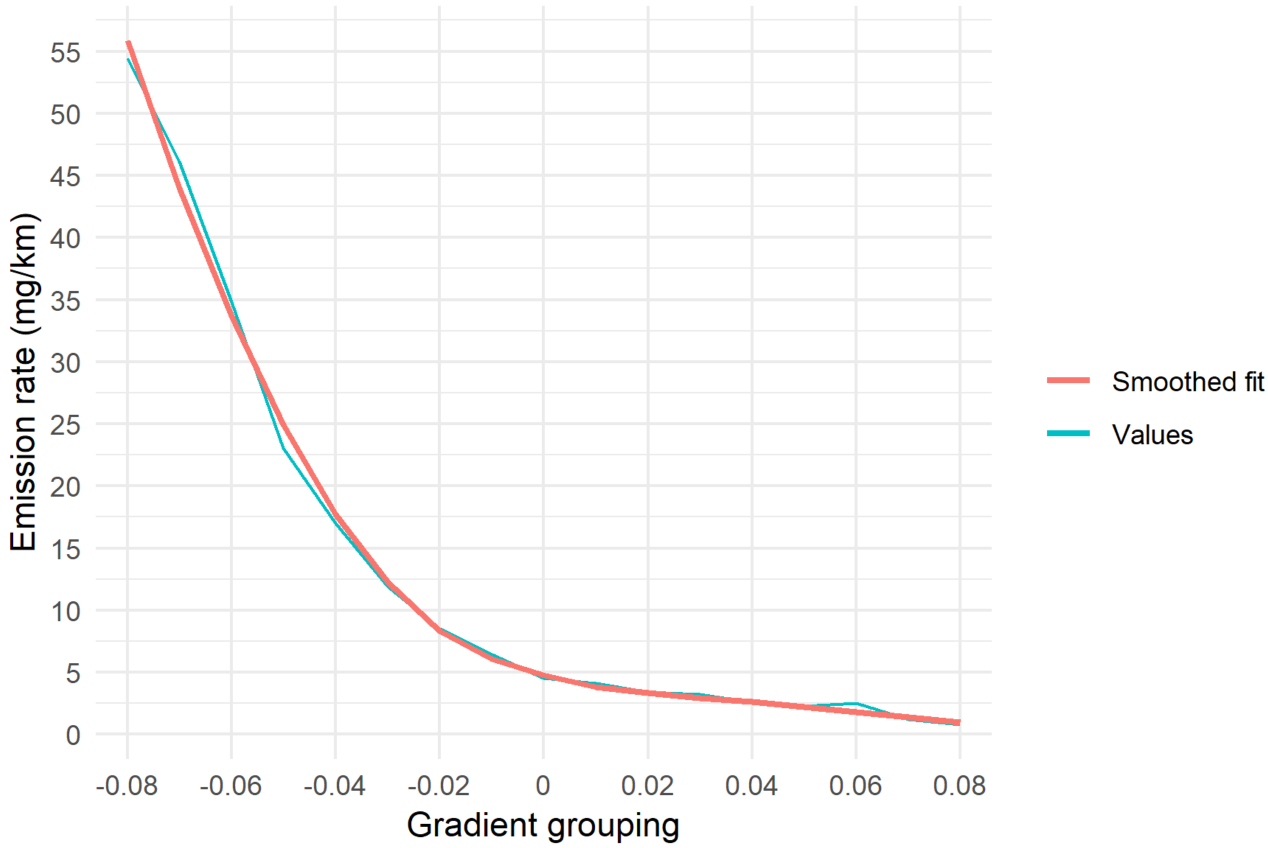


**Figure 11 Average brake wear emission factor (mg/km) by the gradient of the road (averaged over one minute of observations).**

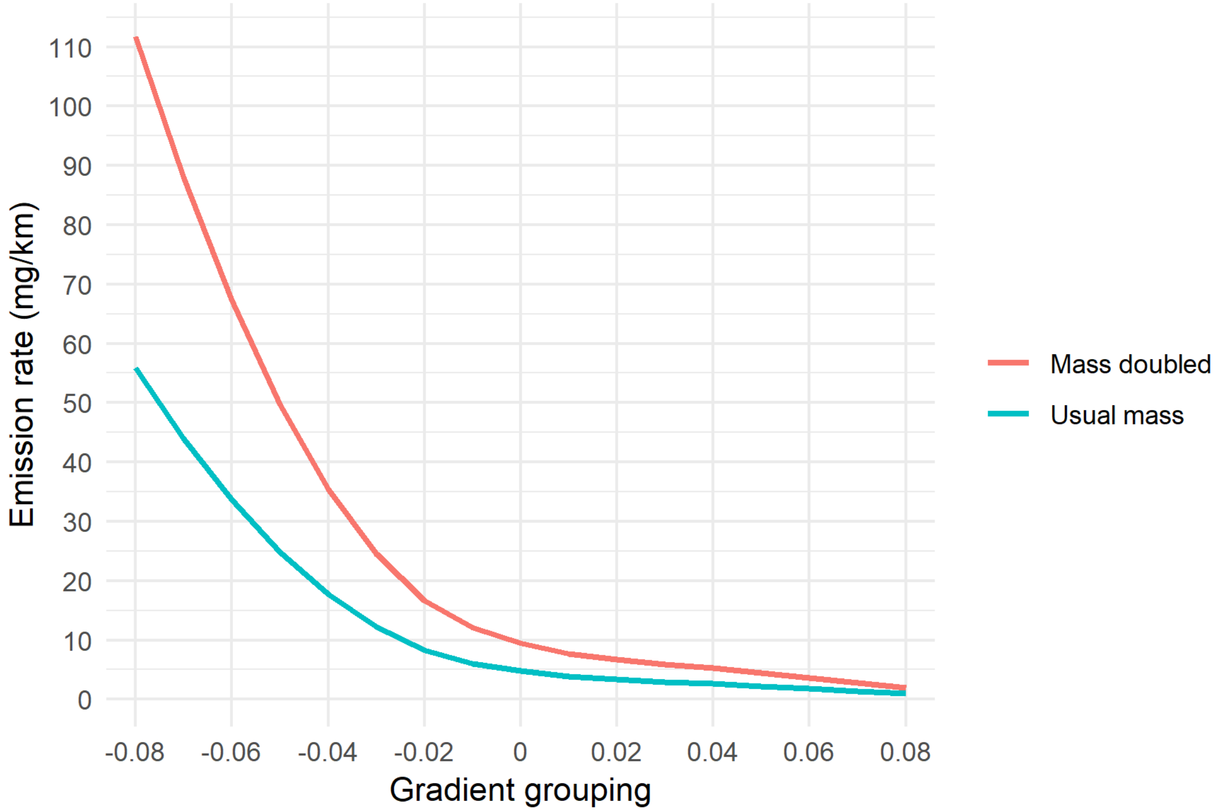


**Figure 12 Average brake wear emission factor (mg/km) by the gradient of the road (averaged over one minute of observations), also with the vehicle mass doubled in the model for comparison.**

# 4 Work Package 3 - Air quality modelling

In this section consideration is given to the impact of brake wear emissions on atmospheric concentrations of $PM_{10}$. Two principal approaches are used. First, a **conventional model** is developed that models brake wear emissions assuming that the emissions are constant along individual road links. This approach is typical of that used in general air quality modelling for other species such as $NO_x$. Second, a detailed, **spatially resolved model** is developed based on the predicted distribution of brake wear emissions, based on the energy lost to the brakes approach described earlier. In both models the total $PM_{10}$ from brake wear is set to be the same. In essence therefore, the detailed model considers the effects of spatially re-allocating the emissions based on actual vehicle activity.

The modelling domain is focused on the Leicester urban area in the UK (population about 440,000). Leicester was chosen for two principal reasons. First, there are considerable numbers of instrumented car trips based on the Leeds data on which to develop alternative emission factor and emissions inventory approaches. Second, there are four continuous air quality monitoring sites in the model domain that measure $PM_{10}$. These measurements provide a direct way in which to understand the extent to which brake wear PM contributes to absolute concentrations of $PM_{10}$ for real urban measurements. Moreover, the availability of these measurement sites also enables a detailed understanding of source apportionment to be developed.

While the availability of $PM_{10}$ measurement sites is of benefit to this study, it is not possible to use the data to validate the model in a direct way. This is because $PM_{10}$ from brake wear typically constitutes only a small proportion of the total concentration, which will almost certainly be smaller than the uncertainty of the measurements themselves. However, the conventional model used has been validated against a much wider range of measurements.

## 4.1 Modelling System

The RapidAir Urban Air Quality Modelling Platform was used to predict air pollutant concentrations for this project. This is Ricardo Energy & Environment's proprietary modelling system developed for small scale (road to urban scale) predictions of air pollutant concentrations.

RapidAir has been developed to provide graphic and numerical outputs which are comparable with other models used widely in the United Kingdom. The model approach is based on loose-coupling of three elements:

- Road traffic emissions model conducted using fleet specific COPERT 5 (via the Defra Emissions Factors Toolkit) algorithms to prepare g $km^{-1}$ $s^{-1}$ emission rates of air pollutants originating from traffic sources.
- Combination of dispersion kernels derived from the US EPA (United States Environmental Protection Agency) AERMOD[7] model with an emissions grid, at resolutions ranging from 1 m to 20 m. AERMOD provides the algorithms that govern

[7] https://www3.epa.gov/ttn/scram/dispersion_prefrec.htm#aermod

the dispersion of the emissions and is an accepted international model for road traffic air quality studies.

- The kernel-based RapidAir model running in GIS software to prepare dispersion fields of concentration for further analysis with a set of decision support tools coded in Python/arcpy.

RapidAir includes an automated meteorological processor based on the US EPA AERMET model which obtains and processes meteorological data of a format suitable for use in AERMOD. Surface meteorological data is obtained from the National Oceanic and Atmospheric Administration (NOAA) online repository[8] and upper air data is downloaded from the NOAA Radiosonde database[9].

The model produces high resolution concentration fields at the city scale (down to a 1 metre scale). A validation study has been conducted in London using the same datasets as the 2011 Defra air quality model inter-comparison study[10]. Using London Atmospheric Emissions Inventory 2008 data and the measurements for the same time period the model performance is consistent (and across some metrics performs better) than other modelling solutions currently in use in the UK. This validation study has been published in *Environmental Modelling and Software*, in partnership with the University of Strathclyde (Masey, Hamilton and Beverland (2018)).

### 4.1.1 Traffic activity data and representation of traffic sources

The traffic activity data used is that used for the UK Government's Pollution Climate Mapping model. The method used to obtain this data is detailed in section 3.2.2 of the UK Emission Mapping Methodology Report[11], and summarised below. This is the method used in the UK for compliance reporting to the Commission.

The base map of the UK road network derived from the Ordnance Survey Open Roads (previously Meridian 2). This gives locations of all roads (motorways, A-roads, B-roads and minor roads) in Great Britain. The traffic flow data are available on a census count point basis[12]. The calendar year considered was 2015.

An important component of the modelling was to represent the series of straight-line road links in a spatially accurate way, taking account of dual carriageways and other real road features. This step, while time consuming to develop, was required because of the need to represent the conventional model and spatially detailed model in the same way and to provide more realistic distributions of $PM_{10}$ concentrations.

The traffic flow data on major roads includes counts of each type of vehicle as an annual average daily flow, which were aggregated up to annual flows. The Annual Average Daily Flow (AADF) statistics take account of seasonal variation using 'expansion factors' applied

---

[8] ftp://ftp.ncdc.noaa.gov/pub/data/noaa

[9] https://www.esrl.noaa.gov/roabs/

[10] https://uk-air.defra.gov.uk/research/air-quality-modelling?view=intercomparison

[11] http://naei.beis.gov.uk/reports/reports?report_id=946

[12] http://www.dft.gov.uk/traffic-counts/

to the single day counts based on data from automatic counts for similar roads and vehicle types. Each traffic count point is allocated to a section of the major road network according to the road name and its proximity to the road i.e. each link has the nearest count point with the same road name assigned to it.

Traffic flow data are not available on a link by link basis for the majority of minor roads. But where these data are available they have been used to enhance the accuracy of the mapping. Minor road count points have been allocated to minor roads in a similar way to that described for major roads, but also using census point local parameters (Local Authority, Area type, distance). Traffic flows for the majority of minor roads have been modelled based on average regional flows and fleet mix (data from DfT) in a similar way to previous years. Regional average flows by vehicle type have been applied to each type of minor road – B and C roads or unclassified roads. These data were obtained from DfT as part of the mapping process for the UK Government's Pollution Climate Mapping model. As part of that process, each major road link was assigned an area type using the DfT definitions of urban area types. Vehicle speeds were assigned to different road types (built up and non-built up A-roads and motorways) within each area type. There are some minor roads where traffic activity data isn't available. These are rare and roads where traffic flow would be expected to be low. These are shown in Figure 13.

Air quality model runs have been undertaken for both calendar years 2015 and 2030 in this project to model the annual mean $PM_{10}$ concentrations. To scale the traffic activity data from 2015 to 2030, scaling rates were developed based on the difference between UK total vehicle kilometres travelled by vehicle, fuel, and road type. Background $PM_{10}$ values for 2015 were obtained from the 2015 reference year background maps available on the Local Air Quality Management website[13]. $PM_{10}$ contributions arising from road traffic sources were removed from the background map values to avoid double-counting.

### 4.1.2 Emission factors

Vehicle emission factors for particulate matter ($PM_{10}$) were obtained from COPERT v5 emission functions. Link specific emission factors were calculated with our in-house emission calculation tool RapidEms, which links directly to our RapidAir dispersion modelling system.

The input for RapidEms consists of a basic fleet split based on vehicle categories (diesel cars, petrol cars, LGVs, articulated HGVs, rigid HGVs, buses, and motorcycles) according to the traffic activity information specified in Section 4.1.1. RapidEms is used to provide a more detailed parameterization of vehicle fleets in 2015 and 2030, including all vehicles up to and including Euro 6/VI.

Later in this section, the modelling of the effect of using regenerative braking on all vehicles is considered. Regenerative braking involves the application of energy stored in the electric motor for decelerations. This method of braking does not involve the mechanical action of the friction between brake pads and discs, and so does not lead to particle generation from the brake materials. There is therefore significant potential for reduced brake wear particle emissions where regenerative braking can be used instead of friction braking. Regenerative braking has been introduced in hybrid and fully electric vehicles in recent years. The fraction

---

[13] Department for Environment, Food & Rural Affairs, Background maps, https://laqm.defra.gov.uk/review-and-assessment/tools/background-maps.html, accessed 20/06/2018.

of vehicles that use regenerative braking in Europe is forecast to increase significantly in the next ten years as more hybrid and fully electric vehicles enter the market.

The regenerative braking system is suitable for most braking events; however, it doesn't provide enough braking power for the highest power deceleration events. Therefore, vehicles with regenerative braking also still retain and use friction brakes, both as a back-up braking system, and as a braking system for the most extreme braking events.

The energy dissipation modelling approach developed in this project is well suited for analyses on the effect of regenerative braking on the reduction of brake wear particle emissions. Given, regenerative braking is only applied at braking events below an energy dissipation threshold, such events can be identified and treated as events that do not produce brake particle emissions. Therefore, only events above this threshold are considered to use friction brakes and therefore emit particles from brake wear. This is hypothesised to significantly impact the patterns of where and when brakes are used as well as the overall magnitude of emissions.

Dr Grochowicz (Ford Motor Company, 2018 EuroBrake Conference) investigated the deceleration threshold for which friction brakes aren't required, and it was found that decelerations up to 1.4 $m/s^2$ did not require friction brakes. Work was also done looking at the proportion of braking events on the Mojácar and WLTP test circuit/cycles that require friction brakes. It was found that 82% of braking events on the Mojácar test circuit could be made just using regenerative braking, whereas 98% of braking events could be made just using regenerative braking on the WLTP test cycle. They concluded that regenerative braking can reduce the usage of friction brakes in cities by more than 95% and anticipate lower brake emissions by a factor of 5 relative to conventional vehicles. The Mojácar test circuit is notably more demanding than the WLTP test cycle, with significantly more hills and intense acceleration and deceleration events. In this work, analyses have been done that show the comparability of the driving in the vehicle measurements data used in this work to the WLTP test cycle. Evidence from AUDI AG (2016) also found that almost all decelerations can be fully completed using regenerative braking (although it is not clear what the exact proportion is from the Figure presented there).

For this report, it has been assumed that 95% of braking events in the vehicle measurements datasets used in this project could be made just using regenerative braking (i.e. don't require friction brakes). This is a more conservative value than the 98% threshold value from Dr Grochowicz (Ford Motor Company, 2018 EuroBrake Conference). The analysis done in this work identified brake use energy dissipation rates for the top five percent of brake energy dissipation conditions (corresponding to conditions where the energy loss exceeded 11.5 kW). Below the $95^{th}$ percentile energy dissipation value, brake wear was assumed to be zero.

Table 4 summarises the emission factor approaches used for the model scenarios.

**Table 4 Emission factor approaches used for the model scenarios.**

| Model | Source of Emission Factors |
|---|---|
| Conventional | Vehicle emission factors for $PM_{10}$ were obtained from COPERT v5 emission functions (via the Defra Emissions Factors Toolkit). Link specific emission factors (g $km^{-1}$ $s^{-1}$) were calculated with our in-house emission calculation tool RapidEms, which links directly to our RapidAir dispersion modelling system.<br><br>The input for RapidEms consists of a basic fleet split based on vehicle categories (diesel cars, petrol cars, LGVs, articulated HGVs, rigid HGVs, and buses, and motorcycles) according to the traffic activity information |
| Spatially resolved | Academic literature review to find suitable passenger car mg/km emissions factor (6 mg $PM_{10}$/km). Based on 6 mg/km for car. Emissions apportioned according to energy estimated to the brakes in the 1 Hz vehicle datasets. Factors for other vehicle types are scaled according to the difference between passenger car emissions factors from the national German emissions inventory. |
| Regenerative braking | The same approach as the for the spatially resolved model, except that it is now assumed that 95% of braking events can be made just using the regenerative braking system. By ordering the braking events based on the energy intensity, emissions are assigned only to the top 5% most energy-intense braking events. |

### 4.1.3 Meteorological data

RapidAir includes an automated meteorological processor based on AERMET which obtains and processes meteorological data of a format suitable for use in AERMOD. Surface meteorological data was obtained from the NOAA online repository[14] and upper air data is downloaded from the NOAA Radiosonde database[15].

For this study, 2015 surface meteorological data was obtained from three stations located near Leicester (Coventry, Church Lawford and Nottingham East Midlands) and upper air meteorological data was obtained from two stations (Nottingham and Larkhill). RapidMet was used to carry out data filling where necessary according to the methodology provided by the US EPA in their “Meteorological Monitoring Guidance for Regulatory Modelling

[14] ftp://ftp.ncdc.noaa.gov/pub/data/noaa

[15] https://www.esrl.noaa.gov/roabs/

Applications" guidance document[16]. Data gaps from the primary meteorological stations (Coventry and Nottingham) are first filled using data from the other nearby stations (Church Lawford and Nottingham East for surface stations, and Larkhill for the upper air station). Remaining data gaps were filled based on the persistence method, where a missing value is replaced using data from the previous hour(s), for data gaps up to and including three hours.

The same meteorological dataset was used for both the 2015 and 2030 model scenarios, due to the availability of data and to ensure a consistent basis for comparison.

### 4.1.4 Model Uncertainties

There are several sources of model uncertainty inherent in this type of study, as discussed below:

- Uncertainties in the traffic model outputs on modelled road links, with regards to number of vehicles, type of vehicles and vehicle speed. The number of low emission vehicles in the future development scenarios may also be underestimated if the UK government is successful in ending the sale of all conventional diesel and petrol cars and vans by 2040, which could result in a systematic over-estimation of future air quality impacts.
- Uncertainties in the background concentrations used, including other sources of pollution, such as industrial sources, domestic heating, port activity and forest fires.
- Uncertainties in future projections of traffic activity, fleet composition etc.
- Uncertainties in the dispersion modelling process.

### 4.1.5 Choosing a Model Domain

A model domain has been selected as the focus for the air quality modelling undertaken. The factors considered when deciding upon the model domain were:

- how many vehicle measurement points were available (i.e. data from Work Package 1);
- availability of data on the vehicle flows along roads within the domain;
- whether there were areas of highly spatially variable braking;
- inclusion of urban areas, to consider urban air quality;
- availability of $PM_{10}$ measurement stations.

As discussed in section 2, most of the vehicle activity data was collected in the Leeds dataset, mainly collected in the Leeds and Leicester regions. Ricardo also have ready access to vehicle traffic flow data on major roads, and most minor roads within the UK but not in Germany. The Leeds and Leicester urban regions were the best candidates, and it was found that there were more particulate matter measurement stations in the Leicester region. As a result, the Leicester urban area was chosen as the model domain. This model domain is shown in Figure 13. A receptor height of 1.5 m was modelled to represent human exposure at ground level and is similar to the inlet height of the $PM_{10}$ measurement stations.

---

[16] United States Environmental Protection Agency, "Meteorological Monitoring Guidance for Regulatory Modelling Applications" available via https://www3.epa.gov/scram001/guidance/met/mmgrma.pdf, accessed June 2017.

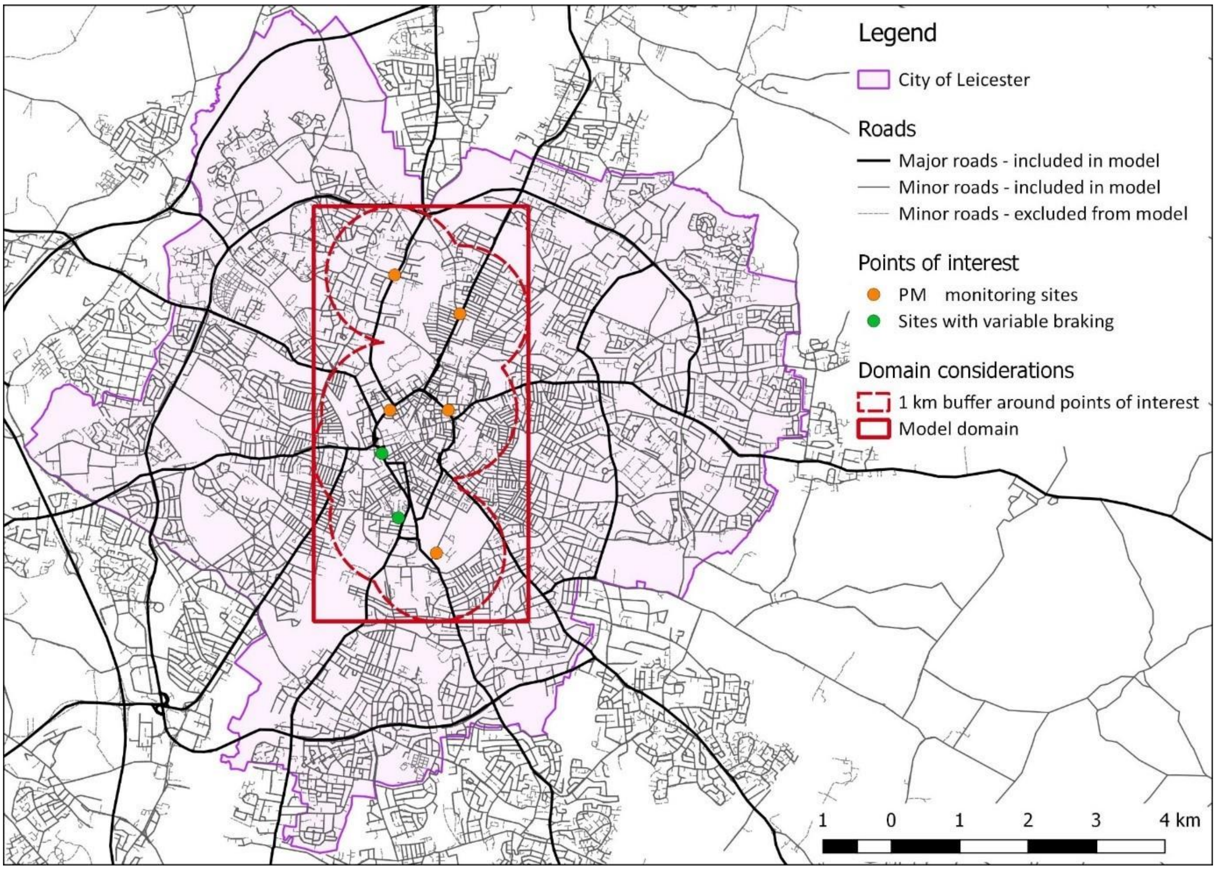


**Figure 13 The Leicester urban area, and the model domain (within the unbroken red rectangle).**

Of specific interest is the location of the four ambient measurement sites for $PM_{10}$, which are shown more clearly in Figure 14. These sites are located close to some of the major roads in the Leicester urban area and are classified as ‘traffic influenced’. In this respect, these sites are interesting locations at which to predict $PM_{10}$ concentrations and specifically the $PM_{10}$ from brake wear emissions.

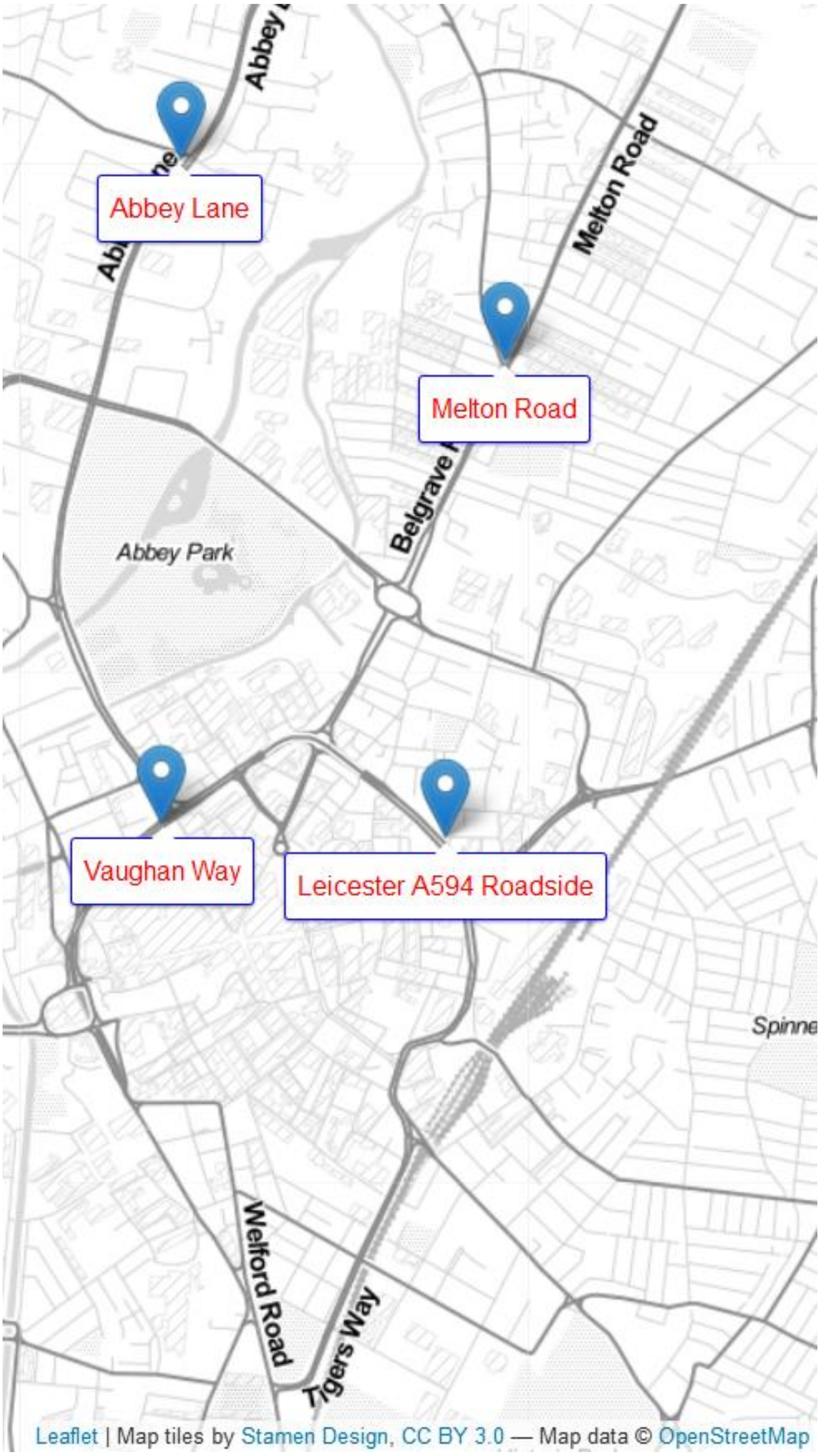


**Figure 14 Four $PM_{10}$ measurements stations within the model domain.**

## 4.2 Model runs

### 4.2.1 Conventional model

This section describes the ‘conventional’ approach to the allocation of emissions along road links is described in this section. The conventional model acts as a useful control and allows comparisons to be made with the more spatially detailed treatment of brake wear emissions, described later.

A smaller subset of the model domain is shown in the following Figures, which helps to show the detail of individual road links. This smaller subset still covers the main ring road, the central urban area, and as it is a smaller domain i.e. covers a wide range of driving conditions and road types. Figure 15 shows the predicted distribution of $PM_{10}$ across the model domain for 2015 and 2030 in the conventional model. As expected, the highest concentrations are restricted to the near-road environment. Concentrations in 2030 increase slightly due to the predicted increased in vehicle km by that time (emission factors for brake wear are assumed to be constant over the 2015 to 2030 period).

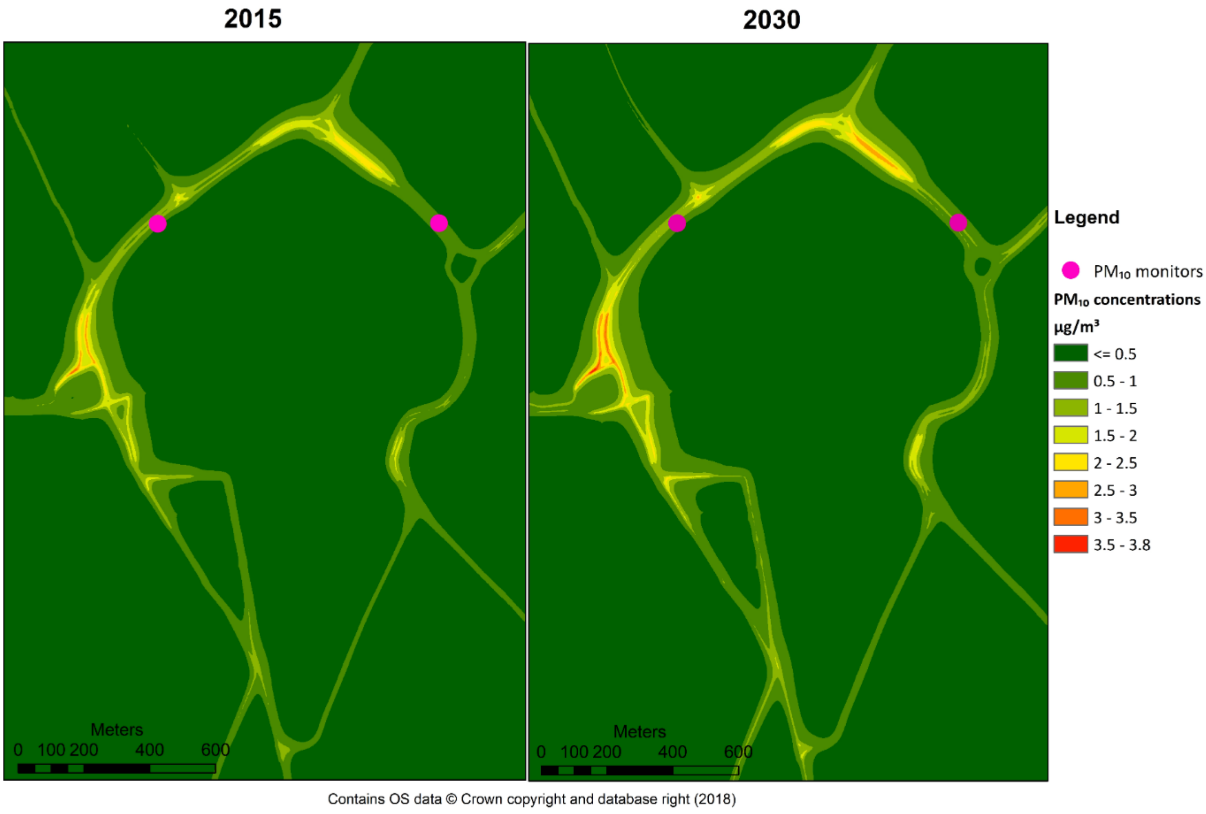


**Figure 15 Modelled brake wear contribution to annual mean $PM_{10}$ concentrations.**

Absolute concentrations of $PM_{10}$ are shown in Figure 16 which shows the dominance of background sources of $PM_{10}$ (which will be mostly regional sulphate and nitrate). The predictions do still reveal the importance of major roads in affecting absolute $PM_{10}$ concentrations. In this case, total $PM_{10}$ concentrations decrease due to reductions in background sources and the virtual elimination of exhaust $PM_{10}$.

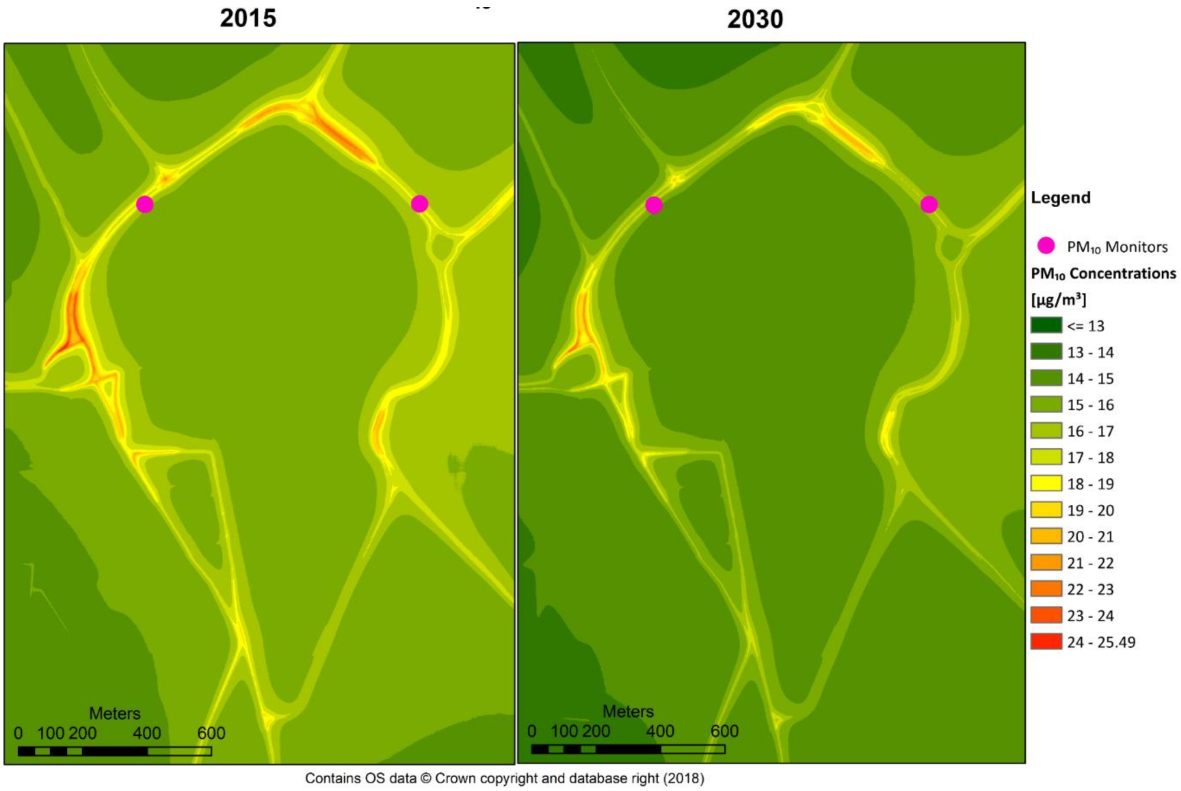


**Figure 16 Total modelled annual mean $PM_{10}$ concentrations.**

It is also useful to consider the contribution made by brake wear to total $PM_{10}$ concentrations, which is shown in Figure 17. On the roads themselves, the contribution can reach as high as 16% – but for locations where human exposure is more relevant and at air pollution monitoring sites, the brake wear contribution is much lower and typically less than a few percent.

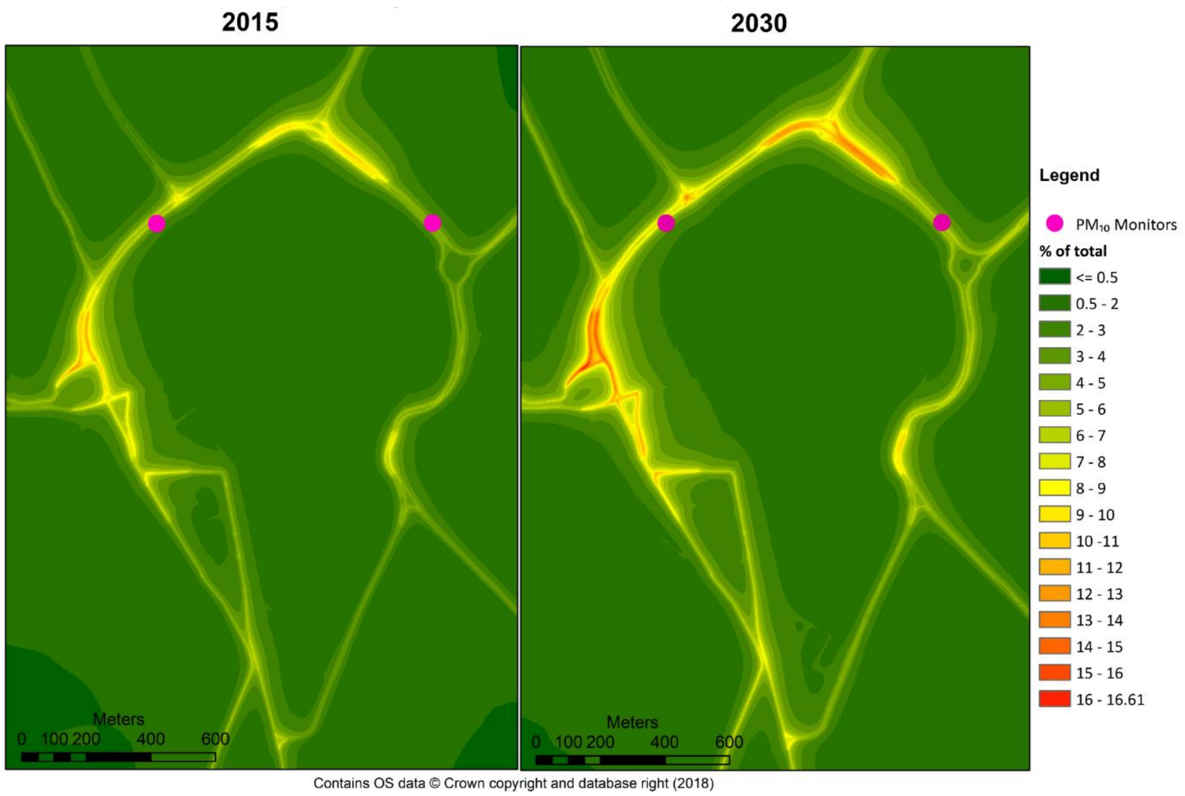


**Figure 17 Modelled brake wear contribution as a percentage of total annual mean $PM_{10}$ concentrations.**

The predictions of $PM_{10}$ at the four measurement sites is shown in Figure 18, which also shows the percentage of the total measured $PM_{10}$ that is predicted to derive from brake wear emissions. It can be seen in Figure 18 that the total modelled $PM_{10}$ (green bars) is lower than the measured $PM_{10}$ (red bars). The explicit modelling of all $PM_{10}$ sources is challenging and it is often the case that modelled concentrations are lower than observed values. There are several sources that are not modelled but which could make an important contribution to overall $PM_{10}$ concentrations in urban areas. These sources include cooking, $PM_{10}$ re-suspension, wood smoke, and ad-hoc activities such as construction. Nevertheless, the predictions show that brake wear makes a minor contribution to total measured or modelled $PM_{10}$ concentrations.

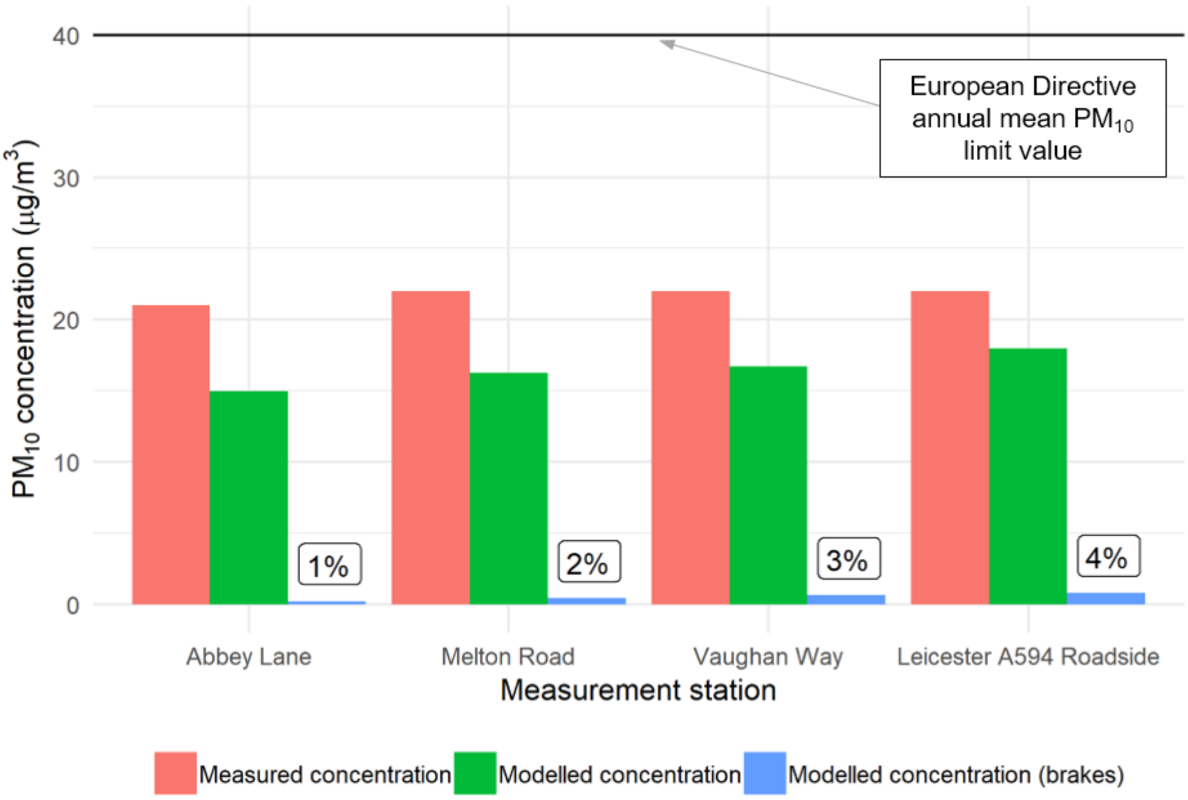


**Figure 18 Measured annual mean $PM_{10}$ concentrations, modelled contribution from brake wear, and total modelled annual mean $PM_{10}$ at four PM measurement stations within the model domain. The model version is the conventional model. The percentage values show the contribution of brakes as a percentage of the measured $PM_{10}$ concentrations. The measurement stations are ordered from left to right according to the % contribution from brake wear.**

### 4.2.2 Spatially-Resolved Model

This section discusses the results from the spatially resolved model i.e. the effect of redistributing the brake wear emissions according to the energy dissipated by brakes based on the detailed vehicle activity data. These predictions provide a comprehensive understanding of the implications of treating brake wear emissions in a more sophisticated way by attempting to allocate the emissions to where brakes are applied based on the energy lost to the braking system. Figure 19 shows a side by side comparison of the conventional model that assumes constant emissions along each road link and the detailed model that allocate the emissions based on energy dissipation. The detailed model shows a much more heterogeneous distribution of concentrations, dominated by some of the major road junctions. However, the main features highlighted in the conventional model (dominated by major roads) are carried through to the spatially resolved model. To a large extent the overall similarity between the two prediction surfaces for $PM_{10}$ reflects the identical traffic flows assumed along each road link in the two models.

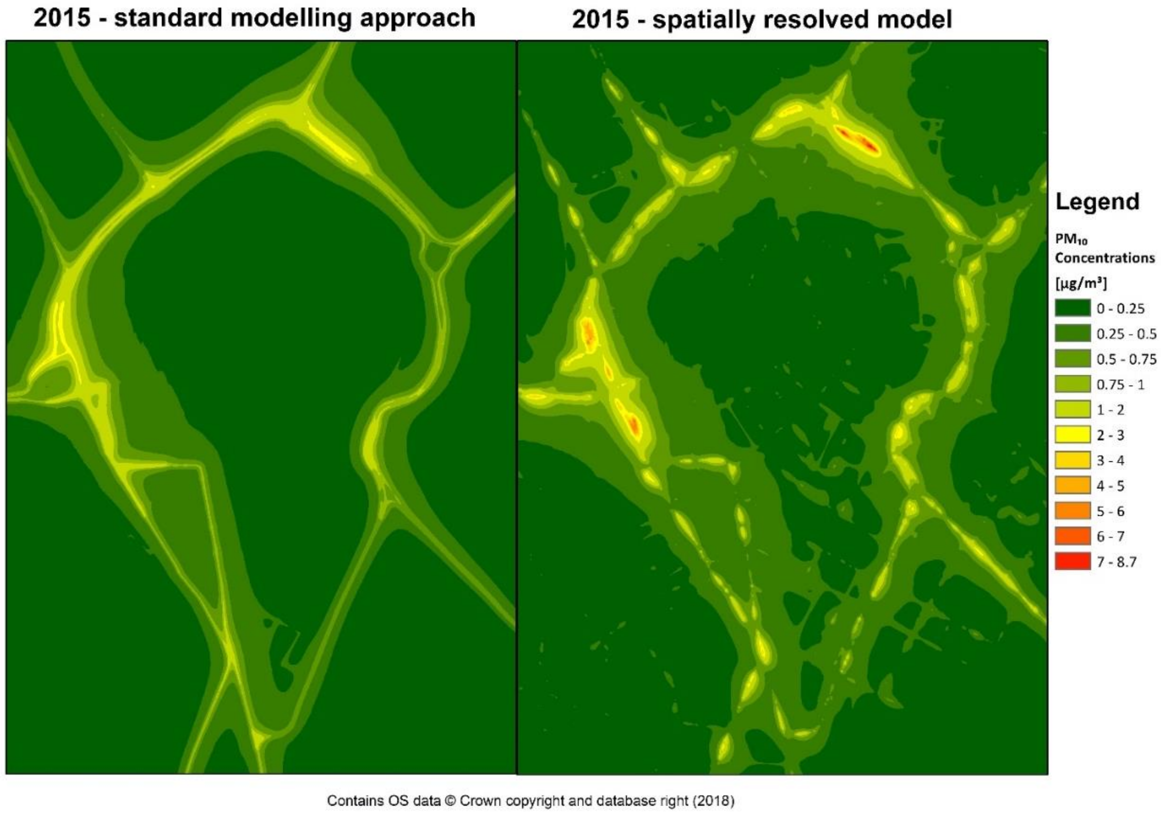


**Figure 19 Modelled annual mean brake wear contribution to $PM_{10}$ concentrations between the conventional model (left) and the spatially-resolved model (right).**

In terms of the contribution at the four measurement sites, Figure 20 shows that the contribution of brake wear emissions does not change by much compared with the conventional model results shown in Figure 18.

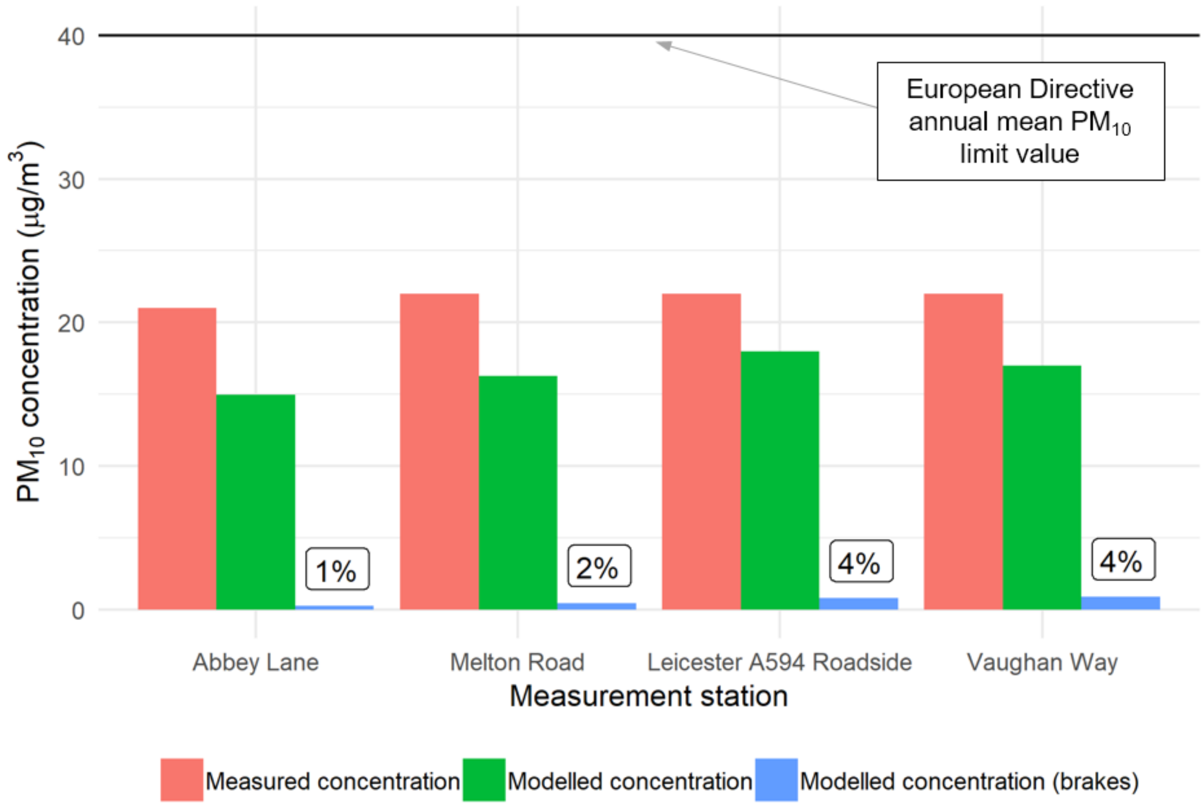


**Figure 20 Measured annual mean $PM_{10}$ concentrations, modelled contribution from brake wear, and total modelled annual mean $PM_{10}$ at four PM measurement stations within the model domain. The model version is the spatially resolved model. The percentage values show the contribution of brakes as a percentage of the measured $PM_{10}$ concentrations. The measurement stations are ordered from left to right according to the % contribution from brake wear.**

The application of the detailed model provides some interesting characteristics in the distribution of brake wear $PM_{10}$ along individual road links. A transect of brake wear concentrations is shown in Figure 21, which illustrates the extent to which emissions from brake wear vary along road links (in this case, from effectively zero emission to 200 mg/km). The location of this transect in Figure 21 is shown in Figure 22.

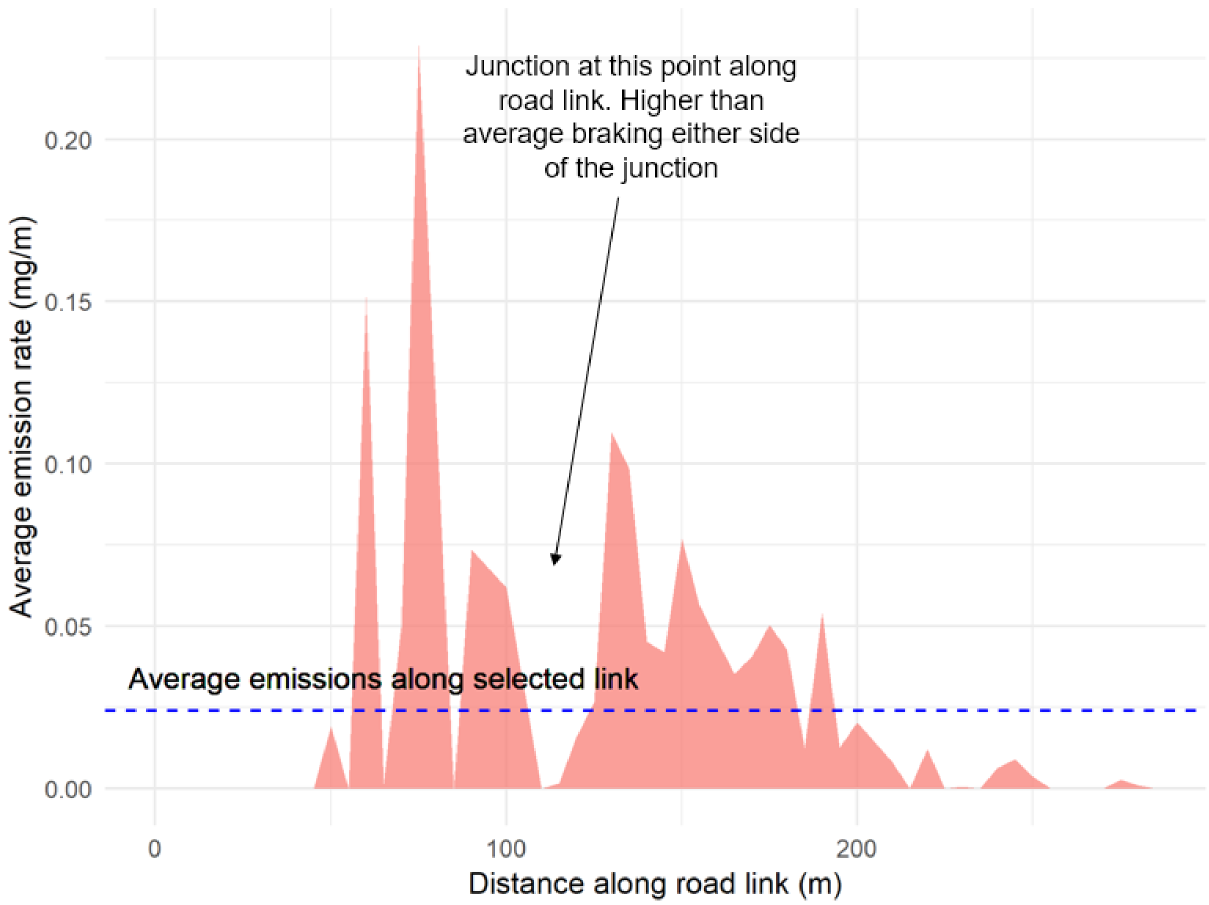


**Figure 21 Transect of brake wear emissions along a select road (Wellington Street, Leicester).**

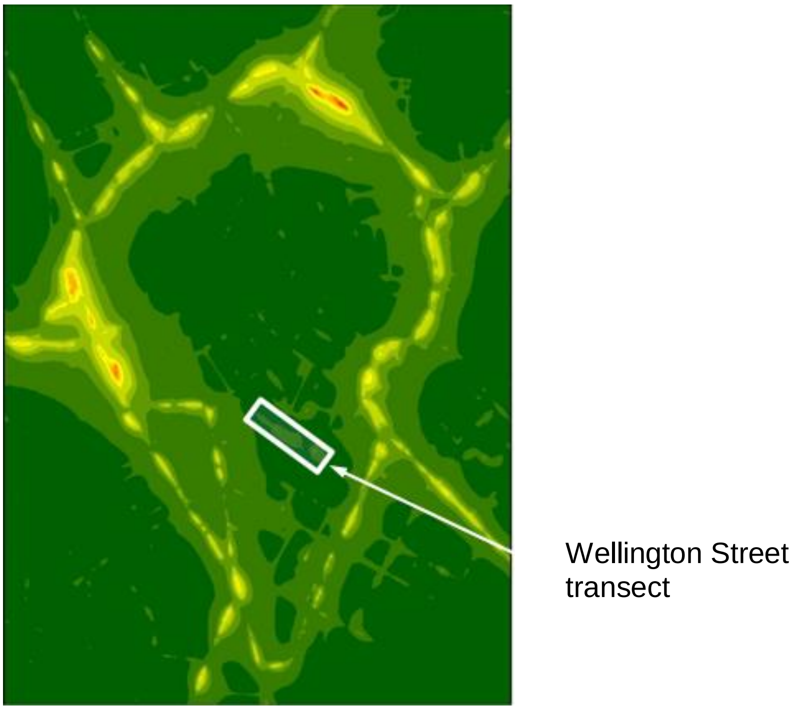


**Figure 22 Location of Wellington Street transect from Figure 21.**

## 4.3 Scenario modelling and sensitivity analyses

In this section consideration is given to a range of scenarios and sensitivity analyses to explore the extent to which brake wear concentrations of $PM_{10}$ vary. The focus of the analysis is the on the quantitative behaviour at a range of receptor locations where source apportionment analysis can also be carried out. The specific scenarios and sensitivity analyses used in this study are summarised in Table 5, which include the effects of halving and doubling brake wear emissions, increased HDV contribution and a consideration of the potential effects of regenerative braking (outlined in section 4.1.2).

**Table 5 Model scenarios and sensitivity tests conducted.**

| Scenario number | Scenario name | Scenario description |
|---|---|---|
| 1 | Conventional model | Using existing assumptions as a control scenario |
| 2 | Spatially-resolved model | Using the newly developed highly spatially-resolved emission rates |
| 3 | Sensitivity analysis (1) | Scenario 2, with the base emission factor doubled to 12 mg/km. |
| 4 | Sensitivity analysis (2) | Scenario 2, with the base emission factor halved to 3 mg/km. |
| 5 | Sensitivity analysis (3) | Scenario 2, with 3 times HDV fleet, and the proportions of all other vehicle types reduced proportionately so that the total traffic flow remains the same |
| 6 | Regenerative braking model | Using highly spatially-resolved emission rates developed for vehicles with regenerative braking |

The predictions from the model were considered at a range of receptor locations shown in Figure 23, and summarised in Table 6. These locations cover the four existing $PM_{10}$ measurement sites, and a series of 'sensitive' receptors including a hospital, two schools and three student accommodation locations. Additionally, a 'high' brake wear location has been considered, which is the location of the highest brake wear contribution to $PM_{10}$ concentrations. The latter location is in fact located at the middle of a complex junction and is not relevant from a human exposure perspective but is still interesting from the perspective of understanding the maximum predicted concentration of $PM_{10}$ across the model domain.

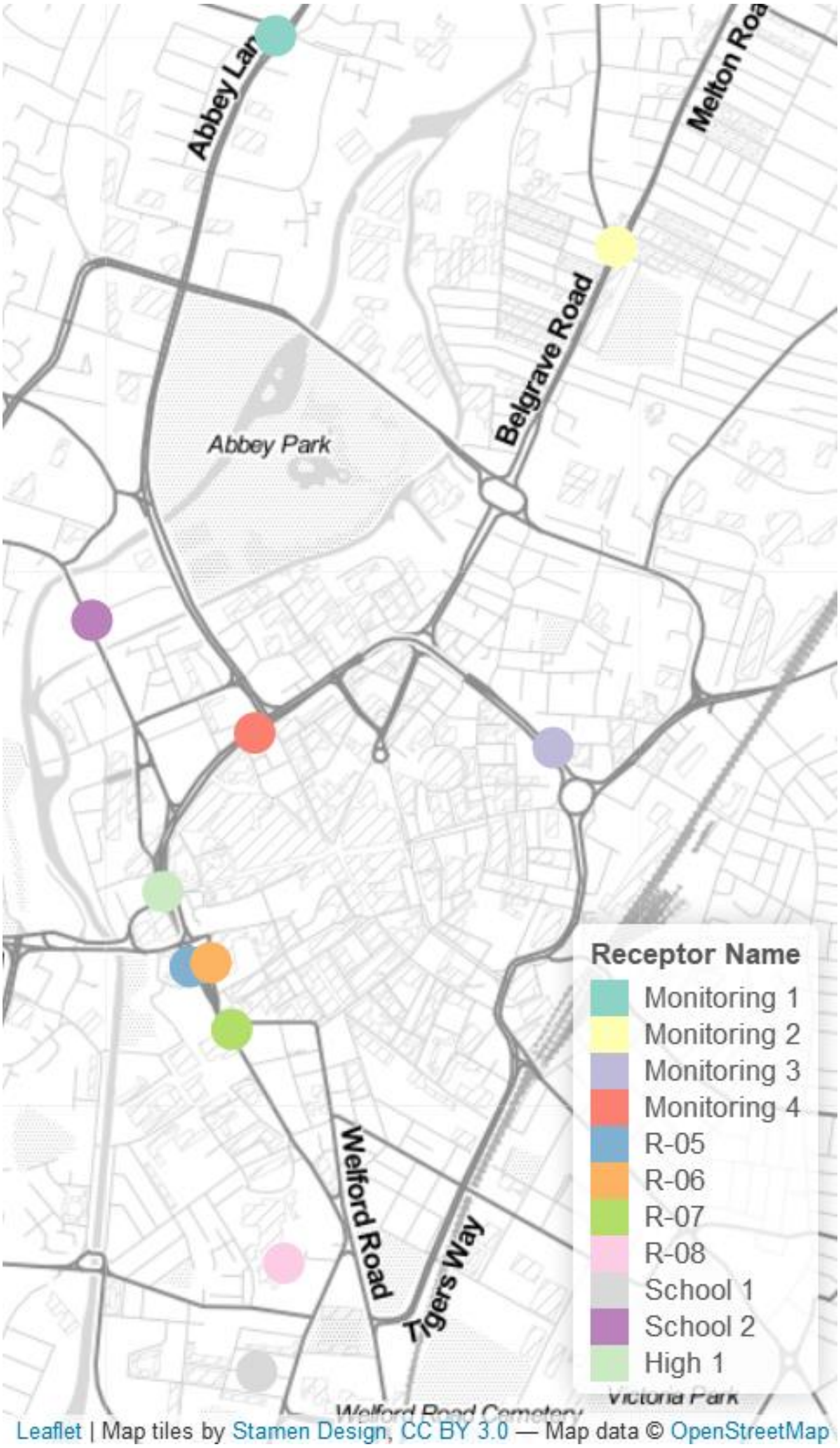


**Figure 23 Receptors chosen for the detailed prediction of concentrations.**

**Table 6 Summary of receptor locations used for detailed source apportionment and sensitivity analysis.**

| Receptor name | Site id |
|---|---|
| Abbey Lane measurement station | Monitoring 1 |
| Melton Road measurement station | Monitoring 2 |
| Leicester A594 Roadside measurement station | Monitoring 3 |
| Vaughan Way measurement station | Monitoring 4 |
| Victoria Hall Leicester - Student Accommodation | R-05 |
| Lumis Student Living - Student Accommodation | R-06 |
| Host The Glassworks - Student Accommodation | R-07 |
| Leicester Royal Infirmary | R-08 |
| Hazel Community Primary School | School 1 |
| Slater Primary School | School 2 |
| A47-A594 Junction | High 1 |
| Average across model domain | Average Domain |

The concentrations of $PM_{10}$ have been split by main source type including background, brake wear, exhaust, and other non-exhaust PM. In this context ‘background’ can be thought of as the $PM_{10}$ that is not explicitly accounted for by the detailed modelling of the road traffic contribution (exhaust and non-exhaust).

A summary of the results of the detailed modelling is shown in Figure 24 for specific receptor locations. The model result values are also presented in a tabular format in Appendix A.7. The $PM_{10}$ concentrations have been apportioned into four major categories; background, exhaust, other_non_exh, brake_wear. ‘background’ is the background $PM_{10}$ from all other sources except the local road sources, ‘exhaust’ is the contribution from road vehicle exhausts, ‘brake_wear’ is the contribution from road vehicle brake wear, and ‘other_non_exh’ is the contribution from other non-exhaust road sources (tyre wear and road abrasion).

In all cases the dominant contribution to absolute $PM_{10}$ concentrations is from background sources (which would be dominated by sources outside Leicester and indeed the UK). At the $PM_{10}$ measurement sites, the brake wear contribution is up to 1 µg $m^{-3}$ of the total $PM_{10}$. However, across the model domain, the brake wear contribution can exceed this in some locations with high intensity braking[17]. An important result from Figure 24 is how spatially variable the brake wear contribution can be, relative to the conventional model. In the spatially resolved model the brake wear emissions are concentrated into a few locations of high intensity braking. This means that in most locations the brake wear contribution is lower in the spatially resolved model, however there are few locations of high intensity braking where the brake wear contribution is predicted to be significantly higher. Understanding local behaviour to understand where these locations are is key to informing urban exposure. Figure 19 suggests that this tends to be at the junctions of busy roads.

[17] The highest concentration predicted is 5.7 µg $m^{-3}$ in the middle of a busy junction on the road itself. However, this location is not relevant from an exposure perspective.

The regenerative braking scenario shows that at all but the highest concentration receptor point, the brake wear contribution to $PM_{10}$ concentrations is reduced to significantly. In fact, the use of regenerative brakes on all vehicles leaves a few locations (‘islands’) where brake wear emissions are considerable. This scenario is of course an extreme case, but it shows how the distribution of brake wear emissions might change in future as more vehicles enter the fleet with regenerative brakes. An interesting aspect of the regenerative brake scenario is that it has the effect of removing brake wear emissions from areas that could be considered urban i.e. where personal exposure is of importance, while leaving only a few small areas of emissions where the hardest braking conditions occur. This is because most urban locations are not associated with the highest braking energies. This behaviour of the regenerative braking scenario could therefore be of importance for exposure to particulate matter in urban populations.

The ‘3x HGV’ scenario has higher overall $PM_{10}$ concentrations than the spatially resolved model using the unadjusted vehicle fleet. This is due to increased road vehicle emissions; however, the effect is quite minor. This is largely as the proportion of HGVs in the traffic fleet is typically very small anyway (around 1-2% within the model domain), so multiplying this by 3 has little effect on the overall $PM_{10}$ concentrations. Even with such typically small proportions of HGVs, the difference between the ‘spatially resolved’ and ‘3x HGV’ scenarios is noticeable as HGVs have much higher non-exhaust vehicle emissions than the most common vehicle type in the model domain, passenger cars.

The “Average Domain” receptor shows the source apportionment averaged across the whole model domain. This shows that in all scenarios, local vehicle sources contribute little to the total $PM_{10}$ concentrations. Looking at the values for the contribution of the different vehicle sources in the “conventional” and “spatially resolved” scenarios more closely shows that “other_non_exh” contributes the most, “exhaust” the least, and “brake_wear” in the middle of these values.

The main focus of the work was to reapportion brake wear emissions according to data on the location and intensity of vehicle braking. In most locations the brake wear contribution is lower in the spatially resolved model relative to the conventional model, however there are few locations of high intensity braking where the brake wear contribution is predicted to be significantly higher. The contribution of brake wear to ambient $PM_{10}$ concentrations at the “High 1” site was over 3 times higher (3.9 $\mu g\ m^{-3}$ difference) using the more refined spatially resolved emissions inputs.

The approach used (analysing the high frequency energy changes from vehicle measurements data) lends itself to a more sophisticated approach to understanding the contribution of brake wear to ambient $PM_{10}$ concentrations in future. The energy-based approach is well-suited for considering a range of scenarios, for example the effect of regenerative braking as has been covered within this project.

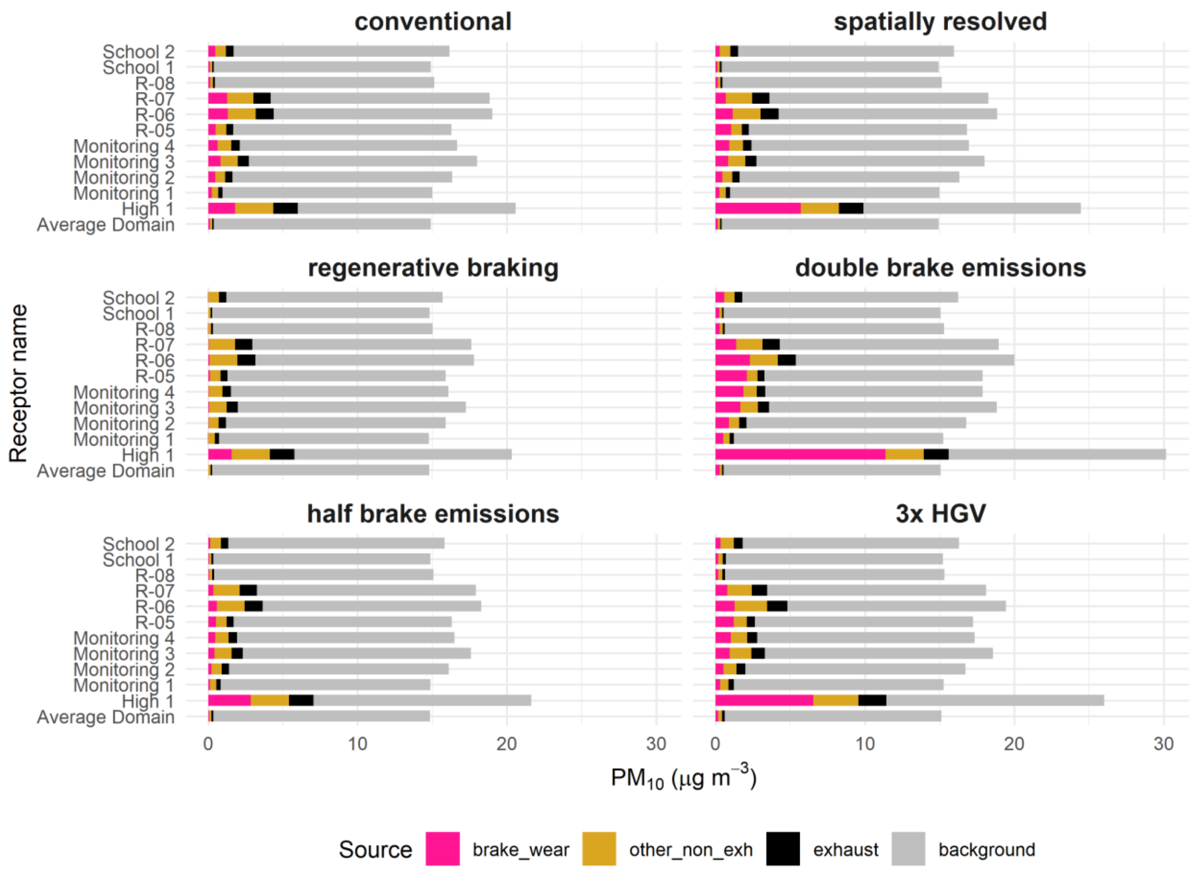


**Figure 24 Results from the detailed modelling of brake wear emissions at specific receptor locations. The annual mean $PM_{10}$ concentrations have been apportioned into four major source categories.**

Figure 25 provides an alternative way of representing the results of the scenarios and sensitivity tests. In this plot, the contribution of each source origin is represented as a fraction of the total.

The results show that the contribution of non-exhaust emissions (‘other_non_exh’ and ‘brake_wear’) exceed that from ‘exhaust’. National emission inventories from the UK and Germany show that this is also the case, with an approximate 60:40 split between non-exhaust and exhaust emissions (FAT (2017)). This split is exaggerated however in Figure 25**.** This is because the model domain chosen is restricted to an urban area. In urban areas it is known that brake wear emission factors are much larger than on motorways as vehicles brake more in urban areas. Also, it may be expected that most of the diesel cars in the urban area would be fitted with diesel particulate filters, vastly reducing particulate emissions from the exhaust.

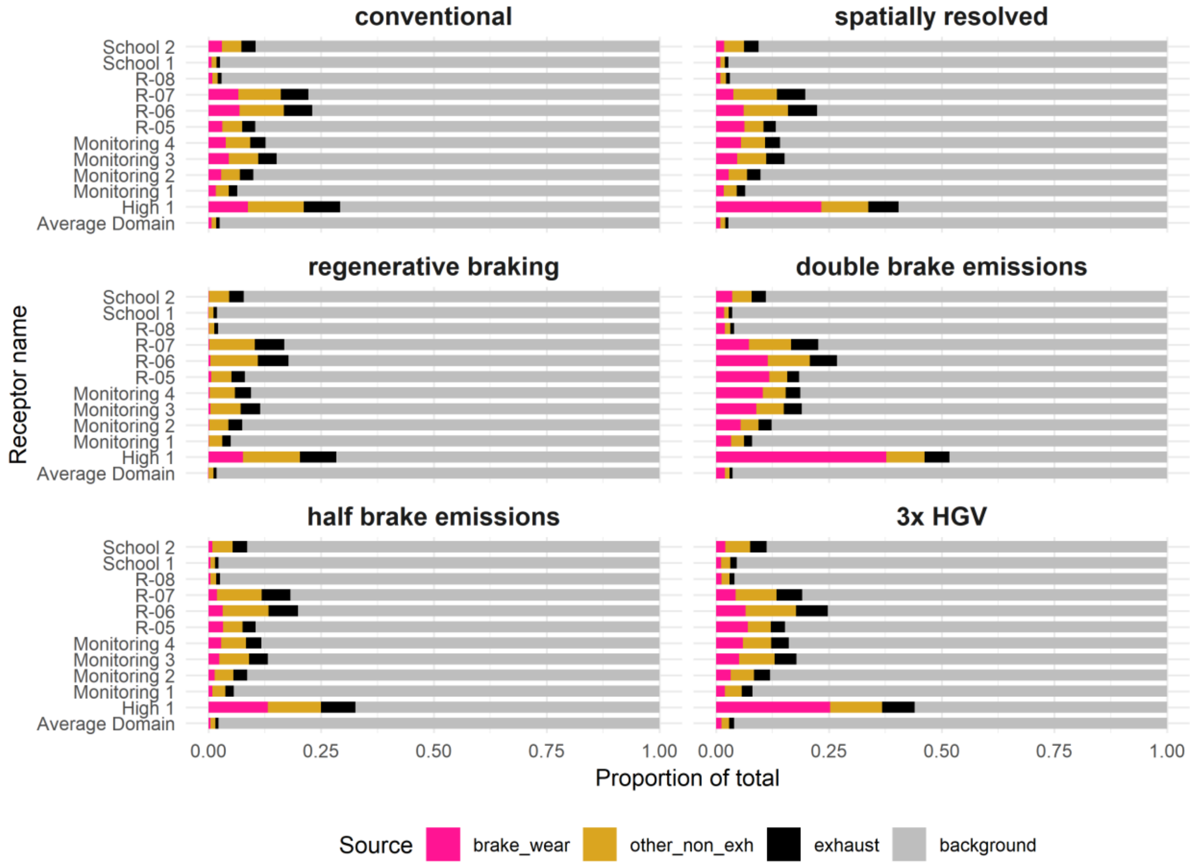


**Figure 25 Results from the detailed modelling of brake wear emissions at specific receptor locations. The concentrations have been apportioned into four major categories to show the relative contribution to the total annual mean $PM_{10}$ concentration at each receptor.**

Figure 26 shows the cumulative distribution of the contribution of brake wear to $PM_{10}$ concentrations across the model domain from the spatially resolved model. Each metre-squared grid in the model domain is represented as a point in the chart. This shows that 99% of values are below 1 µg $m^{-3}$, as most locations in the model domain are away from roads. The refinement in the spatially resolved model only significantly alters locations close to the roads.

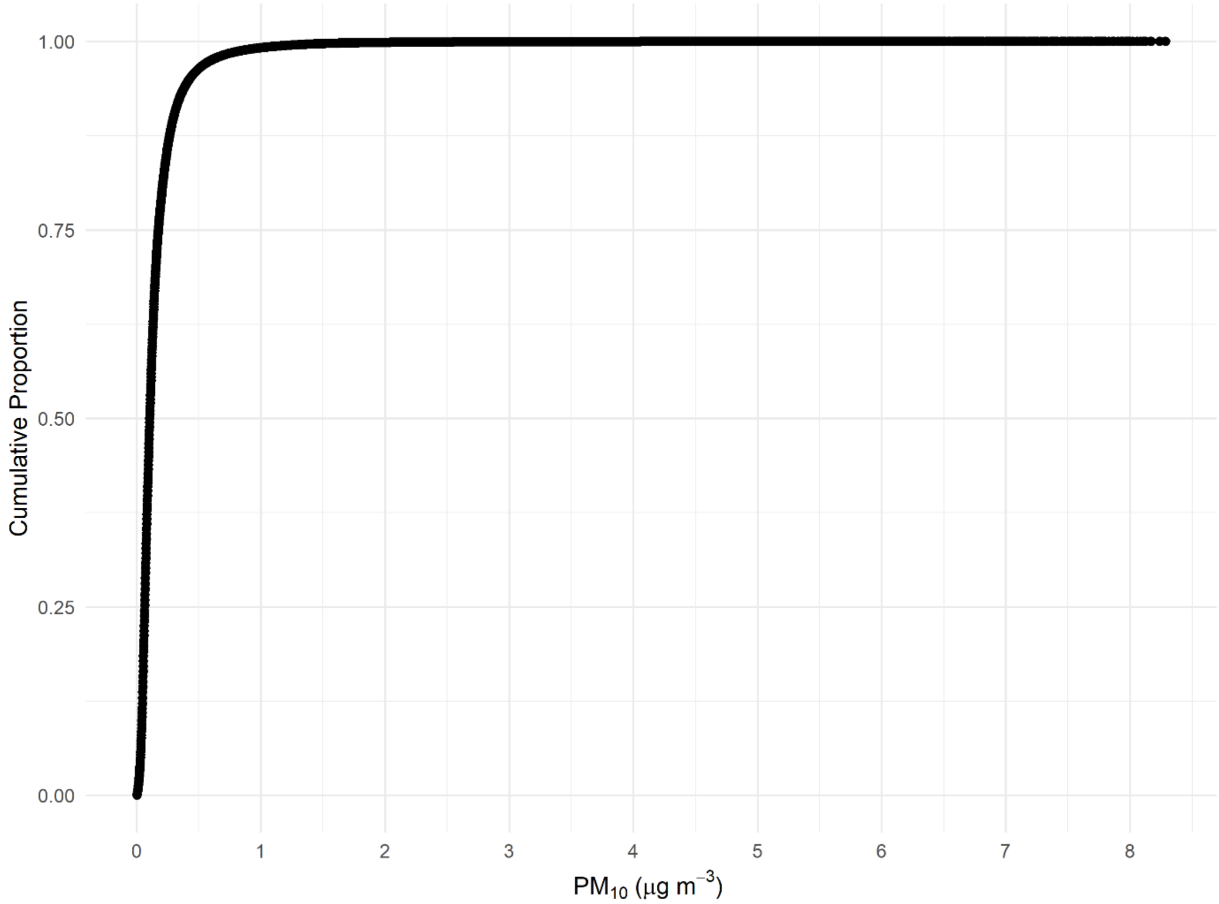


**Figure 26 Cumulative distribution of the contribution of brake wear to annual mean $PM_{10}$ concentrations across the model domain from the spatially resolved model.**

### 4.3.1 Expected $PM_{2.5}$ concentrations

The modelling undertaken has been on $PM_{10}$ concentrations. Although $PM_{2.5}$ wasn't modelled, it is possible to discuss how the results may be similar or different to $PM_{10}$. Table 7 shows $PM_{2.5}$:$PM_{10}$ emissions ratio values by emissions source. It is reasonable to assume that these emissions ratio values would be reflected in the source apportionment of $PM_{2.5}$ concentrations relative to $PM_{10}$. Table 7 shows that brake wear has the highest proportion of $PM_{10}$ in the $PM_{2.5}$-$PM_{10}$ fraction of $PM_{10}$.

**Table 7 $PM_{2.5}$:$PM_{10}$ emissions ratio values by emissions source.**

| Emissions Source | $PM_{2.5}$:$PM_{10}$ | Value Source |
|---|---|---|
| Exhaust | 1 | German national emissions inventory (Hausmann *et al.* (2018)) |
| Brake wear | 0.4 | German national emissions inventory (Hausmann *et al.* (2018)) |
| Tyre wear | 0.7 | German national emissions inventory (Hausmann *et al.* (2018)) |
| Road abrasion | 0.54 | German national emissions inventory (Hausmann *et al.* (2018)) |
| Background | 0.69 | Analysis of UK government background air quality maps[18] |

[18] Department for Environment, Food & Rural Affairs, Background maps, https://laqm.defra.gov.uk/review-and-assessment/tools/background-maps.html, accessed 04/03/2019.

### 4.3.2 Temporal Distribution

The RapidAir model doesn't produce hourly-averaged concentrations (as of writing), however there are other datasets that can help inform how concentrations may vary over time. The temporal traffic distribution is a major determinant of how the contribution of vehicle sources to concentrations are temporally distributed. The temporal traffic distribution used in the model is based on UK government statistics on the traffic distribution in Great Britain[19] and is shown in Figure 27 below.

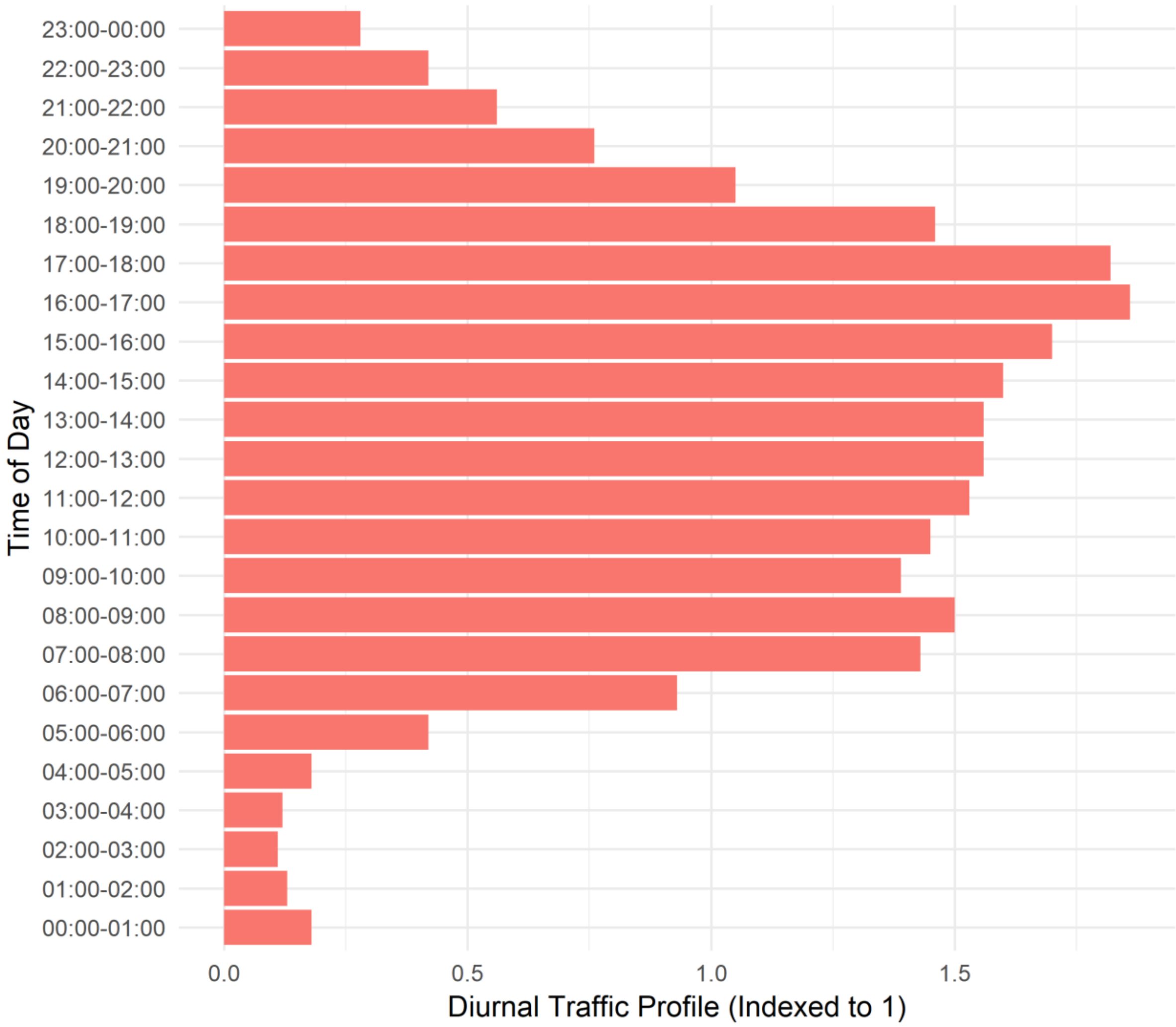


**Figure 27 Diurnal Traffic Profile (Indexed to 1) by Time of Day, based on UK government statistics**

Related to this, the relationship between brake wear emissions and hour of the day based on the vehicle measurements data used in this project has also been analysed (section 3.2.3.1).

[19] Dataset TRA0307: Available here: https://www.gov.uk/government/statistical-data-sets/road-traffic-statistics-tra [Accessed on 05 June 2019]

# 5 Applicability of results to other European locations – including Germany

The air quality modelling has been conducted in a domain within the UK, as there was much more UK vehicle measurement data available to use, and UK traffic data available to use for the model (section 4.1.5). There are several ways in which the results of this work are or could be applied to other European locations including Germany however. These are presented in the numbered bullet points below.

Overall, the work has focussed on challenging conventional approaches to modelling the contribution of brake wear to ambient PM concentrations using a data-driven, universal approach. Given enough German vehicle measurements data and traffic data the approach used is universal enough to be applied in a German or other European context.

1. **Generalised brake wear emission factors by dataset variables**. Section 3.2 presents results of the analyses of brake wear emissions by dataset variables such as speed limit of the road and road gradient. Although the air quality modelling was conducted within a UK domain, these analyses allow more general conclusions to be drawn out. The patterns are also drawn out from analysis of the vehicle measurements data from both the UK and Germany.

2. **Brake wear emissions by road type from OpenStreetMap**. This analysis, presented in section 3.2.2, provides analyses of the effect of road type from OpenStreetMap on averaged brake wear emission rates. The analysis was split between the Leeds (UK) and euroFOT (Germany) vehicle measurements datasets to consider comparability between the two datasets. The main patterns are broadly similar, for example with average brake wear emission factors orders of magnitude larger on “link”-equivalent roads (e.g. larger for “motorway_link” than “motorway”). This pattern is as expected as vehicles will tend to brake much more often on link type roads. Also, the average emission factors are lower on the “motorway” and “trunk” roads which are highest class roads that typically have the highest speed limits. There is not always strong agreement between the two datasets however. As mentioned in section 3.2.2, there are differences in the road classifications between countries, and as the two measurements datasets were collected using different instruments and on different vehicles, this adds extra reason for potential discrepancies. Also, driver behaviour is another key influencing variable, and the euroFOT data is based on measurements from one driver, whereas the Leeds dataset is collected from 79 drivers.

3. **Highly spatially resolved brake wear emissions inventory for Germany**. Section 3.1 describes how the spatially resolved brake emission inventory was developed as an input for the air quality modelling conducted in section 4. A highly spatially resolved brake wear emissions inventory has been developed based on the German euroFOT data. Figure 28 shows an extract of the highly spatially resolved brake emissions inventory developed based on the euroFOT data. The patterns are similar to that seen for the highly spatially resolved brake wear emissions inventory developed based on the analysis of UK vehicle measurements data, with the highest brake wear emissions concentrated before road junctions.

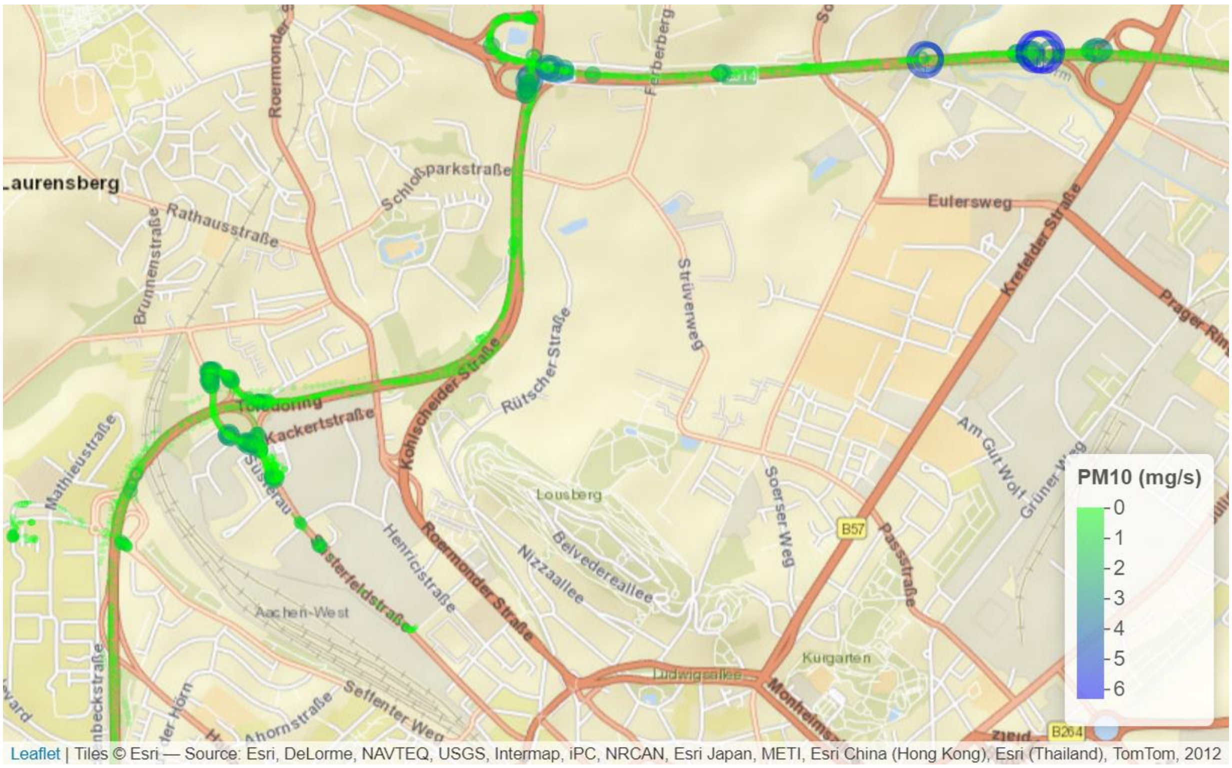


**Figure 28 Extract of the highly spatially resolved brake emissions inventory developed based on the euroFOT data. This extract shown is for north Aachen, Germany.**

4. **Model sensitivity runs**. Sensitivity model runs have been conducted to consider the effect of using different brake wear emission factors and vehicle fleet mix data (section 4.3). If a given location is thought to have a different average passenger car brake wear emission factor to the one used in this work (6 mg/car) then this analysis helps show the sensitivity of the results to the emission factor used.

5. **Transect chart to illustrate the highly resolved spatial variability along roads**. The focus of this work has been to challenge the conventional approach to modelling the contribution of brake wear to ambient $PM_{10}$ concentrations. As a result, the results show higher spatial variability of brake wear emissions, and this is presented for example in Figure 21. This pattern should be universally applicable.

# 6 Conclusions and recommendations

## 6.1 Conclusions

### 6.1.1 Work Package 1

In the first part of the project (Work Package 1), an innovative approach has been developed to estimate brake use on a highly resolved spatial and temporal basis. Real vehicle measurements data, covering over 150,000 kilometres driven has been analysed, and estimates made of the energy dissipated to brakes each second. These estimates have been validated against measured records of brake use within these datasets, where possible. The approach developed for estimating the energy dissipation to the brakes can be extended and applied to datasets without a record of brake use (e.g. PEMS data).

### 6.1.2 Work Package 2

In the second part of the project (Work Package 2), contemporary estimates of brake wear emission rates were distributed according to the spatial and temporal energy dissipation inventory from Work Package 1. A literature review was undertaken to consider the most appropriate emission rates to apply to the results of Work Package 1, to develop emissions rates for brake wear. The highly resolved brake wear emissions inventory was analysed to investigate the relationship between brake wear emissions and variables including the speed limit of the road, the road type classification, the time of day, and gradient of the road, with significant relationships observed in many cases. This information could be used by air quality practitioners going forward if they have information available on these variables.

The highly resolved brake wear emissions inventory was analysed to investigate the relationship between brake wear emissions and variables including the speed limit of the road, the road type classification, the time of day, and gradient of the road. It was found that the speed limit of the road had a significant effect on brake wear emissions, with higher average brake wear emission rates on lower speed limit roads. It was also shown however that there were more high intensity braking events on higher speed limit roads. As a result, it may be expected that emissions from brakes on higher speed limit roads may be more spatially variable, with few highly localised areas of high brake wear emissions, which could lead to high $PM_{10}$ concentrations.

The road type was also investigated using the OpenStreetMap road classifications. Here it was found the average brake wear emissions were significantly larger on “link” type roads (i.e. slip/ramp roads), as vehicles tend to brake more on these types of roads. Brake wear emissions were also investigated as a function of the time of day, by grouping the data into one-hour time groups. It was found that the largest emission rates were found during the typical peak hours (07:00 -19:00), however there was not a stark difference between peak and non-peak hours. Although vehicles brake more often in peak hours, given the roads are more congested during these times, the braking intensity is typically less than during non-peak hours. A similar pattern was found when investigating the difference in average weekday vs. weekend brake wear emissions; vehicles brake more often on weekdays, but given the roads are more congested during these times, the braking intensity is typically less than during weekends.

The relationship between the estimated brake wear emissions and the gradient of the road was also investigated. The gradient of the road was averaged over a minute of consecutive observations and grouped into 1% groups from -8% to +8%. It was found that there was a significant relationship between the gradient of the road and the brake wear emissions.

### 6.1.3 Work Package 3

In Work Package 3, the spatially resolved brake wear emissions inventory has been used as an input to the RapidAir model to investigate impacts on ambient particulate matter ($PM_{10}$) concentrations at a high spatial resolution. Comparisons with current modelling assumptions (i.e. constant emission rates along each road link) were made to understand the effect of using the new approach. This modelling showed that the contribution of brake wear to $PM_{10}$ concentrations was more spatially variable using the new approach, with larger contributions more focussed around busy road junctions. In most locations the brake wear contribution is lower in the spatially resolved model, however there are few locations of high intensity braking where the brake wear contribution is predicted to be significantly higher.

Additional model runs were made to determine the sensitivity of the results to the brake wear emission factor and fleet composition used, and to investigate the effect of regenerative braking on the contribution of brake wear emissions to particulate matter concentrations. The regenerative braking scenario shows that at all but the highest concentration receptor point, the brake wear $PM_{10}$ emission is effectively reduced to zero. An interesting aspect of the regenerative brake scenario is that it has the effect of removing brake wear emissions from areas that could be considered urban i.e. where personal exposure is of importance, while leaving only a few small areas of emission where the hardest braking conditions occur. This is because most urban locations are not associated with the highest braking energy. This behaviour of the regenerative braking scenario could therefore be of importance for exposure to particulate matter in urban populations.

### 6.1.4 Applicability of results to other European locations – including Germany

This work has focussed on challenging conventional approaches to modelling the contribution of brake wear to ambient PM concentrations using a data-driven, universal approach. Although the air quality modelling domain was in the UK, there are several ways in which the results of this work are or could be applied to other European locations including Germany however. These include generalised brake wear emission factors by dataset variables such as speed limit of the road and road gradient, and model sensitivity runs. Given enough German vehicle measurements data and traffic data however, the approach used is universal enough to be applied in a German or other European context.

### 6.1.5 Additional concluding thoughts

The approach used (analysing the high frequency energy changes from vehicle measurements data) lends itself to a more sophisticated approach to understanding the contribution of brake wear to ambient $PM_{10}$ concentrations in future. The energy-based approach is well-suited for considering a range of scenarios, for example the effect of regenerative braking as has been covered within this project.

The results of the air quality modelling could be used to inform the siting of measurement stations to help understand and verify the contribution of brake wear to ambient $PM_{10}$ concentrations, which itself is highly uncertain. Currently, air quality monitoring sites are not specifically located in regions where brake wear emissions could be high. The approach adopted in this work could be used to help design ambient measurement site choice to maximise the contribution made from brake wear emissions. Locations at busy road junctions were found to often be associated with the highest brake wear emissions.

## 6.2 Recommendations

This sub-section presents recommendations to build up on the work presented here.

The approach developed applies high resolution vehicle measurements data, which should become more readily available, and more frequent in the future. Using this approach with more vehicle measurements data and in different locations would be valuable. For example, large amounts of high resolution vehicle measurements data have been collected in London and it would be interesting to see where the brake wear emission hot spots are. Also, using vehicle measurements data that includes vehicle types other than passenger cars would add value to see the differences in braking behaviour.

A key outstanding uncertainty in this area is the value of the emission factors used. An average value of 6 mg/km for passenger cars has been used in this project. Much of the literature is quiet dated however, and there would be significant value in generating energy-based emission factors from robust modern experiments.

As this work has informed locations where the contribution of brake wear to ambient $PM_{10}$ concentrations is particularly high, this can be used to inform suitable locations for siting measurement stations to validate the model. The results suggest that busy road junctions have particularly high contributions of brake wear to ambient $PM_{10}$ concentrations. Analysing the particle composition from Partisol filter measurements would help to understand the source apportionment.

It was mentioned in section 0 that brake material temperature, and a lag in the release of particles from braking may well be important influencing factors on the release of brake wear emissions. Coincident measurements of brake material temperature at a high resolution would be valuable to factor in top the energy-based approach applied. Also, more literature on the lag in the release of particles from braking would be useful to understand how important this factor is, and the mechanism for how it works.

# 7 Acknowledgements

Ricardo Energy & Environment would like to acknowledge the help and support of the Institut für Kraftfahrzeuge for providing the euroFOT vehicle measurements data, the advice and guidance of the FAT members throughout the project, and especially Dr Rainer Vogt for his guidance and leadership of the project on behalf of the FAT.

# 8 References

Abu-Allaban, M. *et al.* (2003) 'Tailpipe, resuspended road dust, and brake-wear emission factors from on-road vehicles', in *Atmospheric Environment*, pp. 5283–5293. doi: 10.1016/j.atmosenv.2003.05.005.

Alemani, M. *et al.* (2018) 'Scaling effects of measuring disc brake airborne particulate matter emissions – A comparison of a pin-on-disc tribometer and an inertia dynamometer bench under dragging conditions', *Proceedings of the Institution of Mechanical Engineers, Part J: Journal of Engineering Tribology*. SAGE PublicationsSage UK: London, England, p. 135065011875668. doi: 10.1177/1350650118756687.

AUDI AG (2016) *Development foundation brake. Internal investigations of braking systems for plug-in hybrid electric vehicles (via Amato (2018), Chapter 10, cited as AUDI AG (2016a))*.

Carslaw, D. C. *et al.* (2010) 'Comprehensive analysis of the carbon impacts of vehicle intelligent speed control', *Atmospheric Environment*. Pergamon, 44(23), pp. 2674–2680. doi: 10.1016/J.ATMOSENV.2010.04.046.

Carsten, O. *et al.* (2008) 'isa-UK intelligent speed adaptation'. Available at: http://www.its.leeds.ac.uk/projects/isa/deliverables/Executive Summary of Project Results.pdf (Accessed: 10 May 2018).

EMEP (2016) 'EMEP/EEA air pollutant emission inventory guidebook 2016 - Chapter 1.A.3.b.vi-vii Road- tyre and brake wear', pp. 1–32.

FAT (2017) *The Contribution of Brake Wear Emissions to Particulate Matter in Ambient Air*. Available at: https://www.vda.de/de/services/Publikationen/fat-schriftenreihe-301.html.

Garg, B. D. *et al.* (2000) 'Brake Wear Particulate Matter Emissions', *Environmental Science & Technology*, 34(21), pp. 4463–4469. doi: 10.1021/es001108h.

Grigoratos, T., Giorgio, M. and Heinz, S. (2016) 'Analysis of WLTP typical driving conditions that affect non-exhaust particle emissions'. doi: 10.2790/283623.

Grigoratos, T. and Martini, G. (2015) 'Brake wear particle emissions: a review', *Environmental Science and Pollution Research*, 22(4), pp. 2491–2504. doi: 10.1007/s11356-014-3696-8.

Grochowicz, J. (2016) *BRAKE WEAR & DUST: COMPARISON OF TEST PROCEDURES*. Available at: https://wiki.unece.org/download/attachments/29229228/PMP-39-08 Grochowicz Wear and Dust _ Comparison of test procedures.pdf?api=v2.

Hagino, H., Oyama, M. and Sasaki, S. (2015) 'Airborne brake wear particle emission due to braking and accelerating', *Wear*, 334–335, pp. 44–48. doi: 10.1016/j.wear.2015.04.012.

Hagino, H., Oyama, M. and Sasaki, S. (2016) 'Laboratory testing of airborne brake wear particle emissions using a dynamometer system under urban city driving cycles', *Atmospheric Environment*, 131, pp. 269–278. doi: 10.1016/j.atmosenv.2016.02.014.

Hausmann, K. *et al.* (2018) *German Informative Inventory Report 2018 (IIR 2018)*. Available at: https://iir-de.wikidot.com/welcome:welcome (Accessed: 7 June 2018).

Iijima, A. *et al.* (2008) 'Emission Factor for Antimony in Brake Abrasion Dusts as One of the Major Atmospheric Antimony Sources', *Environmental Science & Technology*, 42(8), pp. 2937–2942. doi: 10.1021/es702137g.

Karl, T. *et al.* (2017) 'Urban eddy covariance measurements reveal significant missing NOx emissions in Central Europe', *Scientific Reports*. Nature Publishing Group, 7(1), p. 2536. doi: 10.1038/s41598-017-02699-9.

Kukutschová, J. *et al.* (2011) 'On airborne nano/micro-sized wear particles released from low-metallic automotive brakes', *Environmental Pollution*, 159(4), pp. 998–1006. doi: 10.1016/j.envpol.2010.11.036.

Kwak, J. *et al.* (2013) 'Characterization of non-exhaust coarse and fine particles from on-road driving and laboratory measurements', *Science of The Total Environment*, 458–460, pp. 273–282. doi: 10.1016/j.scitotenv.2013.04.040.

Lawrence, S., Sokhi, R. and Ravindra, K. (2016) 'Quantification of vehicle fleet PM10 particulate matter emission factors from exhaust and non-exhaust sources using tunnel measurement techniques', *Environmental Pollution*. Elsevier, 210, pp. 419–428. doi: 10.1016/J.ENVPOL.2016.01.011.

Masey, N., Hamilton, S. and Beverland, I. J. (2018) 'Development and evaluation of the RapidAir dispersion model, including the use of geospatial surrogates to represent street canyon effects', *Environmental Modelling & Software*. Elsevier. doi: 10.1016/J.ENVSOFT.2018.05.014.

Mathissen, M. *et al.* (2012) 'Non-exhaust PM emission measurements of a light duty vehicle with a mobile trailer', *Atmospheric Environment*. Pergamon, 59, pp. 232–242. doi: 10.1016/J.ATMOSENV.2012.05.020.

Nosko, O., Alemani, M. and Olofsson, U. (2015) 'Temperature effect on emission of airborne wear particles from car brakes', in *Europe's Braking Conference and Exhibition*. Available at: http://kth.diva-portal.org/smash/record.jsf?pid=diva2%3A824604&dswid=-1576 (Accessed: 18 April 2018).

Perricone, G. *et al.* (2016) 'Towards the ranking of airborne particle emissions from car brakes – a system approach', *Proceedings of the Institution of Mechanical Engineers, Part D: Journal of Automobile Engineering*. SAGE PublicationsSage UK: London, England, 231(6), pp. 781–797. doi: 10.1177/0954407016662800.

Sanders, P.G.; Ning Xu; Dalka, T.M.; Maricq, M. M. (2003) 'Airborne Brake Wear Debris: Size Distributions, Composition, and a Comparison of Dynamometer and Vehicle Tests'. American Chemical Society. doi: 10.1021/ES034145S.

Sanders *et al.* (2003) 'Airborne Brake Wear Debris: Size Distributions, Composition, and a Comparison of Dynamometer and Vehicle Tests'. American Chemical Society. doi: 10.1021/ES034145S.

The UK Department for Transport (2016) 'Vehicle Emissions Testing Programme - Moving Britain Ahead', (April).

United States Environmental Protection Agency (2014) *Brake and Tire Wear Emissions from On-road Vehicles in MOVES2014 - Google Books*. Available at: https://cfpub.epa.gov/si/si_public_file_download.cfm?p_download_id=525701 (Accessed: 2 November 2018).

US EPA (2011) *Development of Emission Rates for Light-Duty Vehicles in the Motor Vehicle Emissions Simulator (MOVES2010): Final Report (EPA-420-R-11-011, August 2011)*. Available at: https://nepis.epa.gov/Exe/ZyPDF.cgi?Dockey=P100BVT9.pdf (Accessed: 8 October 2018).

Wakeling, D. *et al.* (2018) *UK Informative Inventory Report (1990 to 2016)*. Department for Environment, Food and Rural Affairs (Defra), Nobel House, 17 Smith Square, London SW1P 3JR helpline@defra.gsi.gov.uk. Available at: http://naei.beis.gov.uk/reports/reports?report_id=956 (Accessed: 7 June 2018).

Westerlund, K. –G. and Johansson, C. (2002) 'Emission Of Metals And Particulate Matter Due To Wear Of Brake Linings In Stockholm', *WIT Transactions on Ecology and the Environment*. WIT Press, 53. doi: 10.2495/AIR020791.

Zhang, S., Chen, W. and Li, Y. (2009) 'Wear of Friction Material during Vehicle Braking', in. doi: 10.4271/2009-01-1032.

# A Appendix

## A.1 Detail on activity datasets

### A.1.1 Leeds

This dataset was collected by the University of Leeds as part of research into driver behaviour and safety with a voluntary Intelligent Speed Adaptation (ISA) system (Carsten *et al.*, 2008). This same dataset was also analysed by Carslaw *et al.* (2010), in research into the carbon impacts of vehicle intelligent speed control.

The original dataset collected included data with and without the ISA system in place. Only data where the ISA system was not in place have been analysed for this work. This is because the use of the ISA system is not typically used in the European fleet and may affect usual braking behaviour.

Key fields in the dataset included:

- Global Positioning System (GPS) longitude and latitude
- Vehicle speed
- Trip ID
- Date and time
- Vehicle ID
- Application of brakes (yes or no)
- Speed limit of the road driven on

The data was collected between August 2003 and May 2006. Data from 21 Skoda Fabia Elegance 1.4 litre estate vehicles was measured, with 79 drivers driving these vehicles. The vehicle weight was estimated to provide a means of calculating the energy dissipated to the brakes. The vehicle weight was estimated by summing the estimated unladen weight, and the load on the vehicle. The unladen weight was taken from the Parkers vehicle website[20]. This was given as 1,155 kg. The load weight of the vehicle was not known but was estimated as 175 kg and includes the weight of the driver and any potential passengers, the weight of the fuel, the weight of the ISA system, and any other potential goods carried. This gives a total estimated weight of 1,330 kg.

The total distance driven of all the vehicles within the dataset was 142,000 km. The data was thinned to remove invalid and unrealistic data, leaving a revised total distance driven of 129,000 km. A measure of the altitude data was not included within this dataset. A measure of the altitude allows for an understanding of the change in height and thus the change in potential energy of a vehicle. Changes in potential energy affect estimates of the energy dissipated to the brakes, as all other parameters being equal, a vehicle traveling down a steep hill requires more energy to reduce its speed than a vehicle travelling on a flat road. To account for the potential energy changes, altitude data was sourced from the Ordnance

[20] https://www.parkers.co.uk/skoda/fabia/hatchback-2000/14-16v-elegance-5d-(ac)/specs/

Survey OpenData OS Terrain 50 map dataset. This dataset was free to use under the UK Open Government Licence[21]. This data was joined to the Leeds dataset by the latitude and longitude fields. The OpenData altitude data provides elevation in metres to the nearest metre. This data was linearly interpolated based on the Digital Terrain Model cells nearest each point, to produce a smoother dataset.

## A.1.2 euroFOT

The euroFOT (European Field Operational Test) dataset used was collected as part of a project, led by Ford, to assess the impact from the usage of intelligent transportation systems and evaluate their effect on transport safety and fuel efficiency. An extract of this dataset was purchased and received from ika[22] in January 2018. The extract covers data from one driver, as privacy issues restricted the use of more data.

The vehicle measured was a Euro 5 Ford station wagon. The vehicle weight was provided by ika as 1,496 kg, and considers one driver (75 kg), 90% tank gasoline load, and all other fluids needed. The total distance driven of all the vehicles within the dataset was 27,850 km. The data was thinned to remove invalid and unrealistic data, leaving a revised total distance driven of 23,750 km.

Some of the fields were provided at 10 Hz (e.g. vehicle speed), whilst others were provided at 1 Hz (e.g. GPS location). To consider all the data at the same resolution and reduce the size of the dataset, the 10 Hz fields were aggregated to 1 Hz. One of the fields, given at 10 Hz, was “Brake_pedal_on_off”, a record of whether the brake pedal was applied. A new field was calculated as a measure of whether the brake was applied in the thinned 1 Hz dataset. This field calculated how many of the current, and previous nine observations, had “Brake_pedal_on_off” as TRUE. If this value was >5 (i.e. more than half of the observations), then it was considered that the brake was applied. This therefore retained information from the 10 Hz data within the thinned 1 Hz dataset.

The altitude of the vehicle was given in the dataset from the GPS and was provided at a 1 Hz resolution. Many of the vehicle trips started at an altitude of about 450 metres and would often descend rapidly after around 100 seconds. This behaviour seemed unusual and so the altitude data was verified against an external altitude data source (the Copernicus Digital Terrain Model). This data was produced with funding from the European Union. Verification showed that the altitude data in the raw dataset and the altitude dataset from the Copernicus Digital Terrain Model generally aligned well, except for the cases where trips in the raw dataset started at about 450 metres. For such trips the altitude data was not applied for the calculation of potential energy due to concerns over data quality. It was decided to retain the use of the altitude data in the raw dataset rather than use the Copernicus dataset. This is as the Copernicus dataset is only given at 25 metre resolution, which is considered too low for use in determining gradient at the high resolution required.

---

[21] http://www.nationalarchives.gov.uk/doc/open-government-licence/version/3/ Contains OS data © Crown copyright and database 2018.

[22] ika – Institut für Kraftfahrzeuge: http://ika.rwth-aachen.de/

## A.1.3 DfT

Data from the UK Department for Transport included measurements of 38 vehicles along a 70 km route. The measurements were made during “normal” day-time traffic conditions in central England, along urban, rural, and motorway roads (The UK Department for Transport, 2016). The vehicles tested were 19 Euro 5 and 19 Euro 6 diesel passenger cars. The measurements were estimated to have been made in late 2015 – early 2016.

In FAT (2017), this dataset was used, however only the data from the 19 Euro 5 vehicles was analysed. Further details of the testing conditions are provided in The UK Department for Transport (2016). The DfT dataset did not include a measure of brake use, unlike the other two datasets considered, however it did have high quality 1 Hz measurements of vehicle speed, location, and altitude necessary to estimate the energy going to the brakes used in the model given in this report.

Unladen vehicle weights were estimated by undertaking an internet search. The model and engine size of the vehicle was given in the dataset, and this information was used to search for an estimated vehicle weight to apply. The load weight was estimated as 150 kg which includes the passenger, weight of the fuel, and the Portable Emissions Measurement System (PEMS) that the vehicles carried. Altitude data was included in the raw dataset and was used to calculate the gradient.

## A.1.4 Routes covered in all datasets

Figure 29 shows the road coverage across the three vehicle activity datasets used.


**Figure 29 Road coverage across the three vehicle activity datasets used.**

# A.2 Comparison to the Worldwide Harmonised Light Vehicle Test Procedure driving cycle – further results

## A.2.1 Brake phase duration distributions

This section considers analysis of brake phase duration distributions. The brake phase duration distributions are considered for different “v_max” groups. It has been interpreted that “v_max” is considered to be the maximum speed in a “short trip”, where a short trip is consecutive data with v_max > 1 km/h. “v_max” and “short trip” fields have therefore been created within the Leeds and euroFOT data for comparison.

Figure 30 shows the chart from Grigoratos, Giorgio and Heinz (2016) against which the euroFOT and Leeds data are compared.

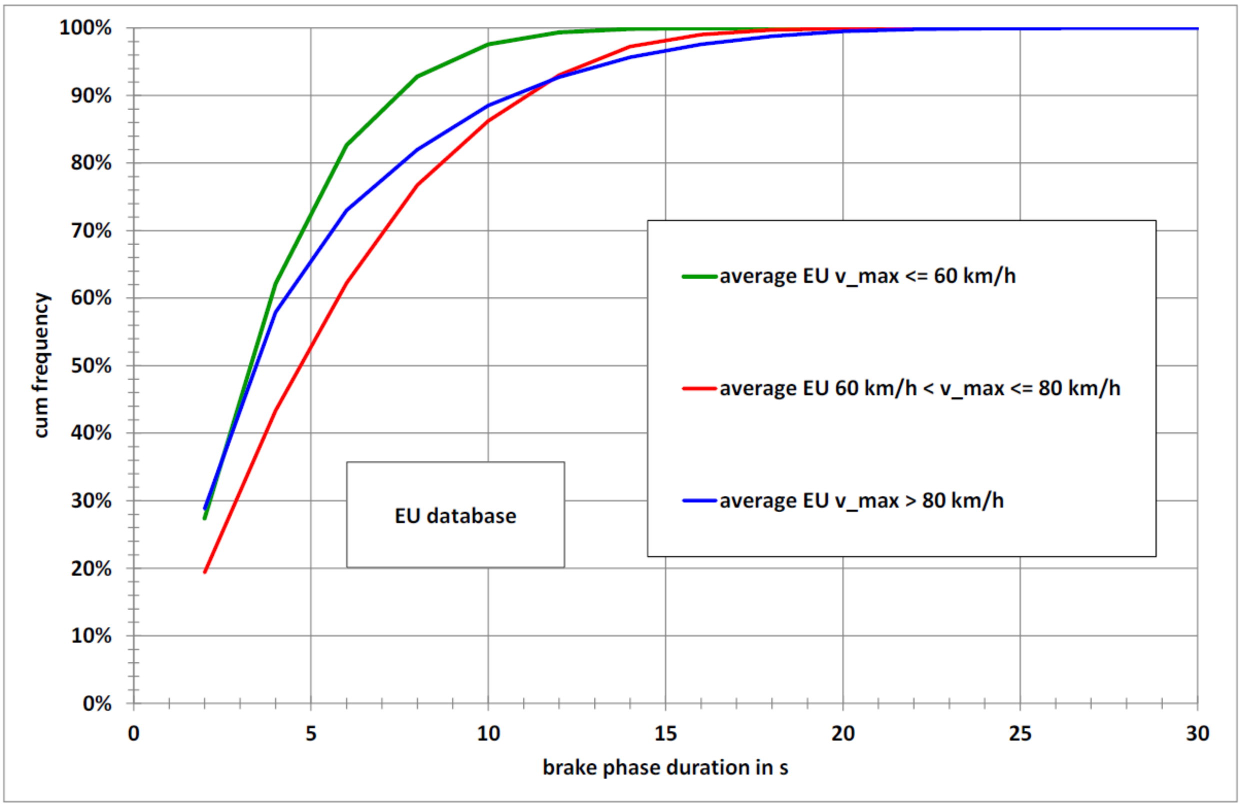


**Figure 30 Figure 181 from Grigoratos, Giorgio and Heinz (2016): Brake phase duration distributions for short trips with different v_max.**

Figure 31 shows the brake phase duration distributions for the Leeds dataset. The patterns are broadly similar, though with some minor differences. In both Figure 31 and Figure 30, the “v_max” < 60 km/h group has the highest proportion of brake phases with lower durations. There is more variation between “v_max” groups in Figure 30, and also a difference in the relative difference between the “v_max” 60-80 km/h and >80 km/h groups.

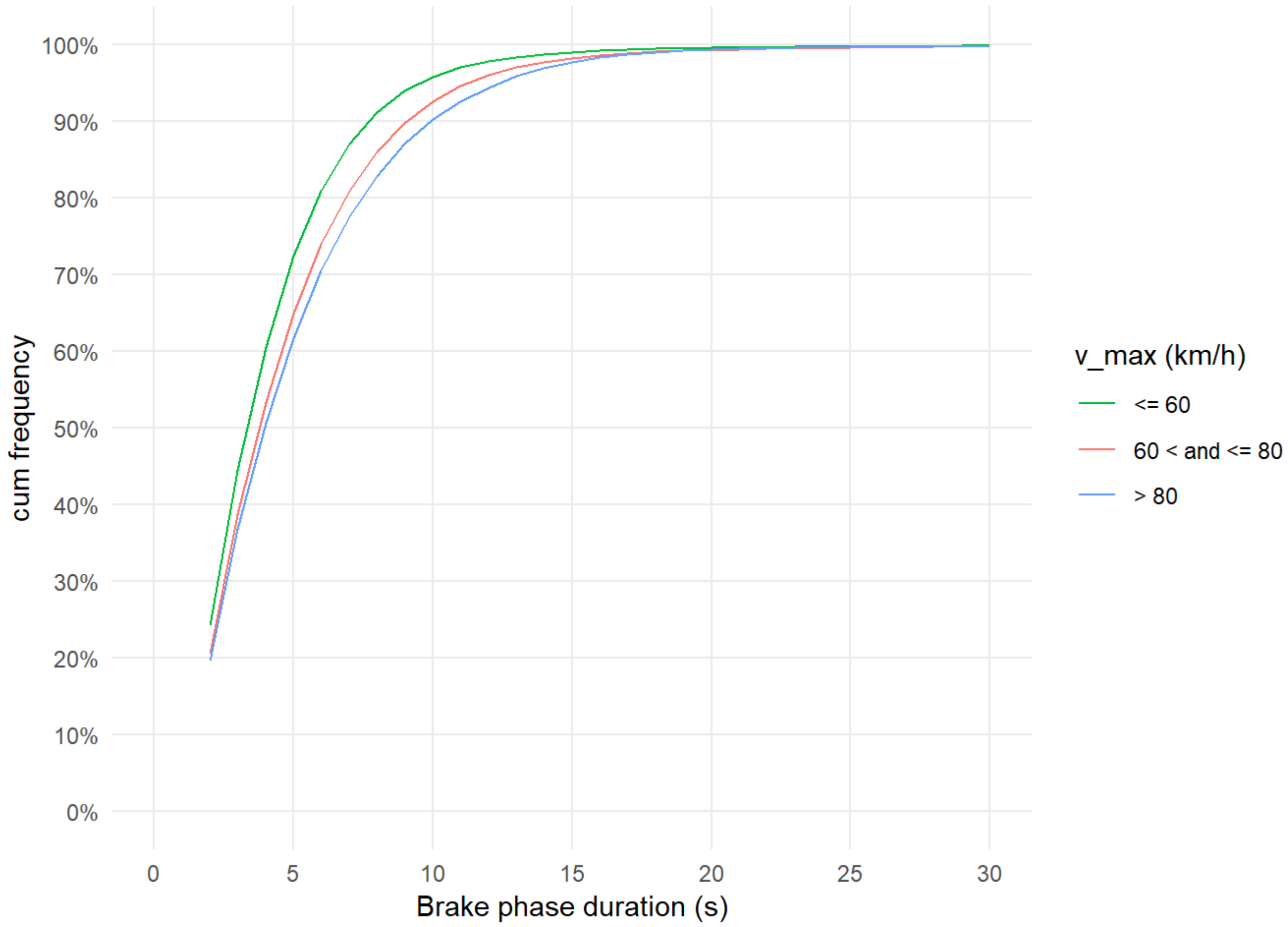


**Figure 31 Brake phase duration in the Leeds dataset**

Figure 32 shows the brake phase duration distributions for the euroFOT dataset. The patterns are broadly similar, though with some minor differences. In both Figure 32 and Figure 30, the "v_max" < 60 km/h group has the highest proportion of brake phases with lower durations. In the euroFOT data there is marginally more data with larger brake phase durations.

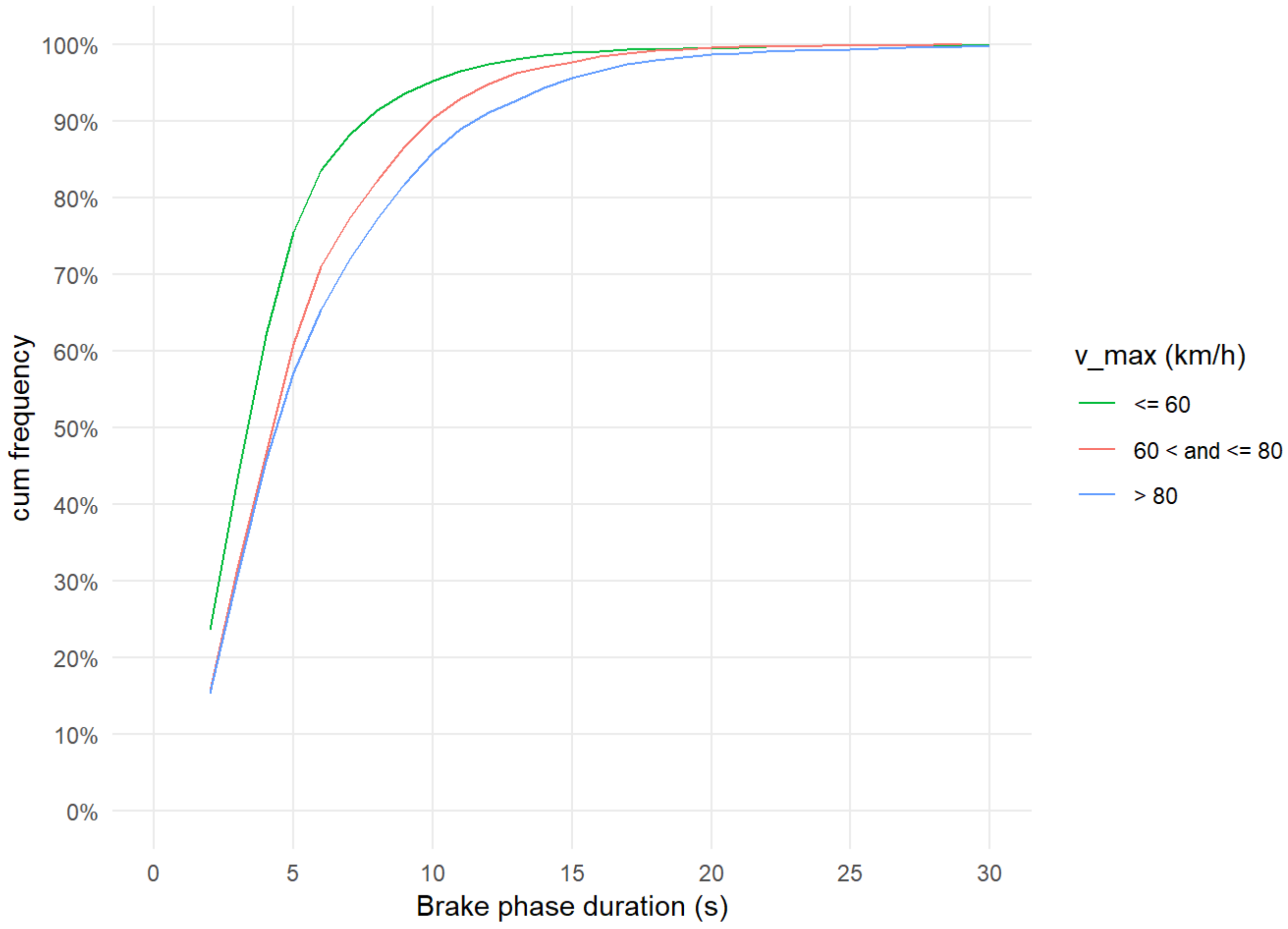


**Figure 32 Brake phase duration in the euroFOT dataset**

## A.2.2 Deceleration distributions

This section considers analysis of deceleration cumulative frequency distributions. These are not braking distributions, as it includes deceleration with braking and without braking. The deceleration distributions consider data with acceleration < -0.15 m/s$^2$. Figure 33 shows the chart from Grigoratos, Giorgio and Heinz (2016), against which the euroFOT and Leeds data are compared.

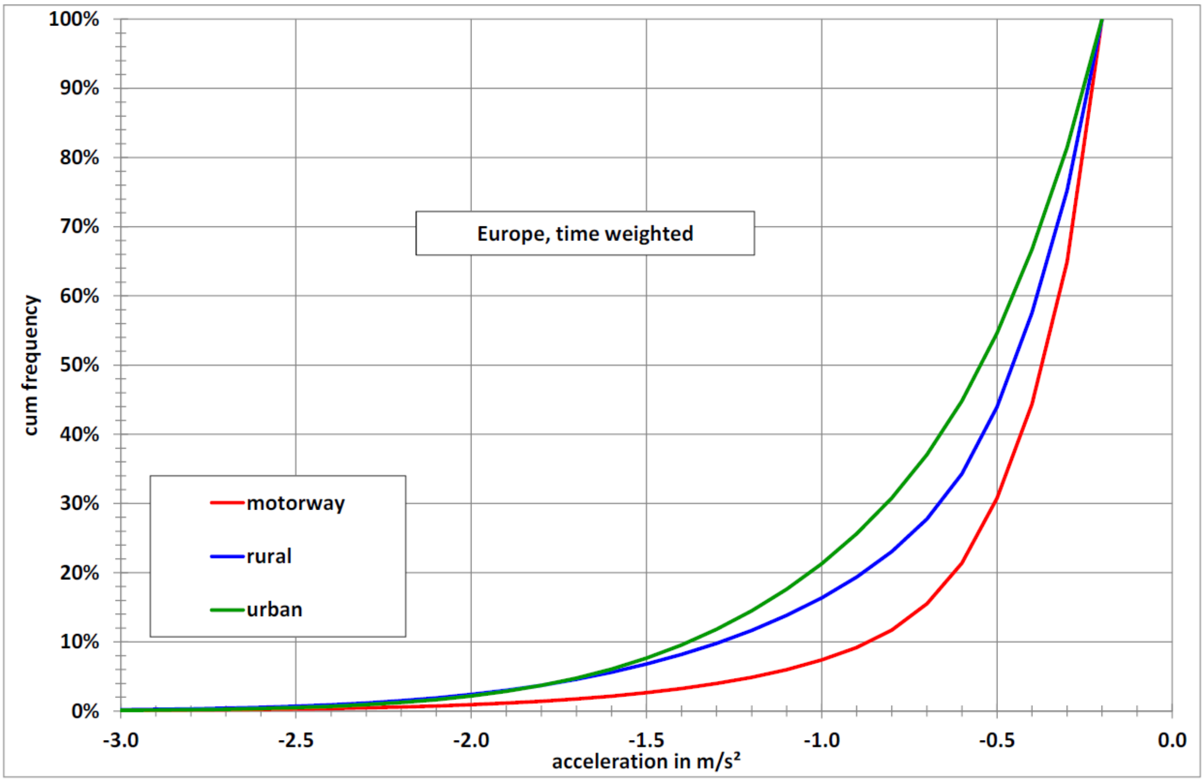


**Figure 33 Figure 254 from Grigoratos, Giorgio and Heinz (2016): Deceleration distributions for road categories, time weighted, Europe**

There is no such urban, rural, motorway split within the Leeds and euroFOT datasets for a direct comparison against Figure 33. There are similar fields we can use to compare the data such as the speed limit of the road and the highway type derived from OpenStreetMap data.

#### A.2.2.1 Pattern by speed limit

The University of Leeds dataset has a record of the speed limit of the road. This includes speed limits from 20 mph to 70 mph, although there are few records at 20 mph. Figure 34 shows the deceleration distributions as a function of speed limit. For comparison, it can be assumed that 30 mph roads are urban roads, 50 mph roads are rural roads, and 70 mph roads are motorway roads. This assumption is more robust for urban and motorway roads.

This chart shows a similar pattern to Figure 33. In both Figure 34 and Figure 33, the intersect at 30% cumulative frequency is at -0.5 $m/s^2$. Also, the highest speed roads have more deceleration data at higher deceleration rates.

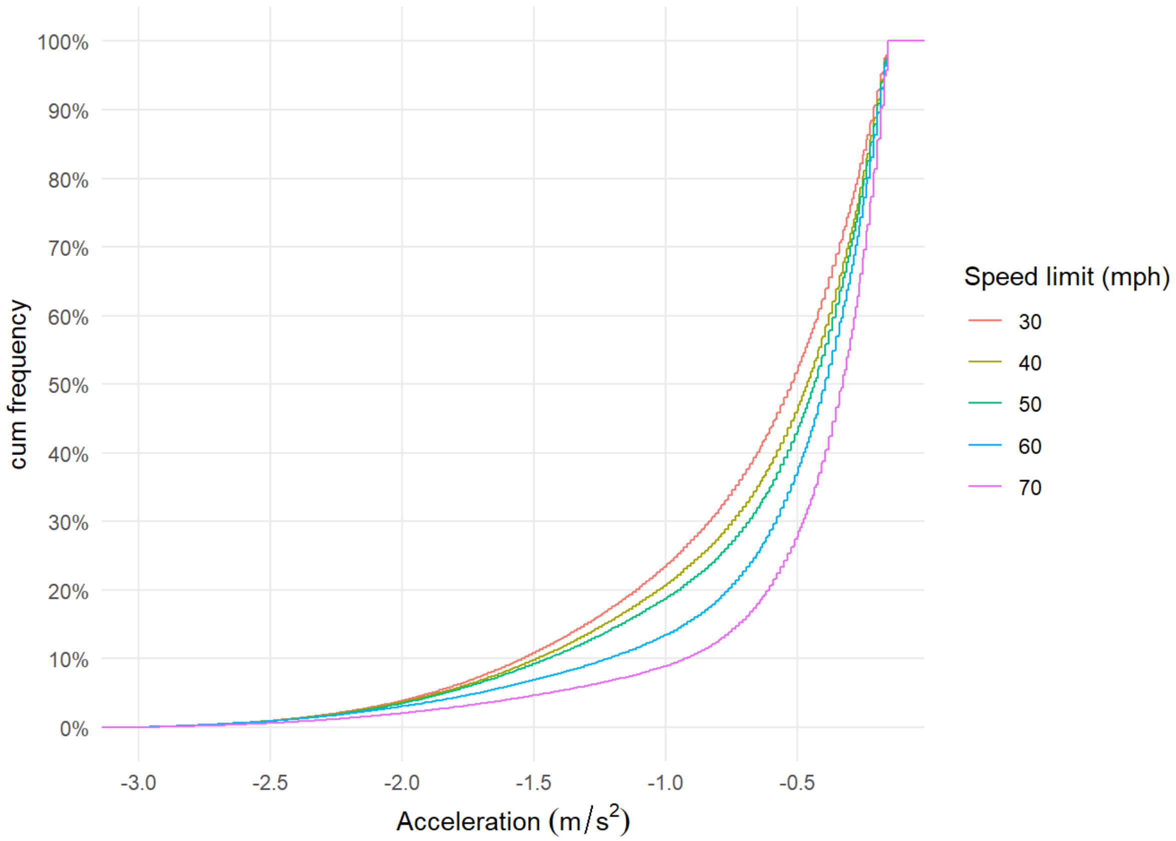


**Figure 34 Decelerations distributions by speed limit of the road from the Leeds dataset**

#### A.2.2.2 Pattern by highway type

OpenStreetMap data contains information about the highway type of the road. Examples include “motorway” and “residential” roads. For the most suitable highway types with sufficient records, the same deceleration distribution has been reproduced below. If not directly comparable with Figure 33, it is useful to see how the Leeds and euroFOT datasets compare.

Figure 35 shows that:

- Motorways have more deceleration data at higher deceleration rates.
- The euroFOT dataset has more deceleration data at higher deceleration rates than the Leeds dataset.
- There is a difference in the patterns in the residential and primary roads between the two datasets.

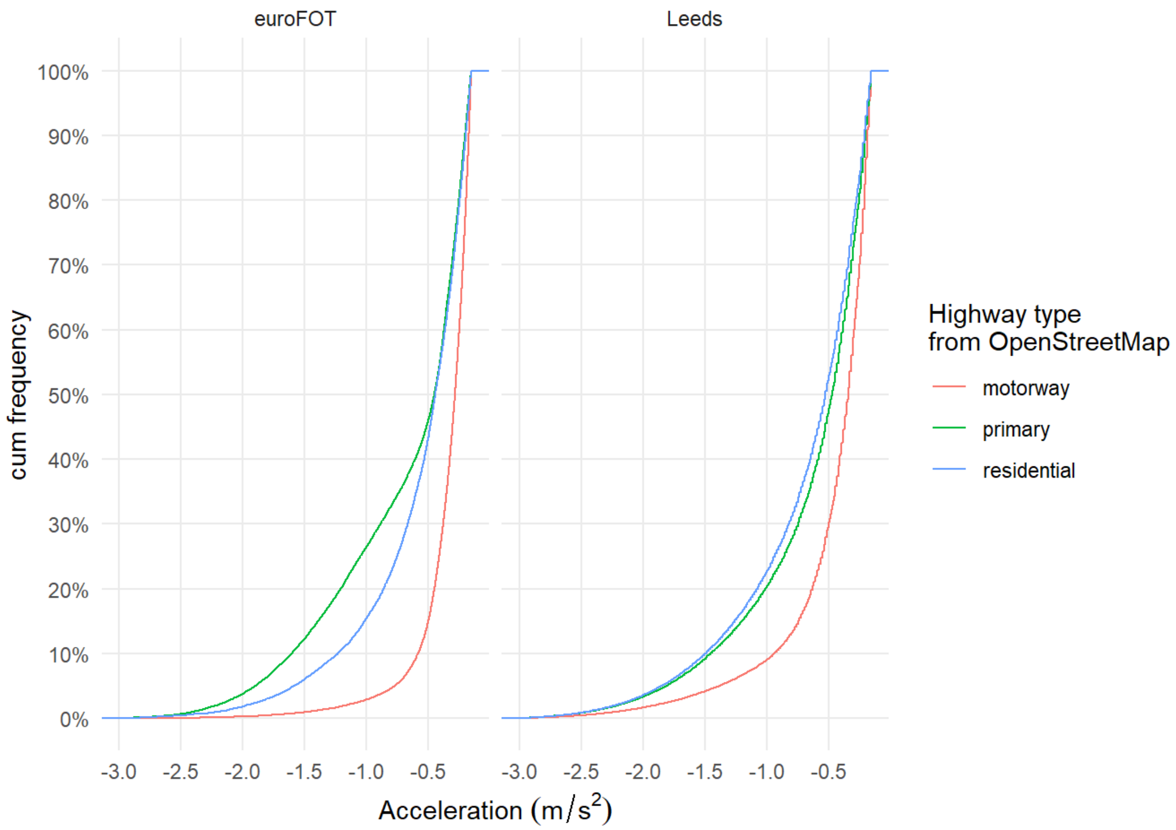


**Figure 35 Decelerations distributions by highway type from OpenStreetMap**

## A.3 Methodology for the estimation of energy going to the brakes

The total energy associated with the vehicles was estimated as the sum of the kinetic energy and potential energies of the vehicles. Data on the vehicle mass, and the speed and altitude at 1 Hz was used to calculate these energies. Further details on the source of this data is given in section 2.1.1.

For each activity dataset the following calculations were made:

- The **kinetic energy** associated with the vehicle was calculated as:

$$\text{Kinetic energy} = 0.5 * m * v^2$$

  - where $m$ is the vehicle mass (kg) and $v$ is the vehicle speed (m/s)

- The **potential energy** associated with the vehicle was calculated as:

$$\text{Potential energy} = m * g * h$$

  - Where $m$ is the vehicle mass (kg), $g$ is the acceleration due to gravity (m/s$^2$), and $h$ is the change in elevation of the vehicle above sea level (m)

These equations were used to calculate the change in kinetic and potential energies of the vehicle at 1 Hz. These calculations were made on a per trip basis, so the first observation of each trip was not applicable (as there is no previous observation to calculate an energy change for).

Estimates of the energy going to the brakes were then made and these results were validated against the measures of brake use in the Leeds and euroFOT datasets. Several approaches were tested to estimate the energy going to the brakes to see which approach best matched the measured brake use and are listed below.

### A.3.1 Approaches to estimate energy going to the brakes

A vehicle can lose speed and energy through natural retarding forces, so consideration was needed to determine at what energy threshold the brakes were applied at. For example, if it was assumed that all the energy lost for decelerations above 0 m/s$^2$ then this would grossly over-estimate the energy going to the brakes as it would ignore the natural retarding forces. In fact, it was found that using 0 m/s$^2$ as a threshold meant that estimates of brake use only agreed with the measures of brake use from the Leeds and euroFOT datasets 57% of the time.

A more sensible deceleration threshold value to use was found to be 0.6 m/s$^2$. However, such a threshold doesn’t factor in that the deceleration threshold will vary with vehicle speed as the many of the natural retarding forces are speed dependent. For example, the aerodynamic drag increases with vehicle speed.

The approach used considered a deceleration threshold that was dependent on the vehicle speed. This was taken from section 9.1 of Grigoratos, Giorgio and Heinz (2016). This equation was derived based on analysis of in-use driving behaviour data from a German

Environment Agency research project ("Investigations on Improving the Method of Noise Measurement for Powered Vehicles", July 1997). Measurements were made on 11 cars in Aachen and the surrounding area, where vehicle speed, engine speed, drive axle torque, and clutch and brake engagement were measured. Several threshold curves were tested in that work, and the best fit was achieved for the following vehicle speed dependent deceleration threshold curve.

$$\mathrm{a\_threshold} = -0.098468 * \ln(\mathrm{v}) - 0.30439$$

where $\mathrm{a\_threshold}$ is the acceleration threshold (m/s$^2$) below which the brakes are assumed to be applied, and $\mathrm{v}$ is the vehicle speed (km/h).

Grigoratos, Giorgio and Heinz (2016) also referred to a $\mathrm{v\_a\_threshold}$ as well as the $\mathrm{a\_threshold}$. It was found that the prediction of brake use against the measures of brake use in the Leeds and euroFOT datasets were similar however.

As well as this, a bottom-up energy-based equation was also developed and tested to see how well it could predict brake use. This equation is shown below.

ΔK.E. = **Brake** – rolling resistance – aerodynamic drag +/- ΔPotential Energy (-*Regen*)

where K.E. is the kinetic energy of the vehicle, Brake is the energy going to the brakes, and *Regen* is an optional add-on variable to factor in energy that could potentially be used from a regenerative braking system.

This approach is useful as it allows the calculation of the energy going to the brakes explicitly based on fundamental physics. It was found however that estimates of brake use were over-predicted compared to the deceleration threshold from Grigoratos, Giorgio and Heinz (2016). This is likely as the former is missing other retarding forces such as engine braking which it wasn't possible to calculate from the data available. As the approach from Grigoratos, Giorgio and Heinz (2016) is based on in-use driving measurements, and not physical equations representing retarding forces, it inherently factors in retarding forces (e.g. engine braking) where there was insufficient information to estimate this using the bottom-up equation immediately above.

Figure 36 shows the deceleration threshold to determine at what point the brakes were applied. Points outside the red area are where the brakes would be applied at. Points within the red area would be associated with decelerations where the brakes wouldn't be needed to be applied. This was derived from the "a_threshold" equation in Grigoratos, Giorgio and Heinz (2016).

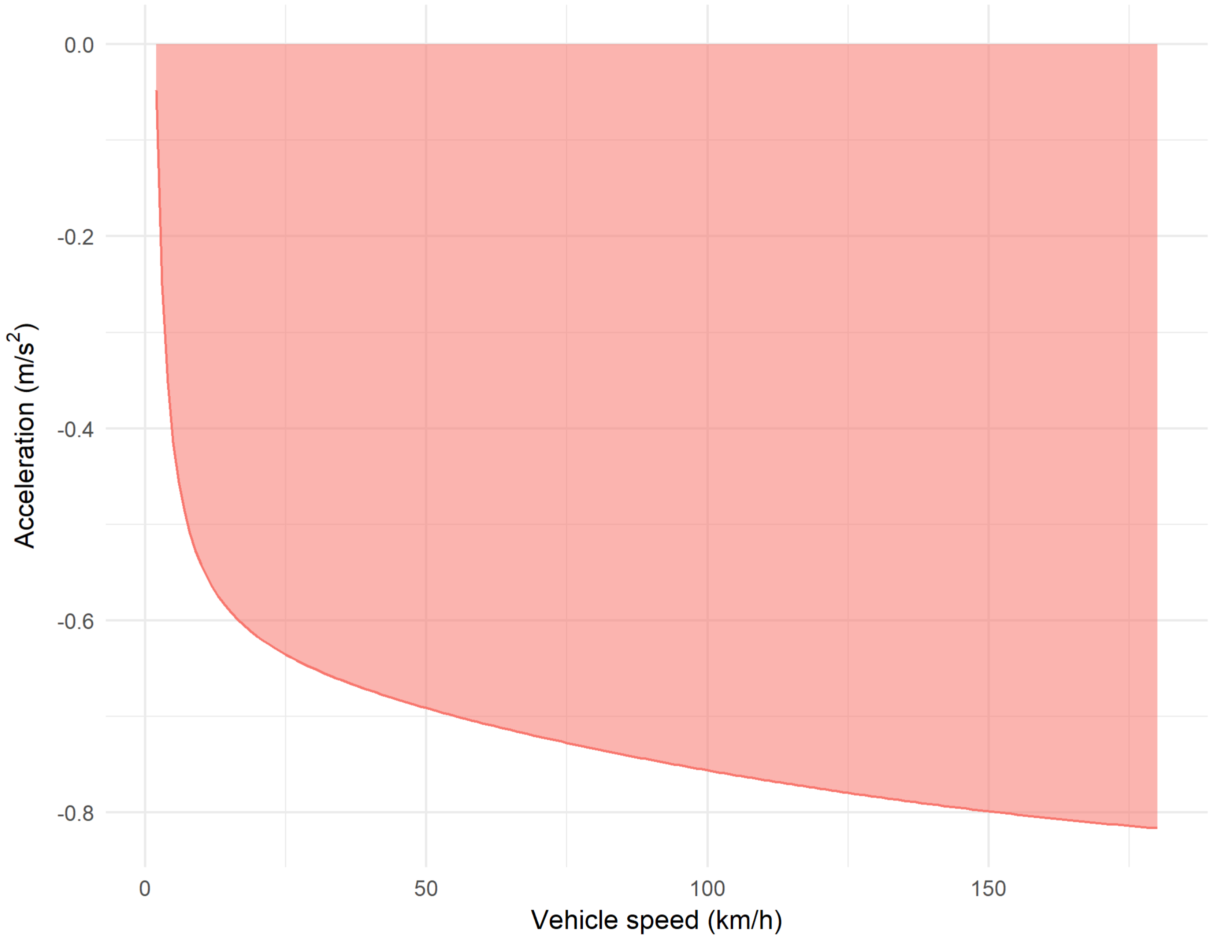


**Figure 36 Deceleration threshold to determine at what point the brakes were applied. Points outside the red area are where the brakes would be applied at. This was derived from the "a_threshold" equation in Grigoratos, Giorgio and Heinz (2016).**

## A.3.2 Potential Energy

The potential energy is an important aspect of the energy-based approach used. For example, a given deceleration and vehicle speed within the white zone in Figure 36 is associated with a certain amount of energy going to the brakes. If the change in potential energy is positive and greater than the calculated energy going to the brakes, then it is assumed that the energy instead does not go to the brakes but is lost as the vehicle gains potential energy whilst going uphill.

Vehicle altitude data was given or derived based on the vehicle GPS longitude and latitude and used to calculate the change in potential energy. Further detail on the altitude data used is given in section A.1. If the absolute gradient calculated was greater than 30% (0.3) then the gradient value was changed to 0 as the data was considered untrustworthy. There is more uncertainty in the altitude data used than many of the other variables such as the vehicle speed and mass and it was found that including changes in potential energy into the energy-based equation used did not significantly increase the accuracy of the prediction of brake use against the measures of brake use in the Leeds and euroFOT datasets.

## A.4 Comparisons/validation against other literature sources

### A.4.1 Comparison to brake wear emission rates in the MOVES model

The emission factors often quoted in the literature and reviewed in Table 2 are given in units of mg/km, a unit well suited to emissions inventory development. The nature of the model developed in this project allows the production of more temporally resolved emission rates, given the data is resolved to 1 Hz.

The United States Environmental Protection Agency (US EPA) has developed the MOtor Vehicle Emission Simulator (MOVES), which is a state-of-the-science emission modelling system. primarily developed for exhaust emissions and adapted for non-exhaust emissions[23]. This modelling system provides a sophisticated method for calculating brake wear emission factors, based on Vehicle Specific Power bins for vehicles (United States Environmental Protection Agency (2014)). Brake wear emission rates are based on $PM_{2.5}$ emission rates vs a deceleration curve/function (Figure 37). The brake wear emission rates are based on literature studies that measured brake wear emissions.

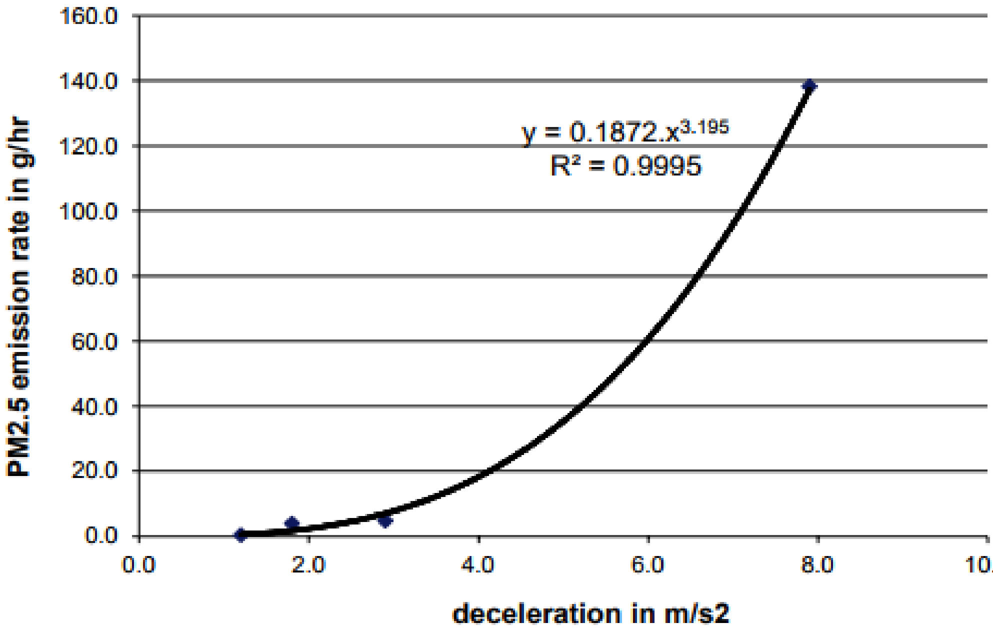


**Figure 37 Brake wear emission rates in units of grams/hour for LDVs, as a function of deceleration rate (Figure 2-1 of United States Environmental Protection Agency (2014)).**

The approach developed in this work has developed estimated brake wear $PM_{10}$ emissions from the 1 Hz vehicle measurements datasets. For each observation therefore, brake wear emissions in g/s have been calculated (section 3.1.2). This can be compared with the brake wear emission rates from Figure 37 in g $PM_{2.5}$/hr. The $PM_{2.5}$:$PM_{10}$ ratio used in United States Environmental Protection Agency (2014) is 1:8, so for this comparison the $PM_{10}$ values from

[23] https://www.epa.gov/moves

this project were divided by 8 to give comparable $PM_{2.5}$ emission rates, and then multiplied by 3,600 to convert from g/s to g/hr.

Figure 38 shows the brake wear $PM_{2.5}$ emission rates as a function of vehicle deceleration from this work (top facet) and from United States Environmental Protection Agency (2014) (bottom facet). The emission rates are comparable between the two approaches where the deceleration is below 3 m/s$^2$. MOVES extrapolates the trend from decelerations of 3 m/s$^2$ to 8 m/s$^2$ based on limited data. Also, decelerations in this range are rare, so the focus here is on decelerations below 3 m/s$^2$.

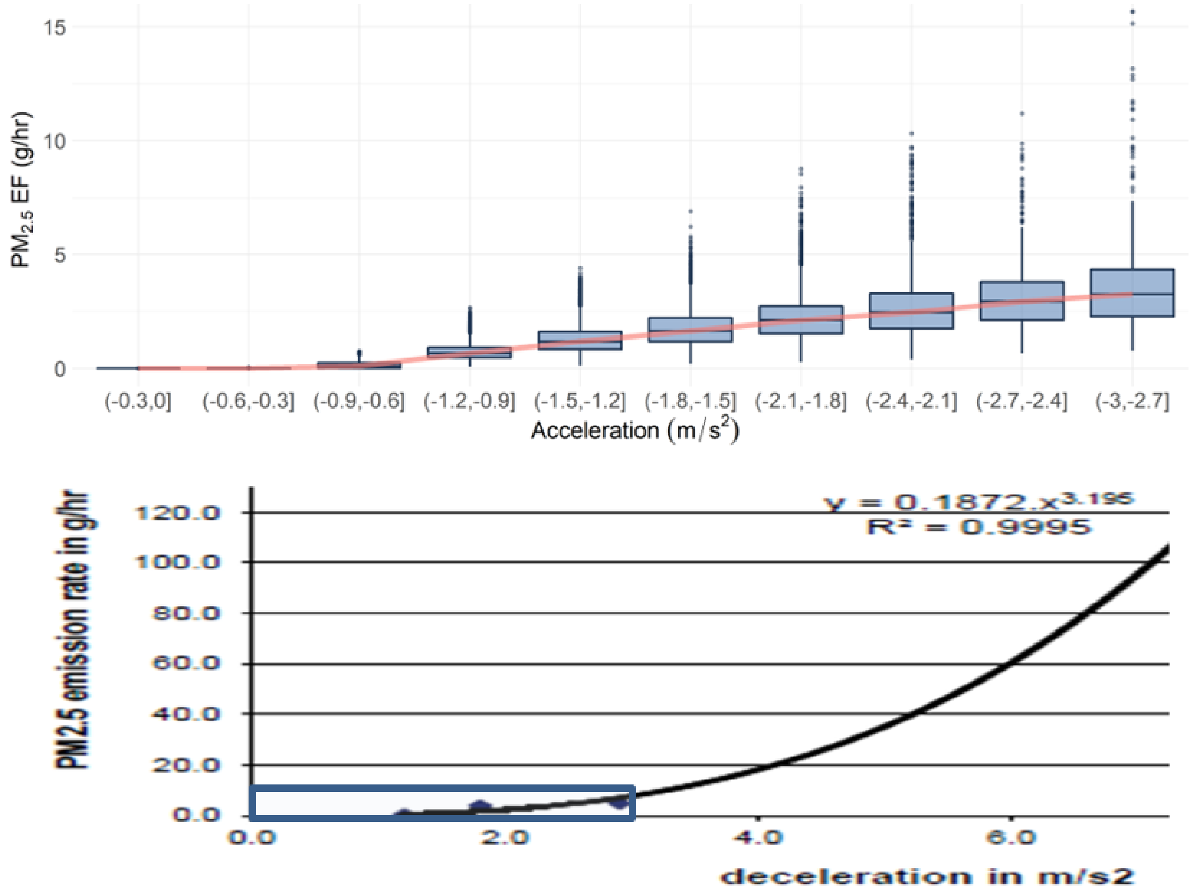


**Figure 38 Brake wear $PM_{2.5}$ emission rates as a function of vehicle deceleration from this work (top facet) and from United States Environmental Protection Agency (2014) (bottom facet).**

## A.4.2 Comparison to literature mg/stop factors

Some literature articles have experimentally researched the mass of particles released over set drive cycles, or from initial speeds and fixed deceleration rates. Therefore, emission rates can be expressed as mg/stop (i.e. braking event), rather than mg/km. mg/stop factors can also be generated from the model developed in this project by replicating the conditions used in the literature articles that developed these mg/stop factors.

Figure 39 shows the estimated mg $PM_{10}$/stop from this project compared to the reported mg $PM_{10}$/stop from the literature articles. Ten scenarios are shown from six literature articles (Garg *et al.* (2000), Hagino, Oyama and Sasaki (2015), Iijima *et al.* (2008), Perricone *et al.*

(2016), Sanders *et al.* (2003), Zhang, Chen and Li (2009)). Each of the ten scenarios shown report mg/stop values or gave initial speeds and deceleration rates that allowed the calculation of mg/stop values. Each scenario considers different a different braking scenario (i.e. different initial speeds and deceleration rates). The amount of energy per stop was calculated for each scenario and using the 0.1 mg/kJ factor from section 3.1.2, the mg $PM_{10}$/stop was derived for comparison against the value from the literature articles.

Figure 39 shows that the estimated mg/stop values are sometimes higher and sometimes lower than the reported mg/stop values from the literature. The discrepancies likely arise due to differences in the experimental conditions between literature articles. Given there is more widespread agreement and use of mg/km brake wear emission factors than mg/stop the work in this project is based on a 6 mg/km average brake wear emission factor rather than a mg/stop value.

Most of these literature articles reviewed considered PM mass as opposed to $PM_{10}$, however $PM_{10}$ should match closely with PM mass, as Kwak *et al.* (2013) noted no brake wear particles were above $PM_{10}$ from on-road and laboratory measurements.

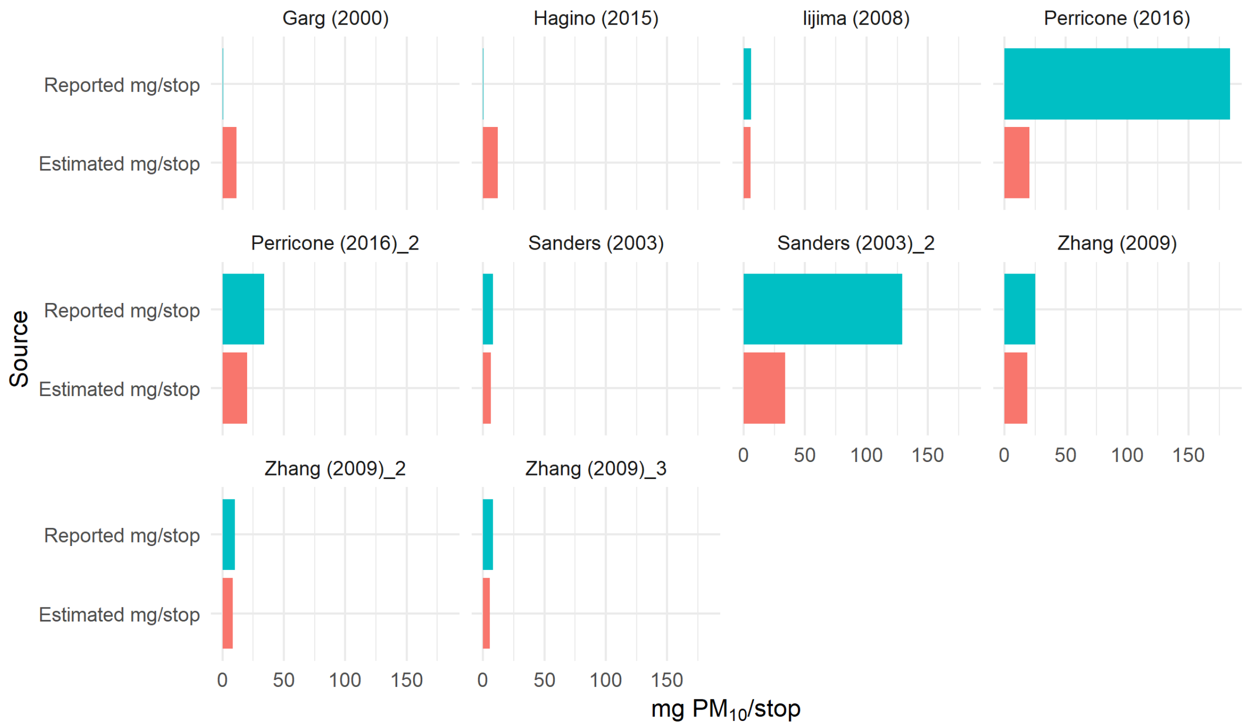


**Figure 39 Estimated mg $PM_{10}$/stop from this project compared to the reported mg $PM_{10}$/stop from the literature articles.**

# A.5 Other influencing variables on brake wear emissions

## A.5.1 Temperature

Research has shown that the brake material temperature can have a significant effect on brake wear emissions. Garg et al. (2000) found that the brake wear emissions increased significantly with increased temperature, especially as the temperature increased above 200 °C (Figure 40). It was also noted that the normal temperature range for braking events was 100-200 °C however. Grochowicz (2016) also found few braking events reached > 200 °C for light-duty vehicles in material presented at the Particle Measurement Programme meeting in Brussels in March 2016.

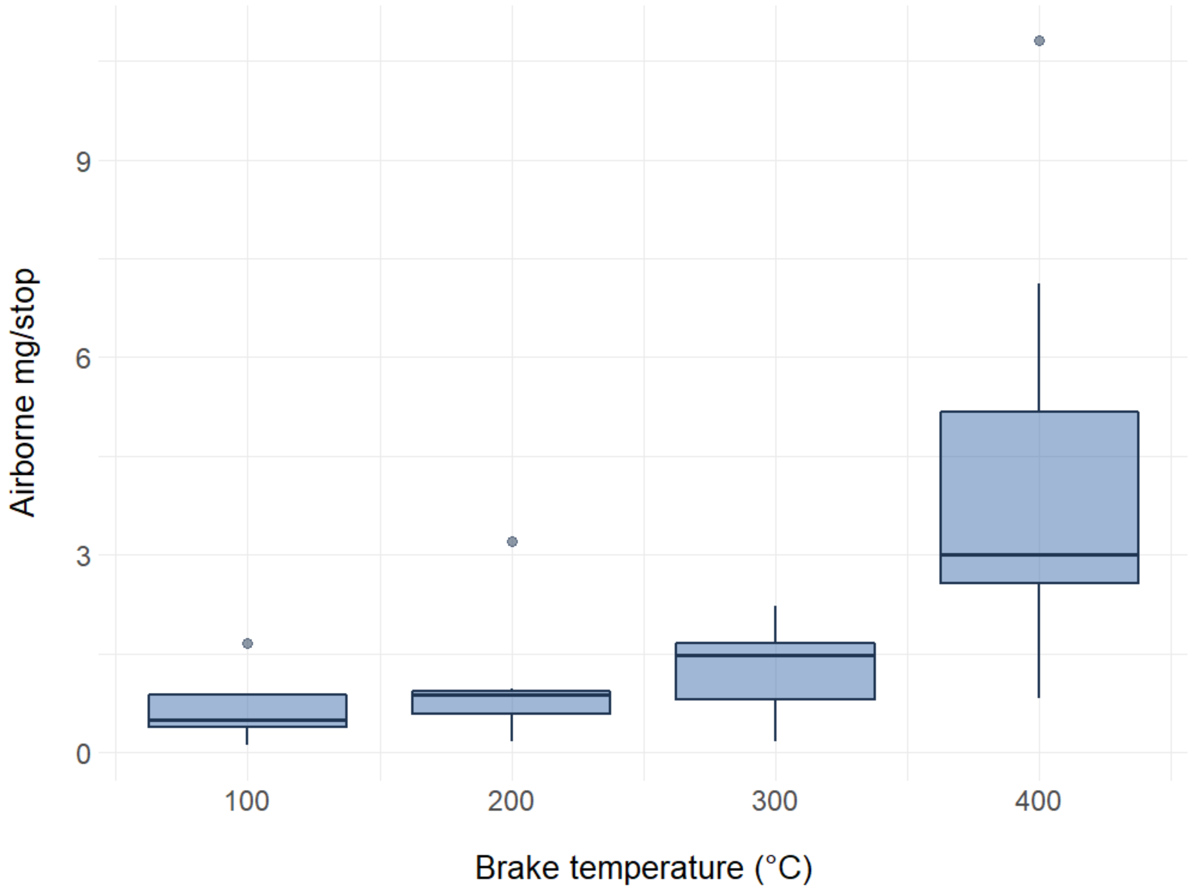


**Figure 40 Airborne PM emissions (mg/stop) as a function of brake pad temperature (Figure created using data from Garg *et al.* (2000)). The grey circles represent outliers in the data.**

Kukutschová *et al.* (2011) found a significant increase in the ultrafine organic particle number concentration above 300 °C, and Nosko *et al.* (2015) and Alemani *et al.* (2018) found a critical temperature for an increase in ultrafine particles of ~165-190 °C. The mechanism for this is that the brake material vaporises at high temperatures. Ultrafine particles given their small size, have a minor contribution to PM mass in the $PM_{10}$ or $PM_{2.5}$ size fractions however. Grochowicz (2016) found that though particle number was related to brake temperature, particle mass ($PM_{10}$) was not (Figure 41).

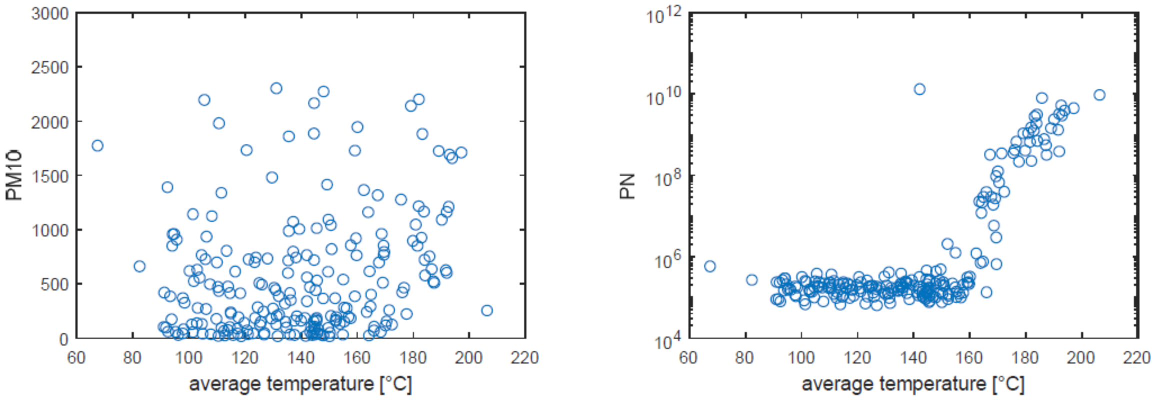


**Figure 41 Relationship between brake temperature and particle mass ($PM_{10}$) and particle number (PN) (Grochowicz (2016)).**

Although temperature may be an important influencing factor on brake wear emissions, there is evidence that there is no clear temperature dependency relationship for typical drive cycles on $PM_{10}$. There would also be significant uncertainties in trying to model this effect. Estimates would need to be made for the rates of cooling of the brake materials, which would vary significantly across the range of pad materials used.

## A.5.2 Lag in emissions release

There is evidence that brake wear particles are emitted during the acceleration after braking. Figure 42 shows an Extract of a time series profile of brake dust particle mass emissions obtained during the measurement of particle mass concentrations from Hagino, Oyama and Sasaki (2015). This shows airborne brake wear particles emissions at deceleration and acceleration, suggesting resuspension of wear particles from friction on the surface of brakes and grooves at acceleration. Hagino, Oyama and Sasaki (2016) showed similar results for disc brakes but not drum brakes however. Mathissen *et al.* (2012) showed phases of braking having higher particle emissions than acceleration phases however. It is not clear exactly what the mechanism is that causes the emissions in acceleration events, and results from more laboratories would be needed before robust conclusions could be made to inform this project.

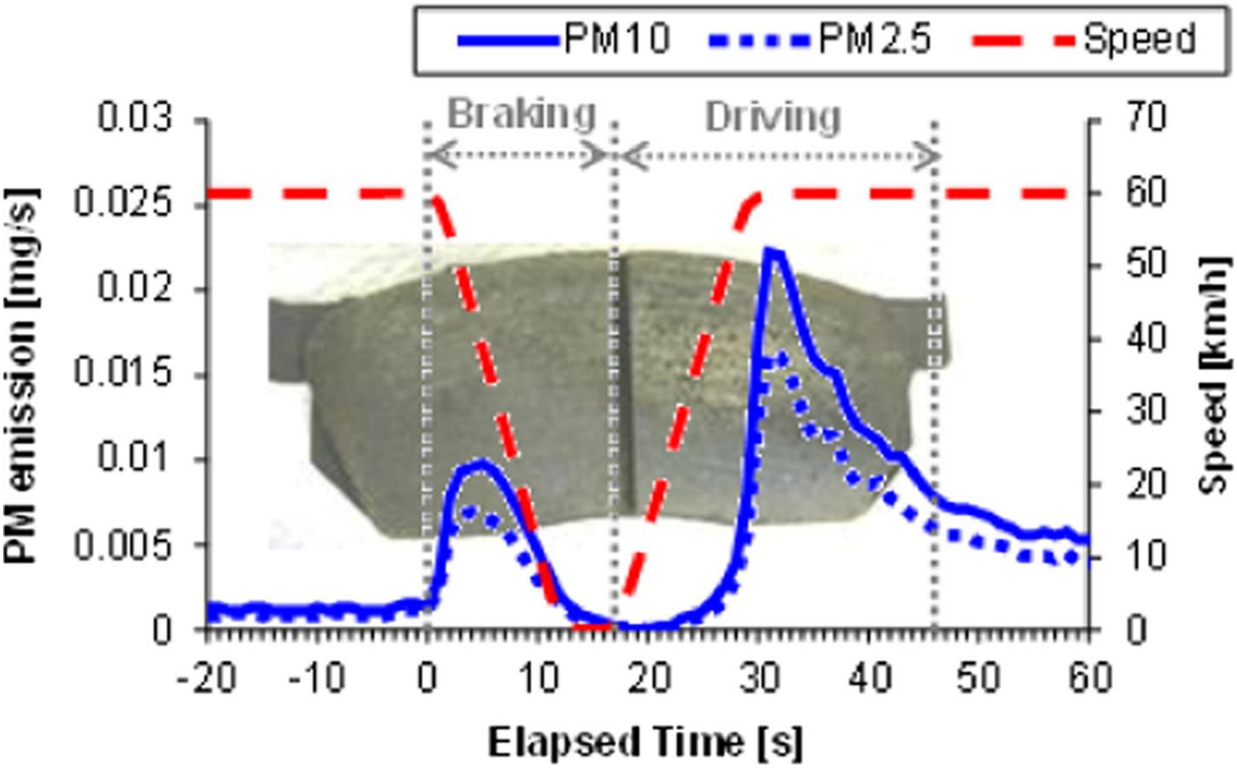


**Figure 42 Extract of a time series profile of brake dust particle mass emissions obtained during the measurement of particle mass concentrations from Hagino, Oyama and Sasaki (2015).**

## A.6 Speed

This section analyses the relationship between the vehicle speed and the brake wear emission rates. The vehicle speed was measured on all three vehicle measurement datasets. It is expected that the average brake wear emission rate will decrease with increased vehicle speed as vehicles tend to brake less at higher speeds.

Figure 43 shows the average brake wear emission factors (mg $PM_{10}$/km) by vehicle speed grouping. The vehicle speed has been grouped into groups of 3 km/h and the average brake wear emission factor has been estimated by dividing the total emissions (mg) by the total distance travelled (km) for each group.

There is a clear pattern of emission factors increasing with lower vehicle speed, with two excpetion to this pattern. Firstly, below 12-15 km/h the emission factors decrease significantly. This is as at such low speeds the energy going to the brakes is so low that very little emissions are apportioned to such events in the energy-based model used.

Secondly, the emission factors do not decrease above 108-111 km/h but instead plateau and slightly increase with increased vehicle speed. This may be due to an over-estimation of braking in the energy-based model compared to the recorded measure of brake use. Figure 44 shows the proportion of observations where brakes are used by vehicle speed grouping from the Leeds dataset with a comparison between the modelled brake use and the recorded brake use from the instrumented vehicles. This shows that the model used over-predicts brake use at the highest speeds and under-predicts brake use at the lowest speeds. The impact of this result on the urban air quality modelling would be minimal however. The lowest speeds are associated with very low vehicle energies and hence brake wear emissions, and the highest speeds are rarely or never found in central urban areas due to speed limit restrictions.

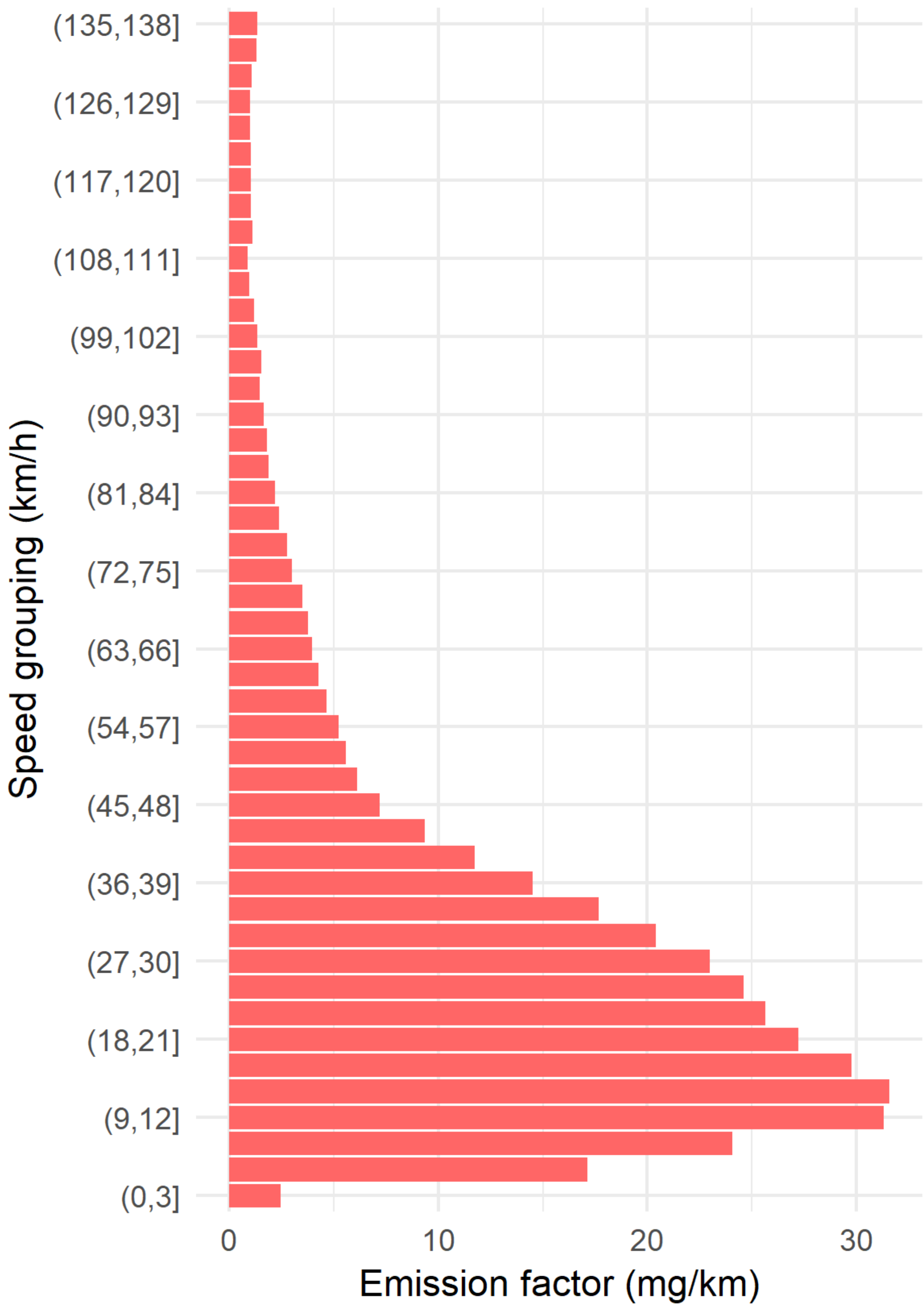


**Figure 43 Average brake wear emission factors (mg $PM_{10}$/km) by vehicle speed grouping from the Leeds dataset.**

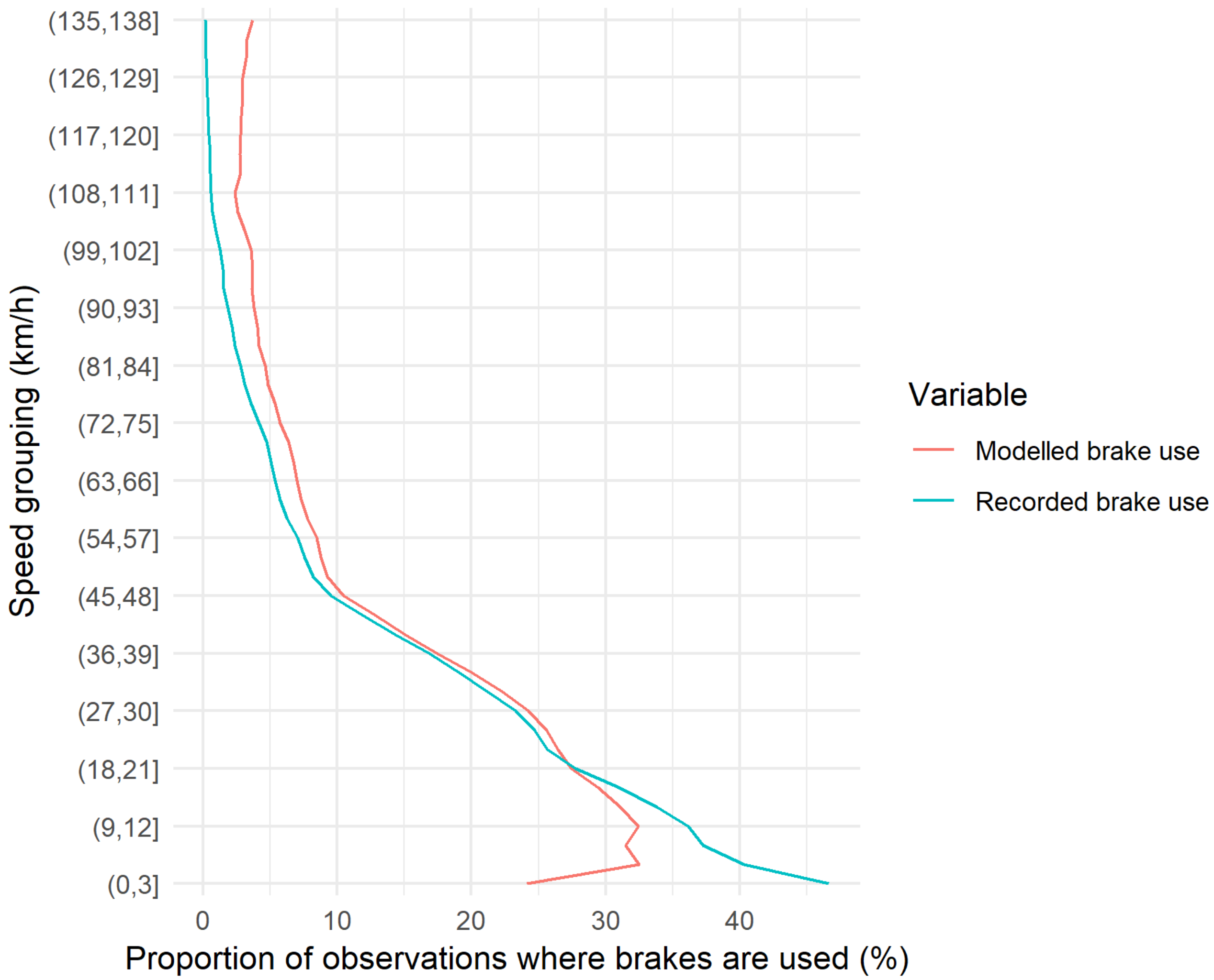


**Figure 44 Proportion of observations where brakes are used by vehicle speed grouping from the Leeds dataset. Comparison between the modelled brake use and the recorded brake use from the instrumented vehicles.**

# A.7 Model result values

**Table 8 $PM_{10}$ concentrations by source, scenario, and receptor, as used in Figure 24. Values are rounded to 1 decimal place.**

| Source | Scenario | School 2 | School 1 | R-08 | R-07 | R-06 | R-05 | Monitoring 4 | Monitoring 3 | Monitoring 2 | Monitoring 1 | High 1 | Average Domain |
|---|---|---|---|---|---|---|---|---|---|---|---|---|---|
| background | conventional | 14.5 | 14.5 | 14.7 | 14.7 | 14.6 | 14.6 | 14.5 | 15.3 | 14.7 | 14.0 | 14.6 | 14.5 |
| background | spatially resolved | 14.5 | 14.5 | 14.7 | 14.7 | 14.6 | 14.6 | 14.5 | 15.3 | 14.7 | 14.0 | 14.6 | 14.5 |
| background | regenerative braking | 14.5 | 14.5 | 14.7 | 14.7 | 14.6 | 14.6 | 14.5 | 15.3 | 14.7 | 14.0 | 14.6 | 14.5 |
| background | double brake emissions | 14.5 | 14.5 | 14.7 | 14.7 | 14.6 | 14.6 | 14.5 | 15.3 | 14.7 | 14.0 | 14.6 | 14.5 |
| background | half brake emissions | 14.5 | 14.5 | 14.7 | 14.7 | 14.6 | 14.6 | 14.5 | 15.3 | 14.7 | 14.0 | 14.6 | 14.5 |
| background | 3x HGV | 14.5 | 14.5 | 14.7 | 14.7 | 14.6 | 14.6 | 14.5 | 15.3 | 14.7 | 14.0 | 14.6 | 14.5 |
| exhaust | conventional | 0.5 | 0.1 | 0.1 | 1.1 | 1.2 | 0.5 | 0.6 | 0.7 | 0.5 | 0.3 | 1.7 | 0.1 |
| exhaust | spatially resolved | 0.5 | 0.1 | 0.1 | 1.1 | 1.2 | 0.5 | 0.6 | 0.7 | 0.5 | 0.3 | 1.7 | 0.1 |
| exhaust | regenerative braking | 0.5 | 0.1 | 0.1 | 1.1 | 1.2 | 0.5 | 0.6 | 0.7 | 0.5 | 0.3 | 1.7 | 0.1 |
| exhaust | double brake emissions | 0.5 | 0.1 | 0.1 | 1.1 | 1.2 | 0.5 | 0.6 | 0.7 | 0.5 | 0.3 | 1.7 | 0.1 |
| exhaust | half brake emissions | 0.5 | 0.1 | 0.1 | 1.1 | 1.2 | 0.5 | 0.6 | 0.7 | 0.5 | 0.3 | 1.7 | 0.1 |
| exhaust | 3x HGV | 0.6 | 0.2 | 0.2 | 1.0 | 1.4 | 0.5 | 0.7 | 0.9 | 0.6 | 0.4 | 1.9 | 0.2 |

| Source | Scenario | School 2 | School 1 | R-08 | R-07 | R-06 | R-05 | Monitoring 4 | Monitoring 3 | Monitoring 2 | Monitoring 1 | High 1 | Average Domain |
|---|---|---|---|---|---|---|---|---|---|---|---|---|---|
| other_non_exh | conventional | 0.7 | 0.2 | 0.2 | 1.8 | 1.9 | 0.7 | 0.9 | 1.2 | 0.7 | 0.4 | 2.6 | 0.2 |
| other_non_exh | spatially resolved | 0.7 | 0.2 | 0.2 | 1.8 | 1.9 | 0.7 | 0.9 | 1.2 | 0.7 | 0.4 | 2.6 | 0.2 |
| other_non_exh | regenerative braking | 0.7 | 0.2 | 0.2 | 1.8 | 1.9 | 0.7 | 0.9 | 1.2 | 0.7 | 0.4 | 2.6 | 0.2 |
| other_non_exh | double brake emissions | 0.7 | 0.2 | 0.2 | 1.8 | 1.9 | 0.7 | 0.9 | 1.2 | 0.7 | 0.4 | 2.6 | 0.2 |
| other_non_exh | half brake emissions | 0.7 | 0.2 | 0.2 | 1.8 | 1.9 | 0.7 | 0.9 | 1.2 | 0.7 | 0.4 | 2.6 | 0.2 |
| other_non_exh | 3x HGV | 0.9 | 0.3 | 0.3 | 1.7 | 2.2 | 0.9 | 1.1 | 1.5 | 0.9 | 0.6 | 3.0 | 0.3 |
| brake_wear | conventional | 0.5 | 0.1 | 0.1 | 1.3 | 1.3 | 0.5 | 0.6 | 0.8 | 0.5 | 0.3 | 1.8 | 0.1 |
| brake_wear | spatially resolved | 0.3 | 0.1 | 0.1 | 0.7 | 1.1 | 1.1 | 0.9 | 0.8 | 0.5 | 0.3 | 5.7 | 0.1 |
| brake_wear | regenerative braking | <0.05 | <0.05 | <0.05 | <0.05 | 0.1 | 0.1 | <0.05 | 0.1 | <0.05 | <0.05 | 1.6 | <0.05 |
| brake_wear | double brake emissions | 0.6 | 0.3 | 0.3 | 1.4 | 2.3 | 2.1 | 1.9 | 1.7 | 0.9 | 0.5 | 11.4 | 0.3 |
| brake_wear | half brake emissions | 0.1 | 0.1 | 0.1 | 0.3 | 0.6 | 0.5 | 0.5 | 0.4 | 0.2 | 0.1 | 2.8 | 0.1 |
| brake_wear | 3x HGV | 0.3 | 0.2 | 0.2 | 0.8 | 1.3 | 1.2 | 1 | 0.9 | 0.5 | 0.3 | 6.6 | 0.2 |

The Gemini Building
Fermi Avenue
Harwell
Didcot
Oxfordshire
OX11 0QR
United Kingdom

t: +44 (0)1235 753000

e: enquiry@ricardo.com

ee.ricardo.com

## Bisher in der FAT-Schriftenreihe erschienen (ab 2014)

| Nr. | Titel |
|---|---|
| 263 | Laserstrahlschweißen von Stahl an Aluminium mittels spektroskopischer Kontrolle der Einschweißtiefe und erhöhter Anbindungsbreite durch zweidimensional ausgeprägte Schweißnähte, 2014 |
| 264 | Entwicklung von Methoden zur zuverlässigen Metamodellierung von CAE Simulations-Modellen, 2014 |
| 265 | Auswirkungen alternativer Antriebskonzepte auf die Fahrdynamik von PKW, 2014 |
| 266 | Entwicklung einer numerischen Methode zur Berücksichtigung stochastischer Effekte für die Crash-simulation von Punktschweißverbindungen, 2014 |
| 267 | Bewegungsverhalten von Fußgängern im Straßenverkehr - Teil 1, 2014 |
| 268 | Bewegungsverhalten von Fußgängern im Straßenverkehr - Teil 2, 2014 |
| 269 | Schwingfestigkeitsbewertung von Schweißnahtenden MSG-geschweißter Feinblechstrukturen aus Aluminium, 2014 |
| 270 | Physiologische Effekte bei PWM-gesteuerter LED-Beleuchtung im Automobil, 2015 |
| 271 | Auskunft über verfügbare Parkplätze in Städten, 2015 |
| 272 | Zusammenhang zwischen lokalem und globalem Behaglichkeitsempfinden: Untersuchung des Kombinationseffektes von Sitzheizung und Strahlungswärmeübertragung zur energieeffizienten Fahrzeugklimatisierung, 2015 |
| 273 | UmCra - Werkstoffmodelle und Kennwertermittlung für die industrielle Anwendung der Umform- und Crash-Simulation unter Berücksichtigung der mechanischen und thermischen Vorgeschichte bei hochfesten Stählen, 2015 |
| 274 | Exemplary development & validation of a practical specification language for semantic interfaces of automotive software components, 2015 |
| 275 | Hochrechnung von GIDAS auf das Unfallgeschehen in Deutschland, 2015 |
| 276 | Literaturanalyse und Methodenauswahl zur Gestaltung von Systemen zum hochautomatisierten Fahren, 2015 |
| 277 | Modellierung der Einflüsse von Porenmorphologie auf das Versagensverhalten von Al-Druckgussteilen mit stochastischem Aspekt für durchgängige Simulation von Gießen bis Crash, 2015 |
| 278 | Wahrnehmung und Bewertung von Fahrzeugaußengeräuschen durch Fußgänger in verschiedenen Verkehrssituationen und unterschiedlichen Betriebszuständen, 2015 |
| 279 | Sensitivitätsanalyse rollwiderstandsrelevanter Einflussgrößen bei Nutzfahrzeugen – Teil 3, 2015 |
| 280 | PCM from iGLAD database, 2015 |
| 281 | Schwere Nutzfahrzeugkonfigurationen unter Einfluss realitätsnaher Anströmbedingungen, 2015 |
| 282 | Studie zur Wirkung niederfrequenter magnetischer Felder in der Umwelt auf medizinische Implantate, 2015 |
| 283 | Verformungs- und Versagensverhalten von Stählen für den Automobilbau unter crashartiger mehrachsiger Belastung, 2016 |
| 284 | Entwicklung einer Methode zur Crashsimulation von langfaserverstärkten Thermoplast (LFT) Bauteilen auf Basis der Faserorientierung aus der Formfüllsimulation, 2016 |
| 285 | Untersuchung des Rollwiderstands von Nutzfahrzeugreifen auf realer Fahrbahn, 2016 |

286 χMCF - A Standard for Describing Connections and Joints in the Automotive Industry, 2016

287 Future Programming Paradigms in the Automotive Industry, 2016

288 Laserstrahlschweißen von anwendungsnahen Stahl-Aluminium-Mischverbindungen für den automobilen Leichtbau, 2016

289 Untersuchung der Bewältigungsleistung des Fahrers von kurzfristig auftretenden Wiederübernahme-situationen nach teilautomatischem, freihändigem Fahren, 2016

290 Auslegung von geklebten Stahlblechstrukturen im Automobilbau für schwingende Last bei wechselnden Temperaturen unter Berücksichtigung des Versagensverhaltens, 2016

291 Analyse, Messung und Optimierung des Ventilationswiderstands von Pkw-Rädern, 2016

292 Innenhochdruckumformen laserstrahlgelöteter Tailored Hybrid Tubes aus Stahl-Aluminium-Mischverbindungen für den automobilen Leichtbau, 2017

293 Filterung an Stelle von Schirmung für Hochvolt-Komponenten in Elektrofahrzeugen, 2017

294 Schwingfestigkeitsbewertung von Nahtenden MSG-geschweißter Feinbleche aus Stahl unter kombinierter Beanspruchung, 2017

295 Wechselwirkungen zwischen zyklisch-mechanischen Beanspruchungen und Korrosion: Bewertung der Schädigungsäquivalenz von Kollektiv- und Signalformen unter mechanisch-korrosiven Beanspruchungs-bedingungen, 2017

296 Auswirkungen des teil- und hochautomatisierten Fahrens auf die Kapazität der Fernstraßeninfrastruktur, 2017

297 Analyse zum Stand und Aufzeigen von Handlungsfeldern beim vernetzten und automatisierten Fahren von Nutzfahrzeugen, 2017

298 Bestimmung des Luftwiderstandsbeiwertes von realen Nutzfahrzeugen im Fahrversuch und Vergleich verschiedener Verfahren zur numerischen Simulation, 2017

299 Unfallvermeidung durch Reibwertprognosen, 2017

300 Thermisches Rollwiderstandsmodell für Nutzfahrzeugreifen zur Prognose fahrprofilspezifischer Energieverbräuche, 2017

301 The Contribution of Brake Wear Emissions to Particulate Matter in Ambient Air, 2017

302 Design Paradigms for Multi-Layer Time Coherency in ADAS and Automated Driving (MULTIC), 2017

303 Experimentelle Untersuchung des Einflusses der Oberflächenbeschaffenheit von Scheiben auf die Kondensatbildung, 2017

304 Der Rollwiderstand von Nutzfahrzeugreifen unter realen Umgebungsbedingungen, 2018

305 Simulationsgestützte Methodik zum Entwurf intelligenter Energiesteuerung in zukünftigen Kfz-Bordnetzen, 2018

306 Einfluss der Kantenbearbeitung auf die Festigkeitseigenschaften von Stahl-Feinblechen unter quasistatisch und schwingender Beanspruchung, 2018

307 Fahrerspezifische Aspekte beim hochautomatisierten Fahren, 2018

308 Der Rollwiderstand von Nutzfahrzeugreifen unter zeitvarianten Betriebsbedingungen, 2018

309 Bewertung der Ermüdungsfestigkeit von Schraubverbindungen mit gefurchtem Gewinde, 2018

310 Konzept zur Auslegungsmethodik zur Verhinderung des selbsttätigen Losdrehens bei Bauteilsystemen im Leichtbau, 2018

311 Experimentelle und numerische Identifikation der Schraubenkopfverschiebung als Eingangsgröße für eine Bewertung des selbsttätigen Losdrehens von Schraubenverbindungen, 2018

312 Analyse der Randbedingungen und Voraussetzungen für einen automatisierten Betrieb von Nutzfahrzeuge im innerbetrieblichen Verkehr, 2018

313 Charakterisierung und Modellierung des anisotropen Versagensverhaltens von Aluminiumwerkstoffen für die Crashsimulation, 2018

314 Definition einer „Äquivalenten Kontakttemperatur“ als Bezugsgröße zur Bewertung der ergonomischen Qualität von kontaktbasierten Klimatisierungssystemen in Fahrzeugen, 2018

315 Anforderungen und Chancen für Wirtschaftsverkehre in der Stadt mit automatisiert fahrenden E-Fahrzeugen (Fokus Deutschland), 2018

316 MULTIC-Tooling, 2019

317 EPHoS: Evaluation of Programming - Models for Heterogeneous Systems, 2019

318 Air Quality Modelling on the Contribution of Brake Wear Emissions to Particulate Matter Concentrations Using a High-Resolution Brake Use Inventory, 2019

# Impressum

Herausgeber FAT
Forschungsvereinigung Automobiltechnik e.V.
Behrenstraße 35
10117 Berlin
Telefon +49 30 897842-0
Fax +49 30 897842-600
www.vda-fat.de

ISSN 2192-7863

Verband der Automobilindustrie e.V. (VDA)
Behrenstraße 35, 10117 Berlin
www.vda.de
Twitter @VDA_online

Forschungsvereinigung Automobiltechnik e.V. (FAT)
Behrenstraße 35, 10117 Berlin
www.vda.de/fat

Verband der Automobilindustrie

Forschungsvereinigung Automobiltechnik